TESTING OF FULL SCALE PRESTRESSED BEAMS TO EVALUATE SHEAR KEY PERFORMANCE

PREPARED IN COOPERATION WITH:
OHIO DEPARTMENT OF TRANSPORTATION AND,
U.S. DEPARTMENT OF TRANSPORTATION,
FEDERAL HIGHWAY ADMINISTRATION

Report # FHWA/OH - 98/019
State Job # 14578(0)

by R.A. Miller, G.M. Hlavacs, and T.W. Long

December, 1998

TESTING OF FULL SCALE PRESTRESSED BEAMS TO EVALUATE SHEAR KEY PERFORMANCE

by R.A. Miller, G.M. Hlavacs, and T.W. Long

University of Cincinnati
Department of Civil and Environmental Engineering

PREPARED IN COOPERATION WITH:
OHIO DEPARTMENT OF TRANSPORTATION AND,
U.S. DEPARTMENT OF TRANSPORTATION,
FEDERAL HIGHWAY ADMINISTRATION

Report # FHWA/OH - 98/019
State Job # 14578(0)

December, 1998

1. Report No.	2. Government Accession No.	3. F
FHWA/OH-98/019		PB99-123200

4. Title and Subtitle	5. Report Date
TESTING OF FULL SCALE PRESTRESSED BEAMS TO EVALUATE SHEAR KEY PERFORMANCE	June, 1998
	6. Performing Organization Code
	8. Performing Organization Report No.
7. Author(s) Richard A. Miller George Hlavacs and Todd Long	10. Work Unit No. (TRAIS)
9. Performing Organization Name and Address The University of Cincinnati Department of Civil and Environmental Engineering Cincinnati, OH 45221-0071	11. Contract or Grant No. State Job No. 14578(0)
	13. Type of Report and Period Covered Final Report
12. Sponsoring Agency Name and Address Ohio Department of Transportation 25 S. Front St. Columbus, OH 43215	14. Sponsoring Agency Code

15. Supplementary Notes

Prepared in cooperation with the U.S. Department of Transportation, Federal Highway Administration

16. Abstract

Adjacent box girder bridges use grouted shear keys to transfer load between beams. These shear keys tend to crack and leak. A full-scale portion of an adjacent box girder bridge was used to test the performance of grouted shear keys under environmental and cyclic loads. Strain gages were placed in the girders and in the shear keys. Displacement gages were placed spanning the shear keys on the top and bottom flanges of the girders. The bridge was subjected to simulated cyclic truck loading as well as environmentally induced thermal loading. The pulse velocity method was employed to find cracks in shear keys. Dye penetration was used to confirm the pulse velocity measurements.

The total research project consisted of: (a) testing of the current keyway detail using the currently specified nonshrink grout, (b) testing of the current keyway detail but substituting epoxy grout for the nonshrink grout, and (c) testing of a modified keyway detail using nonshrink grout in which the keyway is moved to the neutral axis of the girder.

In the first test, the shear keys were grouted in late autumn and cracked soon after casting, before any simulated vehicle loading had been applied. Data from instruments embedded in the beams and shear keys showed large changes in strain due to freezing temperatures. The beams were subjected to 41,000 cycles of loading simulating an HS20-44 truck wheel. No new cracking occurred due to loading, but cracks caused by temperature propagated.

In the second test, the keys were grouted in the summer. However, temperature changes caused by the sun heating the top of the girders again caused large thermal strains, which cracked the shear keys at the abutments. Measurements of beam and shear key deformations and strains under temperature induced loading showed that temperature changes cause large transverse strains in the keyways. These strains are of sufficient magnitude to crack the grout. The keyways were subjected to 1,000,000 cycles of load. As before, the load did not cause new cracks but the existing cracks propagated.

In the third test, keyways located at the neutral axis were grouted in late summer. Thermal stresses caused minimal cracking at the abutments. These keys were subjected to 1,000,000 cycles of load only minimal propagation was observed. In the fourth test, the standard keyways were grouted in early spring using an epoxy grout. No cracking occurred in any of the keyways during the grouting process nor during cyclic or environmental testing.

17. Key Words	18. Distribution Statement
Adjacent, Bridge, Box Girders, Concrete, Cyclic Testing, Epoxy, Full Scale Testing, Prestressed, Shear Keys	No Restrictions. This document is available to the public through the National Technical Information Service, Springfield, Virginia 22161

19. Security Classif. (of this report)	20. Security Classif. (of this page)	21. No. of Pages	22. Price
Unclassified	Unclassified		

ABSTRACT

Adjacent box girder bridges use grouted shear keys to transfer load between beams. These shear keys tend to crack and leak. A full-scale portion of an adjacent box girder bridge was used to test the performance of grouted shear keys under environmental and cyclic loads. Strain gages were placed in the girders, and in the shear keys. Displacement gages were placed spanning the shear keys on the top and bottom flanges of the girders. The bridge was subjected to simulated cyclic truck loading as well as environmentally induced thermal loading. The pulse velocity method was employed to find cracks in shear keys. Dye penetration was used to confirm the pulse velocity measurements.

The total research project consists of three separate trials: (a) testing of the current keyway detail using the currently specified nonshrink grout, (b) testing of the current keyway detail but substituting epoxy grout for the nonshrink grout, and (c) testing of a modified keyway detail developed by CWRU in which the keyway is moved to the neutral axis of the girder and nonshrink grout is used. Four separate tests were conducted in this study utilizing the two different keyway designs.

In the first test, the shear keys were grouted in late autumn and cracked soon after casting, before any simulated vehicle loading had been applied. Data from instruments embedded in the beams and shear keys showed large changes in strain due to freezing temperatures. The beams were subjected to 41,000 cycles of loading simulating an HS20-44 truck wheel. No new cracking occurred due to loading, but cracks caused by temperature propagated.

In the second test, the keys were grouted in the summer. However, temperature changes caused by the sun heating the top of the girders again caused large thermal strains, which cracked the shear keys at the abutments. Measurements of beam and shear key deformations and strains under temperature induced loading showed that temperature changes cause large transverse strains in the keyways. These strains are of sufficient magnitude to crack the grout. The keyways were subjected to 1,000,000 cycles of load. As before, the load did not cause new cracks but the existing cracks propagated.

In the third test, keyways located at the neutral axis were grouted in late summer. Thermal stresses caused minimal cracking at the abutments. These keys were subjected to 1,000,000 cycles of load only minimal propagation was observed.

In the fourth test, the standard keyways were grouted in early spring using an epoxy grout. No cracking occurred in any of the keyways during the grouting process nor during cyclic or environmental testing.

(THIS PAGE INTENTIONALLY LEFT BLANK)

II. ACKNOWLEDGMENT

This research was funded by the Ohio Department of Transportation and the Federal Highway Administration under State Job No. 14578(O); Contract No. 8187.
The authors would like to thank the following ODOT personnel for their help and advice: Mr. W. Edwards (ret.), Mr. Roger Green of ODOT Research and Development; Mr. V. Dalal and Mr. L. Welker of the ODOT office of Structural Engineering.

The authors are grateful to Prestressed Services Inc., Melbourne Kentucky, for providing the testing facilities, cranes and labor for moving the beams and erecting the testing frame. The authors thank Mr. J. McDonald, Mr. D. Bosse and the rest of staff at Prestress Services of Melbourne, Kentucky for the use of their facilities as well as the frequent assistance provided by the entire staff.

The contributions of Dr. Arthur Huckelbridge of the Case-Western Reserve University to the planning of these tests are gratefully acknowledged.

The authors also thank Dr. T. M. Baseheart of the University of Cincinnati for the use of the Pulse-Velocity equipment, and Dr. B. Shahrooz, also of U.C., for the loan of his load cells and jacks. Thanks are also due to all of the members of the University of Cincinnati Technical Staff, particularly Mr. D. Corni, Mr. R. Fitzpatrick, and Mr. D. Breheim, and Mr. B. Munch. Finally thanks are due to Ms. J. Smith ,Mrs. M. Pennington, and Mrs. E. Hutchison for keeping the accounts straight.

III. NOTICE OF UNITS

Numerical information given throughout the text is presented in the International System of Units (SI) first and is followed by U.S. Customary System (USCS) in parenthesis, as required by the Federal Highway Administration. However, it should be noted that actual test data was recorded in USCS units and was subsequently converted to SI units. Since there are slight inaccuracies introduced in conversions (due to rounding), USCS values should be used for any subsequent analysis of the data.

IV. TABLE OF CONTENTS

I. ABSTRACT ii

II. ACKNOWLEDGMENT iv

III. NOTICE OF UNITS v

IV. TABLE OF CONTENTS vi

CHAPTER 1: Introduction 1

CHAPTER 2: Review of Existing Literature 7

CHAPTER 3: Description of the Girders and Testing Facility 17

CHAPTER 4: Construction of the Box Girders 35

CHAPTER 5: Dynamic Load Testing of the Bridge 43

CHAPTER 6: Thermal Movements of the Bridge 73

CHAPTER : Summary, Conclusions and Recommendations 83

REFERENCES 88

APPENDICES 90

(THIS PAGE INTENTIONALLY LEFT BLANK)

CHAPTER 1

INTRODUCTION

1.1 General

Prestressed adjacent box girder bridges (Figure 1.1) are often found on secondary roads throughout the United States. According to a survey taken by the Prestressed/Precast Concrete Institute (PCI) Bridge Committee, these bridges are used in 30 different states (unpublished survey by PCI) and, according to Dunkar and Rabbat (1992), are one of the most common bridge structures in the United States. Using normal strength concrete and 13 mm (0.5 inches) strands, these bridges are often used for spans lengths up to 30 meters (100 feet).

The widespread popularity of the adjacent prestressed box bridge can be attributed to a number of factors including:

1) An excellent depth-to-span ratio, needed when clearance is limited.
2) Erection of these bridges is relatively quick and simple when compared with most other bridge types.
3) The forming of a separate deck structure is not required and a wearing surface may be placed directly on the girders.
4) Compared with most other bridge types, minimal field labor is required.
5) No field drilling or welding is required.
6) Periodic painting of concrete is not required as it is with steel bridges.
7) Concrete is better at resisting the effects of a fire than steel or wood.
8) Better quality control is maintained in a concrete casting plant than is typically obtained when pouring concrete in the field.
9) Precast concrete has had time to shrink and creep before it is in place.

The most serious drawback to the use of adjacent box girder bridges is the widespread failure of shear keys. This problem is the subject of this study.

In Ohio the box girders are set side by side on bearing pads and connected with transverse tie-rods. Some states use transverse post-tensioning and some states do not connect the girders at all (El- Remaily, Tadros, Yamane and Krause, 1995). After the beams are in place, grout is poured into a female - female octagonal shaped gap between the beams which is referred to as either a "shear key" or a "keyway."(Figures 1.1 and 1.2) The state of Ohio currently requires using a non-shrink grout to fill these keyways. Magnesium-phosphate grouts and epoxy grouts have also been used (Gulyas, Wirthlin and Champa, 1995). When the grout hardens, the beams are locked together and form an almost monolithic bridge deck. After grouting the shear keys, a wearing surface may be placed over the bridge. In some cases, the wearing surface is concrete and is made composite with the girders through the use of stirrups. In other cases, a waterproofing membrane is placed on the bridge followed by a non-composite asphalt deck.

In addition to providing a mechanism for load transfer, the shear keys are also intended to seal the joints between the girders. Bridge engineers have noticed that the shear keys tend to crack and leak even when a waterproofing membrane is in place. This allows deicing chemicals to penetrate the longitudinal joints between the beams and attack the concrete between the girders and in the soffit of the bridge. The prestressing tendons become exposed to rust and eventually break.

Failure of prestressing tendons is considered a very serious problem. Miller and Parekh (1994) observed the following phenomenon in a prestressed box girder with three deteriorated strands: 1) Lower precracking stiffness. 2) Lower cracking load. 3) Lower postcracking load. 4) A sudden brittle failure before reaching the ultimate load predicted by the AASHTO Code.

It is believed that failed shear keys can result in overloading a girder because load in not distributed to adjacent girders. Huckelbridge, El-Esnawi and Moses (1995) indicated that the load sharing function of the shear key can be completely eliminated by a fractured keyway.

1.2 Background of the Research

Researchers at Case Western Reserve University (CWRU) in Cleveland, Ohio investigated the problem of shear key failures (Huckelbridge, El-Esnawi and Moses, 1995), (El-Esnawi and Huckelbridge, 1996). After doing field tests to determine the severity of shear key cracking, they performed finite element analysis on a portion of a typical box beam bridge. Next, they conducted laboratory test on 305 mm (12 inch) slices of prestressed concrete box beams. Based upon their analysis and laboratory test, CWRU's determined that:

a) The current keyway design, using nonshrink grout, fails quickly under load. This failure is believed to occur because the top flange and part of the web of the box girder act like a portal frame when a wheel load is applied. The top corners of the box flex in and apply tension to the top of the shear key, creating a crack which propagates under load.

b) A keyway of the same size and proportions as the current keyway located at the neutral axis resists cracking much better than the current design (Figure 1.2).

c) The current keyway design will perform in a satisfactory manner if it is grouted with an epoxy grout.

The University of Cincinnati was chosen to conduct full-scale tests of the current keyway design, the proposed neutral axis keyway and an epoxy keyway.

1.3 Objectives of this Research

Theobjective of this research is to test a full-scale, prestressed adjacent box girder bridge to determine:

1) If shear key cracking occurs due to an inherent flaw in the design or the result of poor construction practices.
2) If the new keyway designs proposed by CWRU resist cracking better than the current design in a full scale bridge.
3) The probable life-span of the current intact shear keys.
4) Load sharing capabilities of adjacent box girder bridges with cracked and uncracked keyways.

1.4 Scope of Research

To achieve the objectives outlined above, a portion of a full-size prestressed adjacent box girder bridge was fabricated and tested to determine the behavior of different keyway designs under cyclic loads. The bridge consisted of four (4) ODOT B33-48 prestressed box girders with a span of 22.4 m (73.5 feet).

Three separate tests were to be conducted:

1) A test of the current ODOT standard shearkey (Figure 1.2, upper detail) grouted with a nonshrink grout.

2) A test of neutral axis keyway proposed by researchers at Case-Western Reserve University. This keyway is identical in size and shape to the current ODOT standard shear key except that it moved down to the neutral axis of the beam (Figure 1.2, lower detail). Another difference between the neutral axis keyway and the current ODOT standard is that the throat (area from the top of the keyway to the top of the beam) is not grouted in the neutral axis keyway detail. A nonshrink grout is used in the neutral axis keyway.

3) A test of the current ODOT standard keyway (Figure 1.2, upper detail), but grouted with an epoxy grout.

All keyway details were to be tested under a loading condition which simulated the wheel loads of HS-20-44 truck passing over the bridge in different directions. The loading was such that it achieved complete shear reversal in the center keyway. All specimens were loaded under cyclic load to 1,000,000 cycles.

Since cracking is the main problem with keyways, all keyways were checked for cracking during the test. This was done using pulse velocity measurements backed up by dye penetration techniques. The keyways were checked for cracking at various intervals to determine the extent of crack formation and crack propagation.

1.5 Organization of Report

The layout of this report is constructed in a chronological order that follows the pattern of construction. Chapter 2 contains the review of existing literature. Chapter 3 details the box girders and the testing facility. Construction of the box girders and initial strains from the internal gages within the box girders taken during construction are covered in chapter 4. The dynamic load testing of the bridge including test results is

covered in chapter 5. From the results of chapter 5 it was determined that environmental testing of the bridge was necessary. The bridge was induced to environmental cyclic loading from the heating and cooling of the sun. Chapter 6 covers the resulting strains and movements provided by this loading. Chapter 7 contains the summary and conclusions from the testing. Several appendices are included to illustrate the calculations used in the preceding chapters.

Figure 1.1 Typical box girder bridge plan and shear key detail.

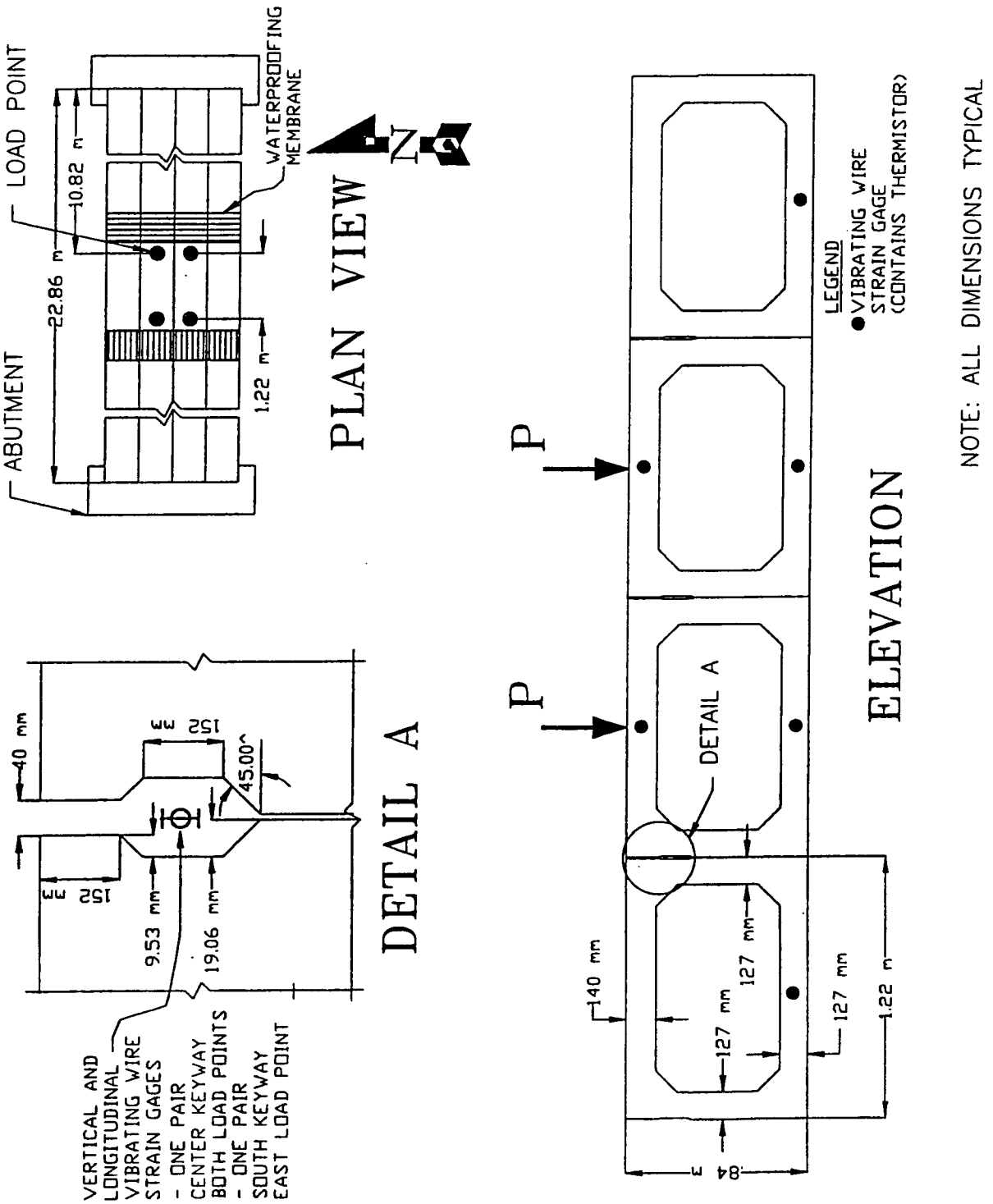

Keyway Locations:

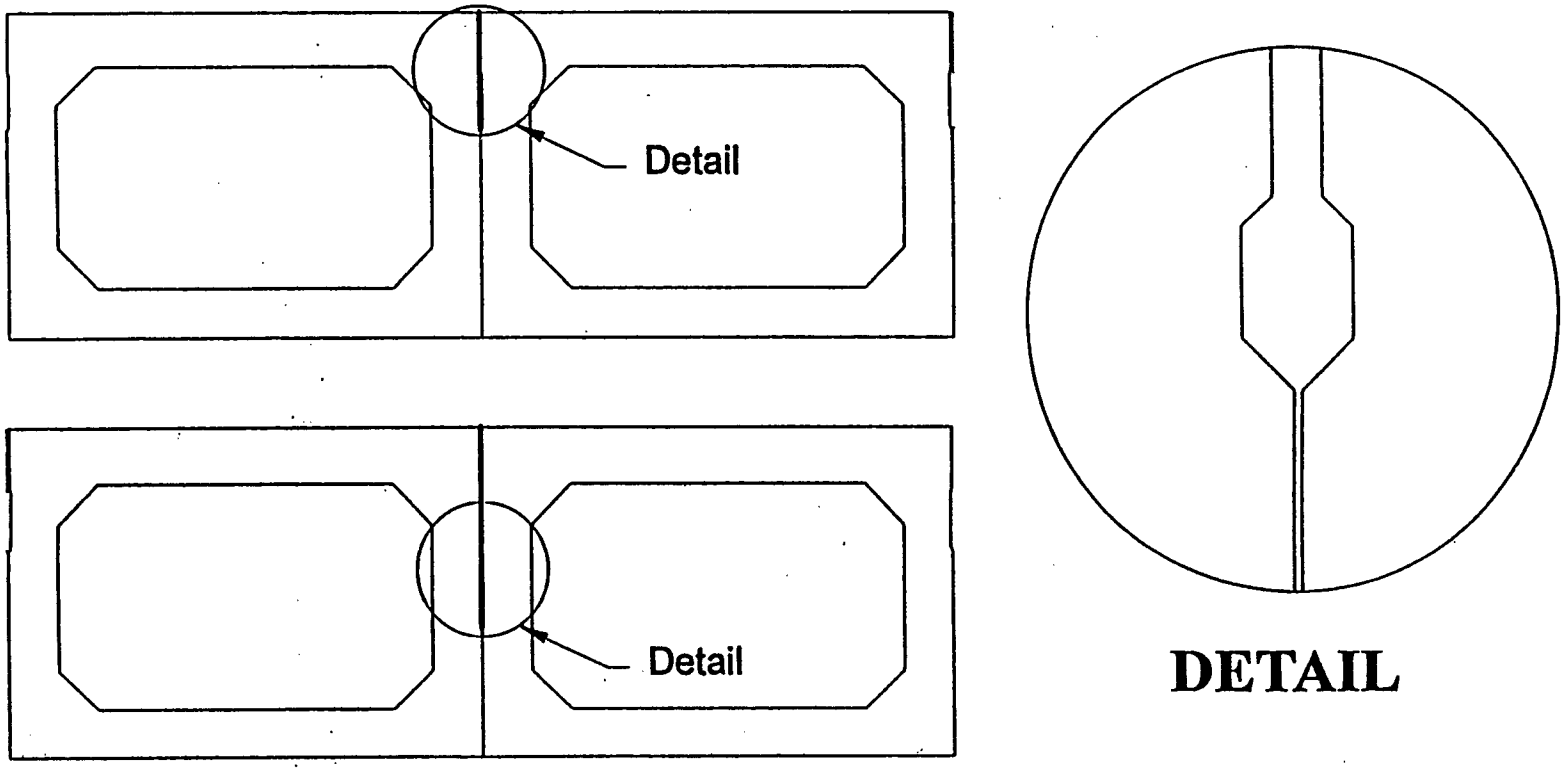

Figure 1.2 Location of current (upper detail) and new (lower detail) keyway.

CHAPTER 2

REVIEW OF EXISTING LITERATURE

2.1 Introduction

A review of existing literature shows that a full-size prestressed box girder bridge has not been erected solely for the sake of testing and monitoring the shear keys. However, several researchers have recently addressed the problem of keyway failures. They attribute the problem to; 1) keyway size, 2) keyway location, 3) lack of transverse post-tensioning, 4) lack of quality control during grouting, and 5) poor performance of non-shrink grouts in keyway. None of the available literature mentions the possibility of environmental effects contributing to the failure of grouted shear keys.

2.2 Huckelbridge, El-Esnawi and Moses - Investigation of Load Transfer in Multi-Beam Box Girder Bridges; And, El-Esnawi and Huckelbridge - Evaluation of Improved Shear Key Design For Multi-Beam Prestressed Concrete Box Girder Bridges

Huckelbridge, El-Esnawi and Moses (1995) conducted field and laboratory tests to quantify the problem of shear key failures in prestressed adjacent box girder bridges. Five bridges in Northeastern Ohio were instrumented and tested. These tests consisted of monitoring the shear keys from below the bridge as a dump truck, with a typical axle weight of 85 kN (19 kips) passed over a bridge in the normal direction of travel (parallel to the bridge girders). Relative displacements between girders were measured with specially designed transducers (deflectometers) which had a resolution of 0.0025 mm (0.00010 inches). Data was taken during multiple passes of the truck traveling at speeds ranging from 8 kph (5 mph) to 65 kph (40 mph). All bridges showed relative displacements across some of the joints indicative of fractured shear keys. These displacements were found to be as high as 0.5 mm (0.02 inches). In comparison, finite element analysis indicated that an intact shear key limited relative displacements to approximately 0.008 mm (0.0003 inches).

One of the bridges that showed severe shear key cracking was disassembled, had the shear keys cleaned, and was re-grouted. Six months later, the researchers conducted a follow up test to determine the condition of the shear keys. They discovered that the same keyways that had previously been cracked, had once again cracked. Nearly the same level of relative displacements were observed in the newly cracked keyways.

To study the problem more closely, El-Esnawi and Huckelbridge (1996) created a finite element analysis of a three-dimensional bridge model (Figure 2.1). This analysis showed that the top flange and webs behave as a portal frame. Under wheel loads, the top corners move inward and create tensile stresses in the shear key grout (Figure 2.2). Further finite element analysis indicated that moving the shear key to the neutral axis, and not grouting the throat, would eliminate these large tensile strains (Figure 2.3).

Next, El-Esnawi and Huckelbridge (1996) performed laboratory test on 305 mm (12 inch) box girder slices. A 223 kN (50 Kip) hydraulic actuator was used to simulate a truck

wheel passing over the center of the box girder. Three laboratory static tests were conducted on the current shear key as well as the neutral axis shear key. Load, relative deflections and strains were measured. Three different grout materials were tested; non-shrink grout, magnesium-phosphate grout and an epoxy grout. For the non-shrink and magnesium-phosphate grouts, shear key failures were observed as the grout debonded from the girder. For the epoxy grout, shear key failures were observed as the concrete in the girder failed. Cracking of the grout material was never observed in any of the laboratory tests performed.

For static tests of the current keyway design, non-shrink grout failure occurred at an average load of 45 kN (10 kips), while mag-phosphate grout failed at an average load of 62 kN (14 kips). The epoxy grout did not fail, but at loads as high as 180 kN (40 kips), the concrete in the box girder failed. For the neutral axis keyway design, the non-shrink grout failed at an average load of 105 kN (23.5 kips). The mag-phosphate and epoxy grouts were not tested at the neutral axis.

Three fatigue life test were conducted on the current shear key, the mag-phosphate shear key, the neutral axis shear key and the epoxy shear key. A load of 45 kN (10 kips) was used to simulate the wheel load of a truck passing over the specimen at a rate of three times per second. For the current shear key design, the non-shrink grout failed on the first cycle. The mag-phosphate grout failed at about 1,000 cycles. The epoxy grout did not fail after 4,000,000 cycles. For the neutral axis keyway test, the non-shrink grout did not fail at 8,000,000 cycles. As with the static tests, the mag-phosphate and epoxy grouts were not tested at the neutral axis. Laboratory testing confirmed that the neutral axis keyway and the epoxy keyway resist cracking much better than the current design.

2.3 Yamane, Tadros, and Arummugasaamy- Short to Medium Span Japanese Bridges;And El-Remaily, Tadros, Yamane, and Krause - Transverse Design of Box Girder Bridges

Yamane, Tadros, and Arummugasaamy (1994) present the "state-of-the-art" Japanese design and construction bridge practices. Several comparisons are made between Japanese practices and American practices. For instance, the Japanese require the strength of prestressed concrete to be 49 MPa (7100 psi), whereas American girders have a concrete design strengths ranging from 34 to 41 MPa (5000 to 6000 psi). The Japanese tendons used are similar to the American tendons. The major difference in the box girder design is in the shear key design. The Japanese box girders have a full-depth keyway (Figure 2.4). The American design typically uses a 150 mm (6 inch) keyway which is set 150 mm (6 inches) below the top face of the girder. The Japanese design uses a 500 mm (20 inches) keyway that extends to 100 mm (4 inches) above the bottom face of the girder. The Japanese keyway design entails the following; 1) After the girders are placed on the abutments, the ducts between the girders are connected with a pipe. 2) Then tendons are inserted into these ducts. 3) Stay-in-place forms made of thin galvanized steel panels are placed between the girders. This will prevent the keyway grout from leaking through bottom gap. 4) The keyway grout is poured. 5) Once the grout has reached the required strength, transverse post-tensioning is applied. The level of transverse post-tensioning is much higher than that commonly used in the United States.

El-Remaily, Tadros, Yamane, and Krause (1996) proposed a new keyway design based upon the success of the Japanese design. The practices of other countries, (only Japan

is named), were reviewed by the authors. Their investigation revealed that longitudinal shear key cracking is rarely reported in Japan. Design charts and typical bridge details are given showing their recommendations. The following changes are recommended: 1) Use a full depth keyway (Figure 2.4). 2) The girders should contain five rigid diaphragms equally spaced along the length of the bridge-- two at the abutments and three at the quarter points. 3) Provide considerably larger amounts of transverse post-tensioning than is currently used in the United States. The level of post-tensioning is based upon the worst-case assumption that if all the keyways are cracked the bridge will be rigidly connected at the five diaphragm locations. These rigid connections will limit the relative deflection between girders to less than 0.5 mm (0.02 inches), which they claim to be an acceptable amount.

2.4 Gulyas, Wirthlin, and Champa - Evaluation of Keyway Grouts

Gulyas, Wirthlin, and Champa (1995) begin by evaluating properties of non-shrink grouts as dictated by the ASTM specifications. Three following weakness in the specifications are noted; 1) There is no requirement for maximum allowable shrinkage. 2) No requirement for the minimum bond strength. 3) The test for compressive strength of grouts uses a 51 mm (2 inch) square cube whereas the precast concrete test are done on cylindrical specimens.

A series of laboratory test were performed to compare the performance of non-shrink grout with a mag-phosphate grout. The specimen, resembling a typical shear key, consisted of two precast concrete elements joined by the grout under consideration (Figure 2.5) Two shear key sizes were used, the standard 152 mm (6 inch) deep keyway and a 305 mm (12 inch) deep keyway. Three different testing modes were performed; 1) direct vertical composite shear test, 2) the composite direct tension test, and 3) the composite direct longitudinal shear test. (Figure 2.5). The mag-phosphate grout tests were performed with and without the presence of carbonation on the faces of the keyway specimens. In all three test modes as well as the carbonation influenced tests, the mag-phosphate grout produced higher failure loads than the non-shrink grout. In the direct tension test, the failure for the non-shrink grout always occurred at the bond line while the mag-phosphate grout always failed in the substrate. In the vertical shear tests, the non-shrink grout always failed at the bond line while the mag-phosphate grout failed partially through the bond and partially through the substrate. The longitudinal shear test produced erratic failure modes probably due to the built-in eccentricity in the testing procedure.

Next, the shrinkage test following ASTM C157 was performed. The mag-phosphate grout experienced five times less shrinkage than 0.32 water-cement ratio concretes having a 19 mm (0.75 inch) maximum size aggregates. The authors presume that non-shrink grout would shrink more than the 0.32 water-cement ratio concrete because there in no aggregate restraining the grout.

Finally, laboratory tests were performed monitoring a 102 mm (4 inch) cube for chloride absorption. The tests showed that the mag-phosphate absorbed less chloride than a portland cement specimen.

2.5 Lall, Alampalli and DiCocco - Performance of Full Depth Shear Keys in New York

A study was published on the performance of experimental shear keys in New York State (Lall, Alampalli and DiCocco, 1998). All bridges in this study were composite. Prior to 1992, NYDOT used the traditional shear key (same as Ohio) and transverse post-tensioning on bridges longer than 1.5 m (50 ft.) For bridges between 15 m (50 ft) and 23 m (75 ft.), a single post-tensioning strand was used at midspan; bridges more than 23 m (75 ft.) long were post-tensioned at the outer quarter points.

The experimental shear key was the traditional shear key (as used in Ohio), except that an additional 25 mm $\pm$ 5 mm (1" $\pm$ 1/8") width of shear key was extended from the bottom of the normal shear key to within 75 mm (3") of the bottom of the beams. NYDOT also increased the amount of transverse post-tensioning, using 3 tendons in bridges up to 15 m (50 ft.) and 5 tendons for larger spans. The new design greatly reduced cracking.

The study also recommended that, in future bridges, the transverse post-tensioning should be increased, the composite deck reinforcing should be increased (NYDOT currently uses mesh) and that alternate bearing pad placements be considered. The alternate bearing pad placements were: 1) use a full width bearing pad; 2) use of 600 mm 24 in.) bearing pads centered on the joint, i.e. bearing 300 mm (12 in.) on each of two adjacent beams.

(THIS PAGE INTENTIONALLY LEFT BLANK)

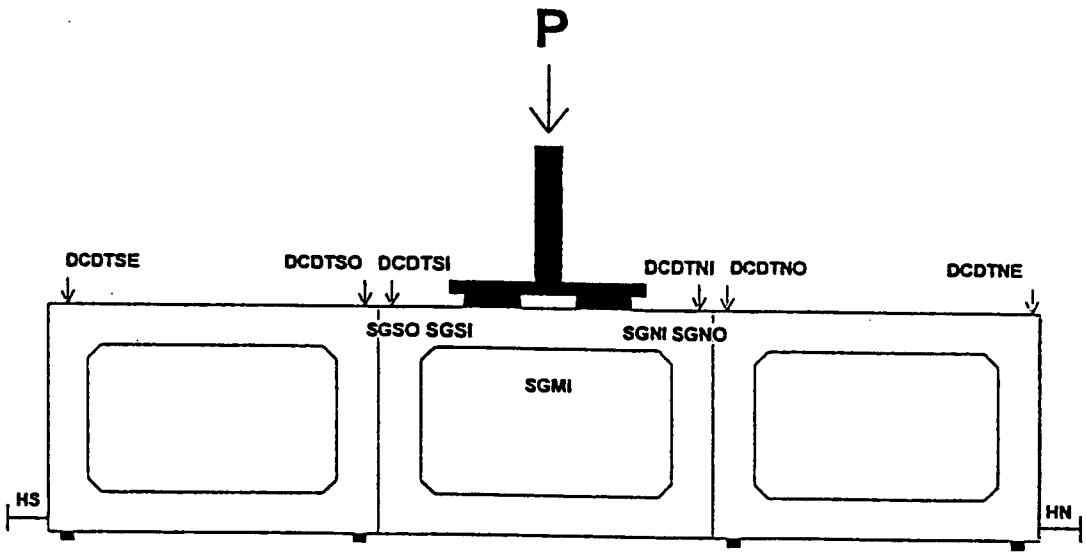

Figure 2.1 Load case used in FE model to determine shear key stresses (From El-Esnawi and Huckelbridge (1996)).

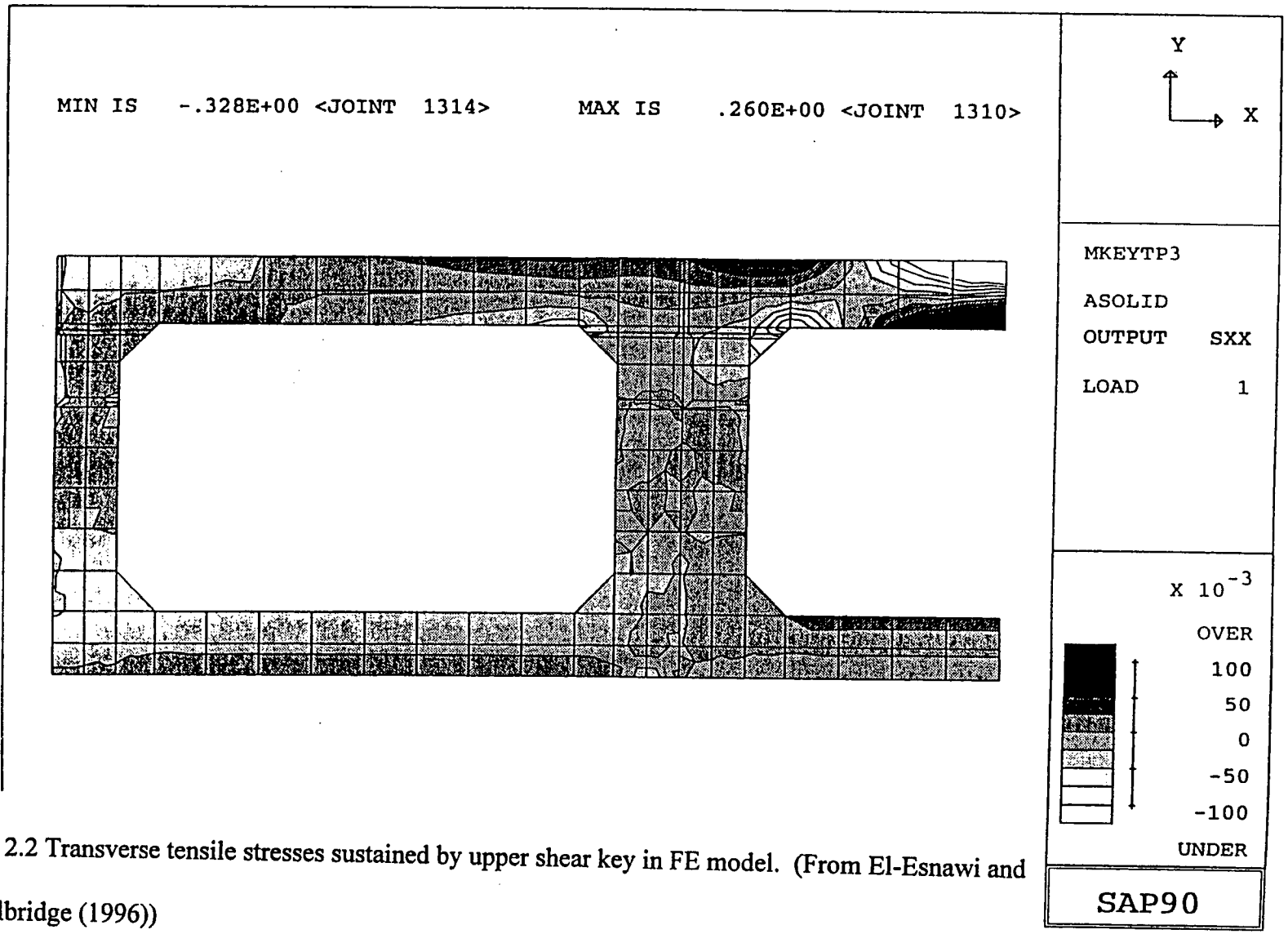

Figure 2.2 Transverse tensile stresses sustained by upper shear key in FE model. (From El-Esnawi and Huckelbridge (1996))

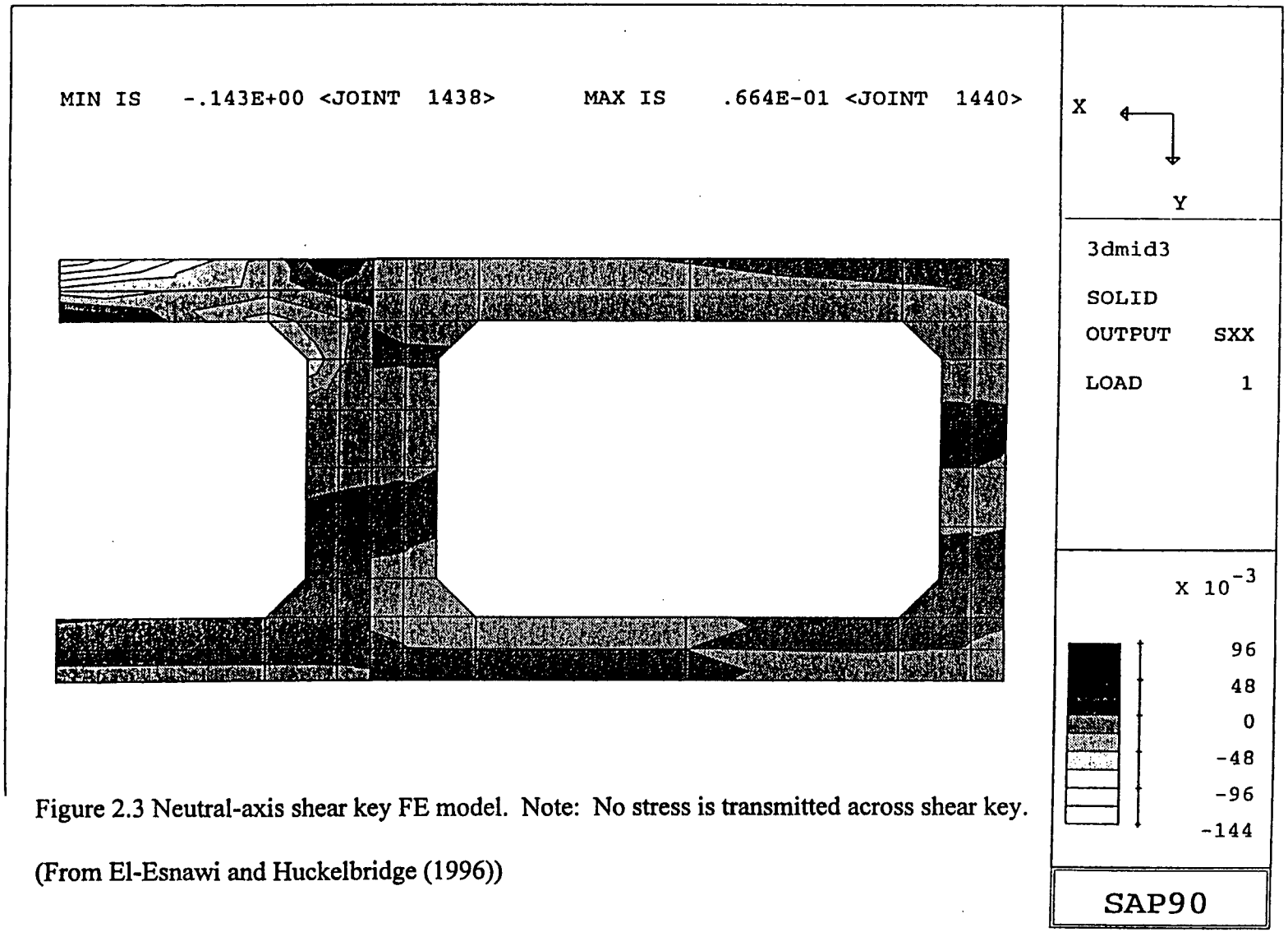

Figure 2.3 Neutral-axis shear key FE model. Note: No stress is transmitted across shear key.

(From El-Esnawi and Huckelbridge (1996))

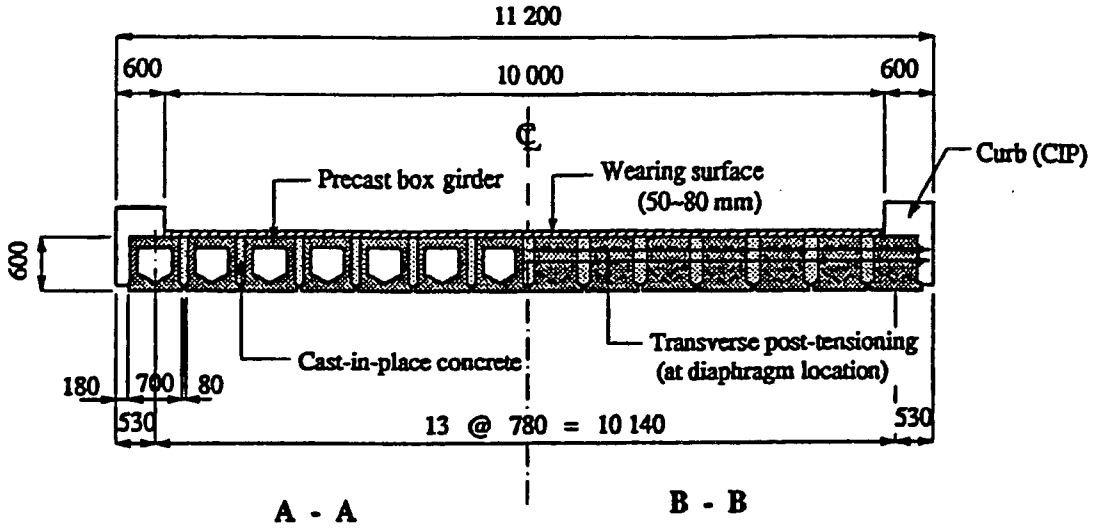

Cross section

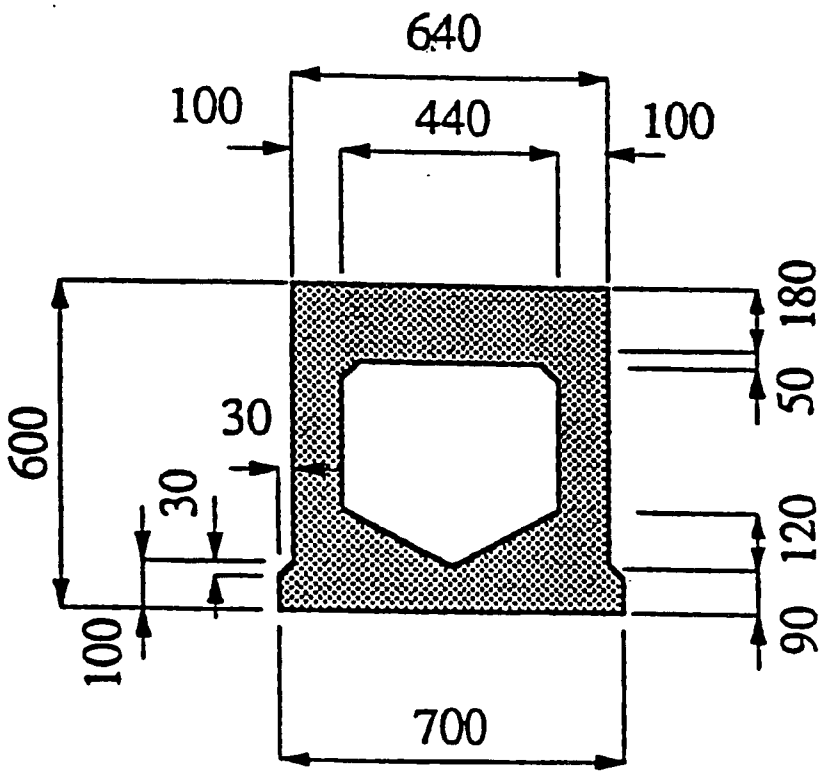

Typical girder cross section

Figure 2.4 Full-depth keyway used in Japan. (From Yamame et. al. (1994))

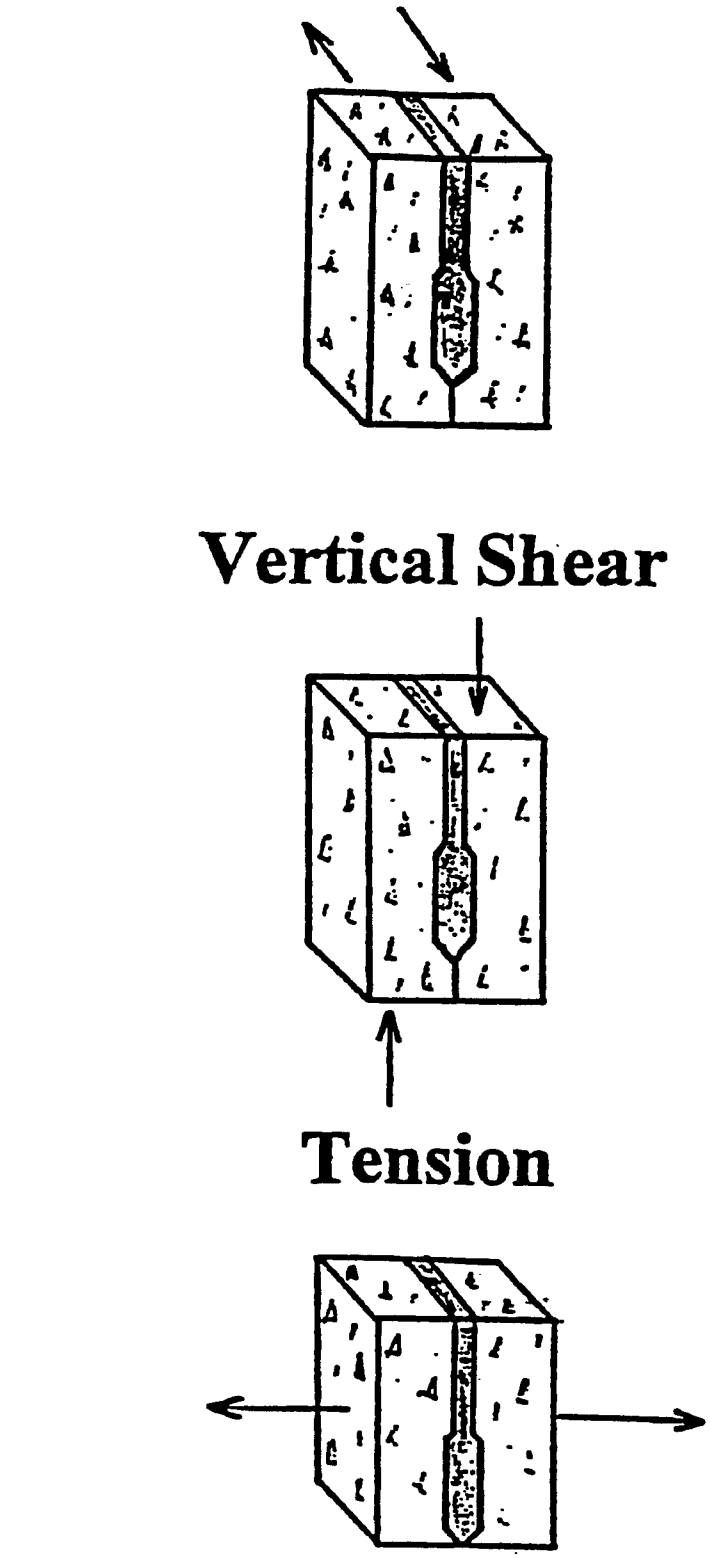

Figure 2.5 Laboratory tests performed by Gulyas et al. (1994)

CHAPTER 3

DESCRIPTION OF THE GIRDERS

AND TESTING FACILITIES

3.1 Description of the Girders

The bridge chosen for this project represented a typical Ohio prestressed adjacent box girder bridge. Prestress Services Inc. of Melbourne Kentucky designed and fabricated the girders using the ODOT specifications in force at the time. AASHTO HS20-44 trucks and the alternate military loading was used for the design live load (Figure 3.1). The bridge consisted of four type B33-48 box beams (Figure 3.2). These beams are 0.838 meters (33 inches) deep and 1.22 meters (48 inches) wide. Each girder is 22.86 meters (75 feet) long, and weighed 245 kN (55 kips). The top flange is 140 mm (5.5 inches) thick, and the bottom flange and the webs are 127 mm (5.0 inches) thick. Each beam has 24 prestressing strands; 22 in the bottom layer 44.5 mm (1.75 inches) from the bottom face, and 2 strands 63.5 mm (2.5 inches) from the bottom face of the girders.

Unlike a typical box girder, these beams were cast with two keyways-- the upper keyway which is 152 mm (6 inches) deep and located 152 mm below the top the beams and the lower (neutral axis) keyway (Figure 1.2) per the recommendations of El-Esnawi and Huckelbridge (1994). The lower keyway was also 152 mm deep and was located 304 mm (12 inches) below the top face of the girders, or directly below the bottom of the top keyway.

3.1.1 Material Properties of the Concrete and Steel

All material properties were as given in ODOT specifications at the time of fabrication:

Minimum concrete strength at release of strand: = 28 MPa (4.0 ksi).
Minimum concrete strength at 28 days := 38 MPa (5.5 ksi)
Strand was (7) wire, uncoated, stress relieved, 12.7 mm (½ inch) diameter, 1850 MPa (270 ksi) ultimate strength (f_{pu}).
Mild steel was grade 60, A.S.T.M. A-615. Yield strength (f_y) of 410 MPa (60 ksi).

During the construction of the each girder, four - 152 x 305 mm (6 x 12 inch) concrete cylinders were made. These specimens were instrumented and tested to determine the ultimate strength as well as the modulus of elasticity of the concrete. To measure elastic modulus, four omega clip gages were placed at 90° intervals around the perimeter at mid-height of the cylinders. The cylinders were then placed in a 1800 kN (400 Kip) Tinius Olsen testing machine and tested until failure. Load data was taken from an internal pressure transducer in the testing machine.

Table 3.1 shows the 28 day compressive strengths and modulus of elasticity for the four cylinders tested. All cylinder strengths exceeded the required strength. The measured modulus of elasticity is based upon averaging the strains from the clip gages (to eliminate any bending effects) and plotting against stress. Modulus of elasticity was measured as the tangent modulus using a linear regression constructed through initial data points. The modulus of elasticity is also calculated from the ACI formula:

$$E_c = 57000(f'_c)^{1/2}$$

The measured modulus of elasticity was 12.7% lower than that predicted by the ACI formula, but variations of ±20% between measured values and the ACI formula are not uncommon, especially for higher strength concrete.

Table 3.1- COMPRESSIVE STRENGTHS OF CYLINDERS

Sample	f'_c	E_c (ACI Formula)	E_c Measured
	MPa (ksi)	MPa (ksi)	MPa (ksi)
#1	56 (8.2)	36,000 (5200)	34,000 (5000)
#2	63 (9.1)	37,000 (5400)	34,000 (5000)
#3	69 (10.1)	39,000 (5700)	33,000 (4800)
#4	67 (9.7)	39,000 (5600)	31,000 (4500)
Average	64 (9.3)	38,000 (5500)	33,000 (4800)

3.1.2 Internal Instrumentation of Box Girders and Keyways

A total of ten vibrating wire gages were placed in the four bridge girders before casting. The gage model used was VCE-4200 fabricated by Geokon Inc. These gages have a gage length of 153 mm (6 inches). Vibrating wire gages contain an internal tensioned wire which is plucked with an electric pulse. As the wire vibrates, the frequency of vibration is measured by a piezoelectric device. Strain in the gage changes the tension of the wire, which in turn changes in the frequency of vibration. Thus strain

can be determined by measuring the difference in frequency. This is done by connecting the gage to a Campbell CR10 Datalogger. Since the frequency of vibration is affected by temperature, the VCE-4200 contains a thermistor, which allows the datalogger software to correct for temperature. According to the manufacturer, these vibrating wire gages are accurate to one microstrain.

Each of the interior beams contained four vibrating wire gages. Two gages were placed 0.61 meters (2.0 feet) on either side of midspan (Figure 3.3). One gage at the level of the prestressing tendons (44.5 mm (1.75 inches) from the bottom face of the girder), and one gage tied to one of the upper longitudinal rebar (64 mm (2.5 inches) from the top face of the girder). The exterior beams contain one vibrating wire gage each (Figure 3.4) -- located directly at midspan and suspended between the prestressing tendons (44.5 mm (1.75 inches) from the bottom face of the girder).

Vibrating wire gages were also placed in the keyways before the keys were grouted (Figure 3.5). Since the model VCE-4200 gages were too big to fit in the keyway, model VCE-4202 gages were used. These gages are only 51 mm (2 inches) long. Shortly before grouting the keyways, several assemblies of these gages were placed in the keyways An assembly consisted of two gages attached perpendicular to each other (Figure 3.6). One gage was hung vertically, and the other was positioned horizontally along the longitudinal axis of the keyway. For the upper keyway test, the gage assemblies were located about 230 mm (9 inches) from the top face of the girder. For the neutral axis keyway, the gage assemblies were located 420 mm (16.5 inches) from the top face of the girder, or directly at the neutral axis of the girders. Tests #1, #2, #3 and #4 had one pair of gages in the center keyway and one pair of gages in the south keyway. Both assemblies were located at the east load point. Tests #2 and #3 had a third assembly in center keyway located at the west load points.

3.2 Testing Facilities

3.2.1 Reaction Frame

The bridge was fabricated, erected and tested on the premises of Prestress Services Inc., Melbourne, Kentucky. A concrete slab cast on a pile foundation was available at the site. The slab had four groups of embedded anchor rods, which had previously been designed for use as tie-downs for a reaction frame. Each of these tie-downs had previously resisted upward vertical loads of over 222 kN (50 kips) (Miller and Parekh, 1994).

Two testing frames were also located on the premisses from an earlier research project. Only one was used for this project. These frames had two W14x30 columns which were 2.74 meters (9 feet) tall and spaced 3.66 meters (12 feet) on center by steel channels (C10x15.3). The columns supported two steel cross beams which had been used to mount hydraulic actuators. The steel channels connected the columns to each other and to a pair of tie downs. Since the bridge for this research project was 4.88 meters (16 feet) wide, the columns could be reused, but the existing cross beams and channels were not long enough. The frame was modified by moving to columns out to a distance of 5.79

meters (19 feet) on center. New channels (C10x20), cross beams (W14x53) and appropriate bracing were fabricated and erected. W18x35 spacer beams were bolted to existing holes in the columns to provide a 1.22 meter (4 foot) distance between the reaction beams. This was done to simulate the wheel spacing of a tandem axle (Figure 3.9). Holes were drilled in the bottom flanges of the W14x53 reaction beams so four hydraulic actuators could be attached -- two on each steel beam spaced 1.22 meters (4 feet) apart (0.61 meters (2 feet) from centerline of the box girder bridge). This distance was chosen so the load would be applied in the center of the flanges of the interior box girders as it was believed that flexure in the top flange of the box contributed to shear key failure (El-Esnawi and Huckelbridge (1994)). Fatigue of the steel beams was also a design considered. They beams were designed according to the AISC Code (9^{th} edition) provisions for a fatigue life of 3 million cycles.

3.2.2 Abutments

Since the test specimen was meant to simulate the center joint in a bridge, the bridge was made with a crown. To achieve this, prestressed abutments were cast at the same time and in the same bed as the box girders (Figure 3.8). However, the abutments were solid slabs, 610 mm (24 inches) high and 5.08 meters (16'-8") long. The prestress force caused a 9.5 mm (0.38 inch) camber to the abutments. This produced the crowning effect desired in the bridge.

The abutments were positioned 22.88 meters (75 feet) apart on center. The beams were placed on the abutments such that midspan of the beams was directly under the center of the reaction frame. Each beam sat on four elastomeric pads-- two at each end as required by ODOT Specifications. The pads are centered about 229 mm (9 inches) from the ends of the beams making the span of the bridge was actually 22.4 meters (73'-6").

3.2.3 Fluid Power Facilities

Load was applied to the bridge using hydraulic actuators. Each had a 101.6 mm (4.000 inch) diameter bore, a 44.45 mm (1.750 in.) diameter rod, and 305 mm (12 in.) of stroke. These actuators were capable of applying 167.8 kN (37.7 kips) push or 135.7 kN (30.5 kips) pull at 20.67 MPa (3000 psi). For this project, they were only used to push down on the bridge. The four actuators were arranged in a square pattern over the two interior box girders. The hydraulic system was configured so that the two north actuators would move in phase and the two south actuators would move in phase. The desired effect was to simulate a truck crossing the bridge with one wheel centered on an interior beam immediately followed by another truck crossing in the opposite direction with one wheel load centered on the other interior beam (Figure 3.9). This was done to achieve a complete load reversal on the center keyway. A wheel load of 89 kN (20 kips) was used because the weight of the design truck (HS20) is 142.4 kN (32 kips), or 71.2 (16 kips) per wheel. An impact factor of 1.25 was used to arrive at 89 kN (20 kips), which corresponds to 44.5 Kn (10 kips) per actuator.

A power unit was used to provide hydraulic power to the actuators. The power unit consisted of a high flow, variable displacement piston pump. The pump contained a type "CM" pressure compensator, which enabled it to provide a continuously modulated flow to meet changing load demands at the pre-adjusted pressure. The pump was capable of producing a flow of 98.4 liters/minute (26 gpm) at 24.98 MPa (3625 psi), however, actual performance was limited by the motor power output. With the provided 29.8 kW (40 hp) motor, the pump could produce a flow of 71.5 liters/minute (18.9 gpm) at 24.98 MPa (3625 psi).

The flow to the actuators was split and controlled by two Vickers SM4-10 electro-hydraulic servo valves (Figure 3.10). Each could provide a precisely modulated flow of up to 37.85 liters/minute (10.00 gpm). One valve provided fluid to the two actuators over the north interior beam (beam #2). The other valve controlled the two actuators over the south interior beam (beam #3). A Vickers high pressure filter was used to provide the necessary fluid cleanliness levels required by the servo valves. This filter was sized for the pump's maximum flow rate.

A servo valve controller was fabricated by technicians at the University of Cincinnati. The controller consists of a variable time-delay relay controller, current amplifier, a potentiometer, two relays, a counter, and a cooling fan. The two servo valve cables could be plugged into the ports so that the servo valves would produce a flow in phase with each other or the cables could be plugged in such that the servo valve produced a flow π radians (180 degrees) out of phase. This allowed for both beams to be loaded together or be loaded separately to achieve load reversal in the keyway.

3.2.4 Data Acquisition Systems

The vibrating wire gages were monitored using a CR10 Datalogger made by Campbell Scientific Inc. The wire leads from each gage were hooked into ports on a sixteen-channel multiplexer which the CR10 controlled. It took about 23 seconds for the multiplexer to cycle through all sixteen channels. Due to the relatively slow speed of this system, the vibrating wire gages could only be used for static testing and long term monitoring of the bridge. The CR10 was connected to the COM port on an IBM compatible computer to download data. Software provided by Geokon Inc. was used to interface the IBM computer with the CR10.

The CR10 datalogger required DC power, so a standard automobile battery was used to provide 12 volts to the CR10. By using battery power, the CR10 could monitor gages over long periods of time when the researcher could not visit the bridge site. Also, use of a battery made the unit portable so strain in the beams could be measured during curing.

In addition to vibrating wire gages, direct current linear variable differential transformers (DCDTs), and wire potentiometers were used at various times to measure deflections. Omega strain gages were used to measure dynamic concrete and shear key strains and crack openings. All gages were monitored using two, Strawberry Tree data acquisition cards. Each card monitored sixteen channels and was plugged into a separate IBM compatible computer. Two computers were necessary in order to collect data at

rates up to 10 hertz. Raw data was collected in ASCII format and processed using a spreadsheet. These gages were powered with 10 volts of DC electric power from a very precise power supply.

3.2.5 Crack Measurement System

3.2.5.1 Pulse Velocity Method

The pulse velocity method was first used by Leslie and Cheeseman (1949) to detect and measure cracking. Today, commercially available low frequency ultrasonic test systems can be used directly to measure the velocity of a pulse transmitted through a porous material such as concrete. These systems use a transmitter, which is a sending transducer that transfers ultrasonic energy pulses to the concrete, and a receiver, which captures the first received signal. The system then displays the transit time of the pulse through the concrete. A meter with 150 kHz transducers was used to determine when cracks occurred in the shear key at the interface between the side of the box girder and the adjacent grout.

At the time of the first test, the concrete in the beams was 5 months old and the physical properties of the concrete were not changing significantly with time. Therefore, the pulse velocity in the concrete material did not change appreciably throughout the testing program. Any changes in the transit time of a pulse across the shear key joint at a specific location along the beam could then be attributed to an increase in the transit length of the ultrasonic pulse. These changes in the transit time are the result of the inability of the ultrasonic pulse to transmit energy across a concrete-air interface, such as a crack, thereby requiring the diffraction of the pulse around the periphery of the crack. As illustrated in Figure 3.11 this results in a transit time that increases as the depth of the crack increases. A crack totally through the depth of the shear key could not transmit a pulse and is identified by an infinite transit time.

Transit time measurements were taken by placing the sending and the receiving transducers on either side of the shear keyways at 0.90 m (3 feet) intervals along the three longitudinal joints between the four box girders. The transducers were mounted in a fixture that kept the transducers 75 mm (3 inches) apart, but allowed for rotation so that the transducers would be able to uniformly contact the concrete surface of the top of the box girders on both sides of the shear key. A 22 N (10 lb) weight was applied to the fixture to assure uniform and consistent contact pressure. The concrete surfaces at the test positions were ground flat and wax pads were used to facilitate the coupling of the transducers to the concrete. While it is possible to use this procedure to estimate the actual depth of a crack visible at the surface, the technique is used here to qualitatively determine whether the shear key has cracked. The cracks were divided into four types: superficial cracks which occurred only on the surface and caused no appreciable increase in transmission time; moderate cracks, which showed some increases in transit time; severe cracks, which had very large transit times and cracks which completely penetrated the shear key and had an infinite transit time. Sound concrete and concrete with superficial cracks (< 3 mm) had pulse transmission times of less than 50 ms. Moderate

cracks were arbitrarily defined to be pulse transmission times between 50 ms and 500 ms. A severe crack had pulse transmission times over 500 ms. Completely cracked keyways had infinite pulse transmission times.

3.2.5.2 Dye Penetration

Dye penetration was used as a second method of crack detection to verify the pulse velocity method results. The dye penetration method has been successfully used to measure crack propagation (Swartz, 1991). The drawback to this method is that only cracks wide enough to allow admission of the dye are detected whereas pulse velocity will detect much thinner cracks. Some difference in the results obtained between the dye penetration and the pulse velocity methods were expected.

Since the major problem with cracks in shear keys is leakage, only cracks which admit water are of concern. A standard fabric dye was chosen since it was water based and would detect those cracks which could be penetrated by water. After drying, the dye was semi-permanent and did not easily wash out so the penetration of the dye could be seen when the beams were separated after the tests. However, after separation of the beams, several weeks of weathering and a light sandblasting removed the dye for the next test.

The first dye used was black and successive dyes were of lighter colors. The purpose of using lighter colors is that they will not dye over the existing darker color and will only color new areas exposed by the crack. Crack propagation is seen as an advancing line of successively lighter colors.

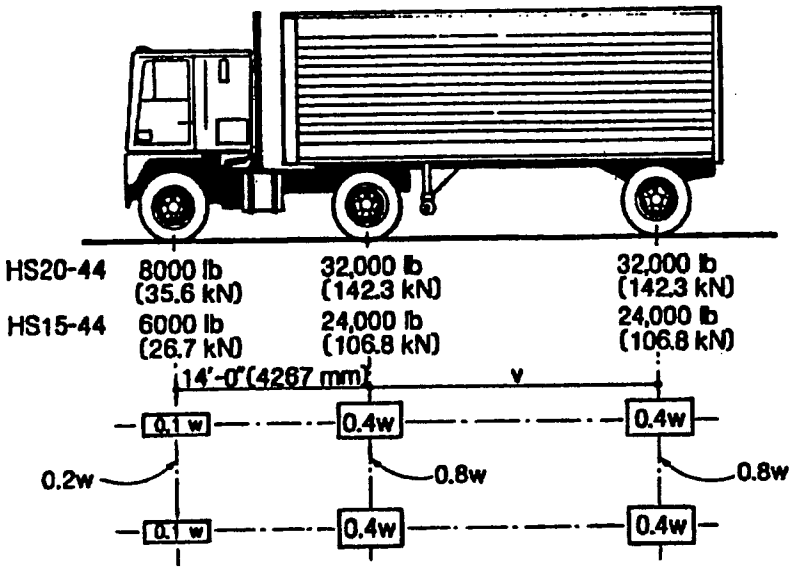

w = combined weight on the first two axles which is the same as for the corresponding H truck.

v = variable spacing-14 feet(4267 mm) to 30 feet(9144 mm) inclusive -spacing to be used is that which produces maximum stresses.

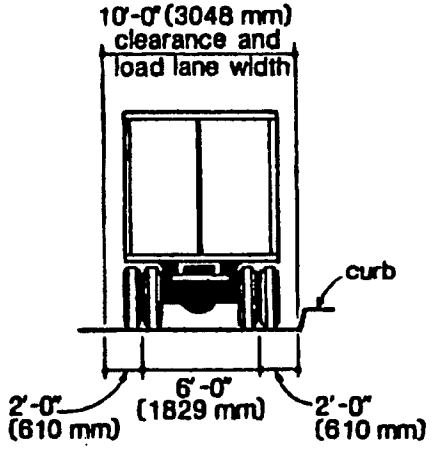

standard HS trucks

Figure 3.1 AASHTO Standard HS Truck

(From AASHTO(1992))

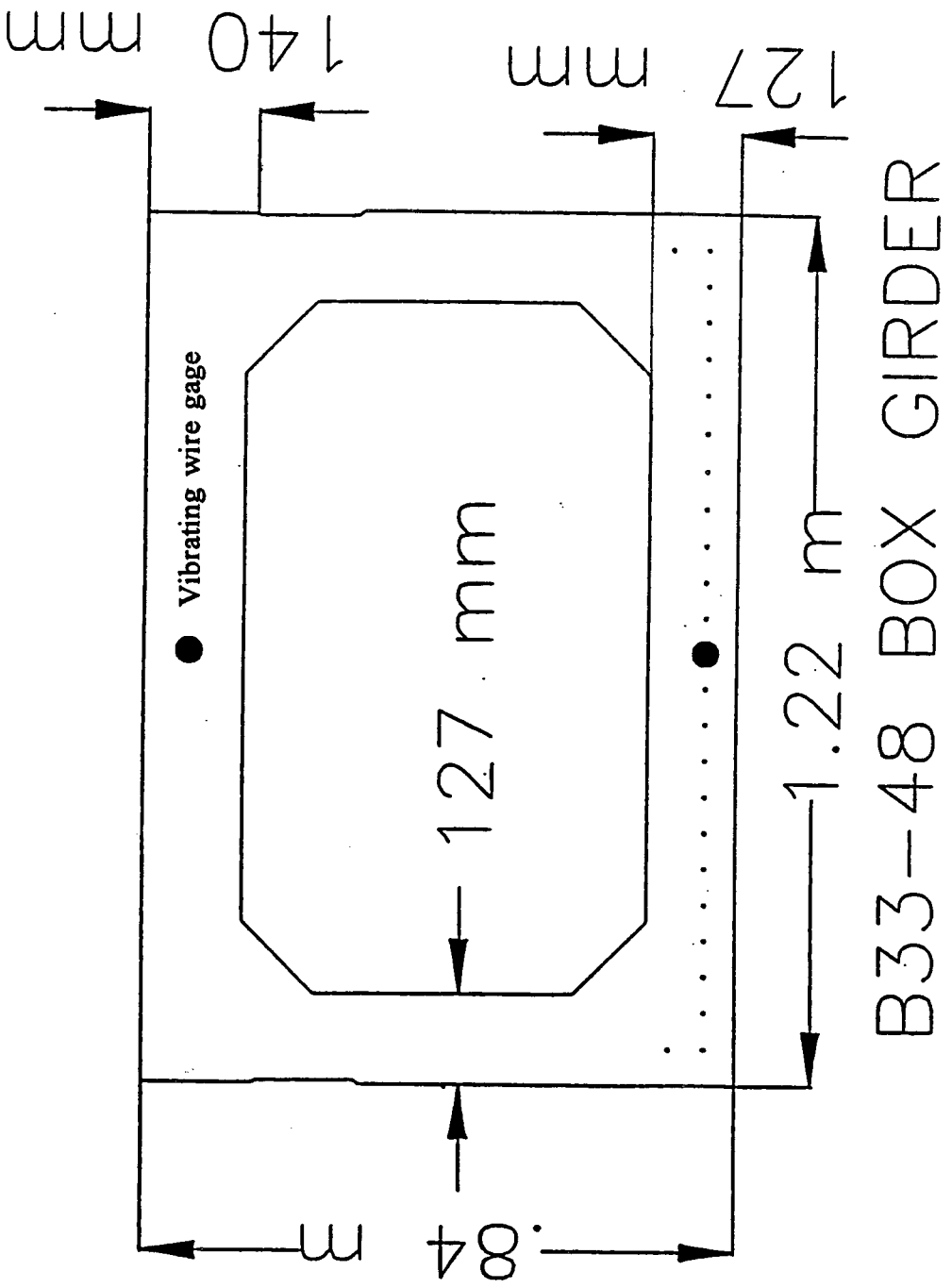

Figure 3.2 Cross section of B33-48 box girder.

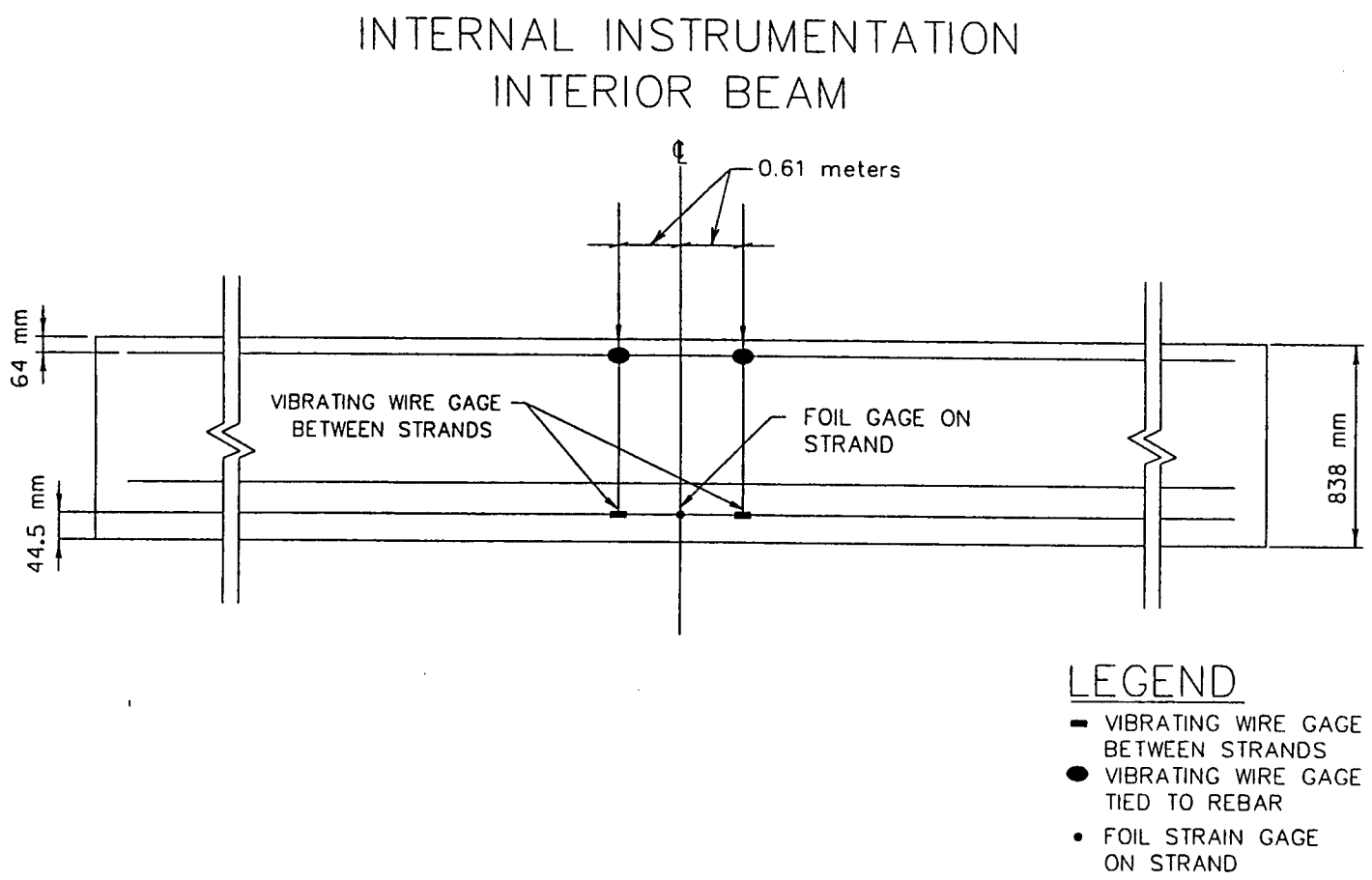

Figure 3.3 Location of vibrating wire gages in interior girders.

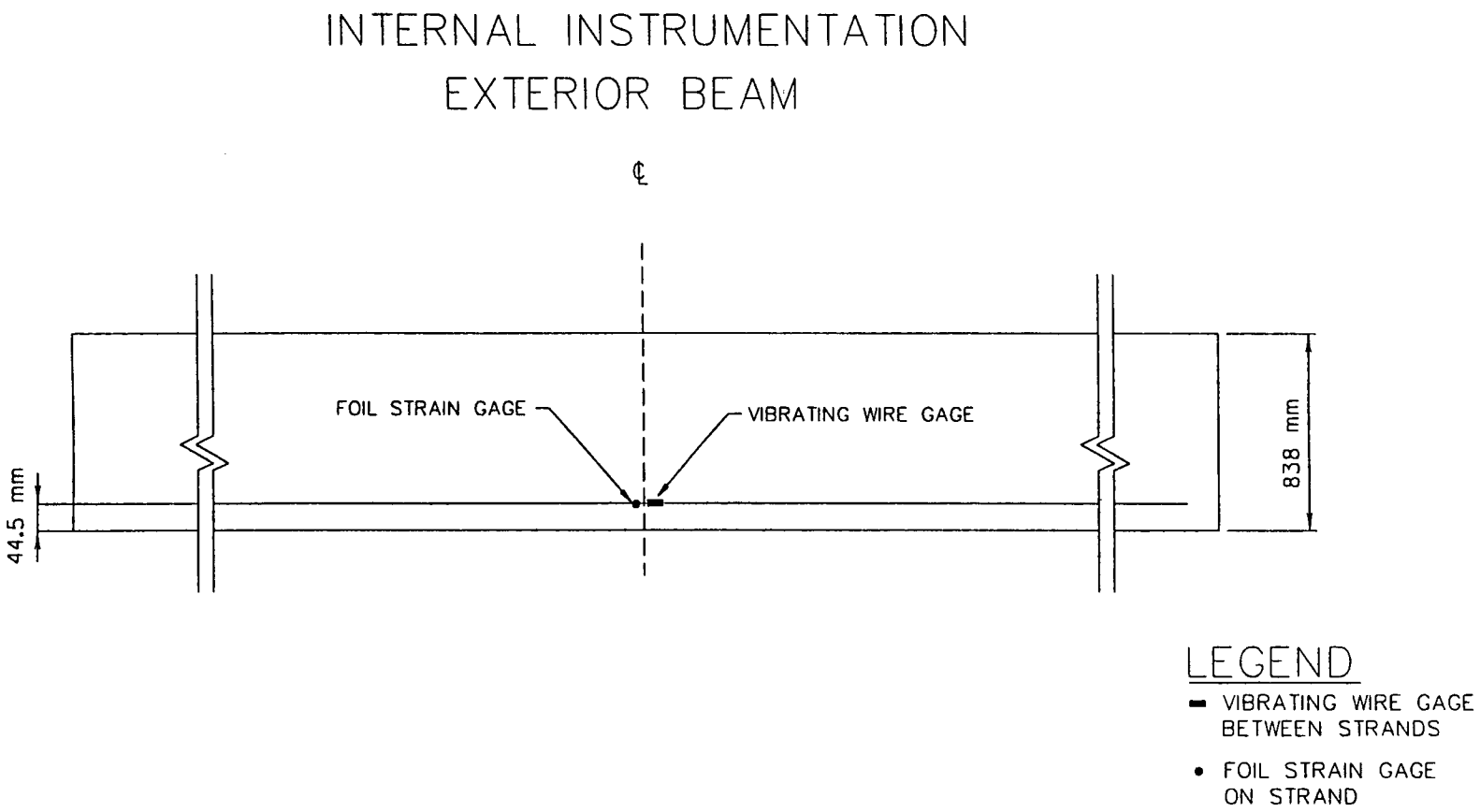

Figure 3.4 Location of vibrating wire gages in exterior girders.

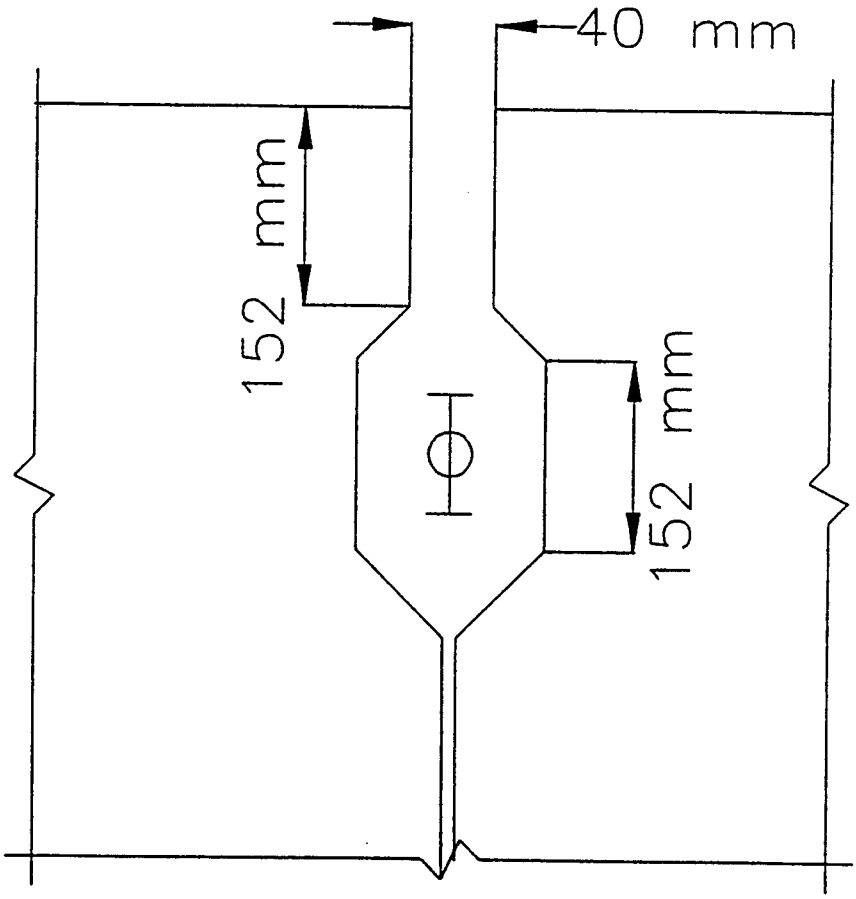

Figure 3.5 Location of keyway vibrating wire gages.

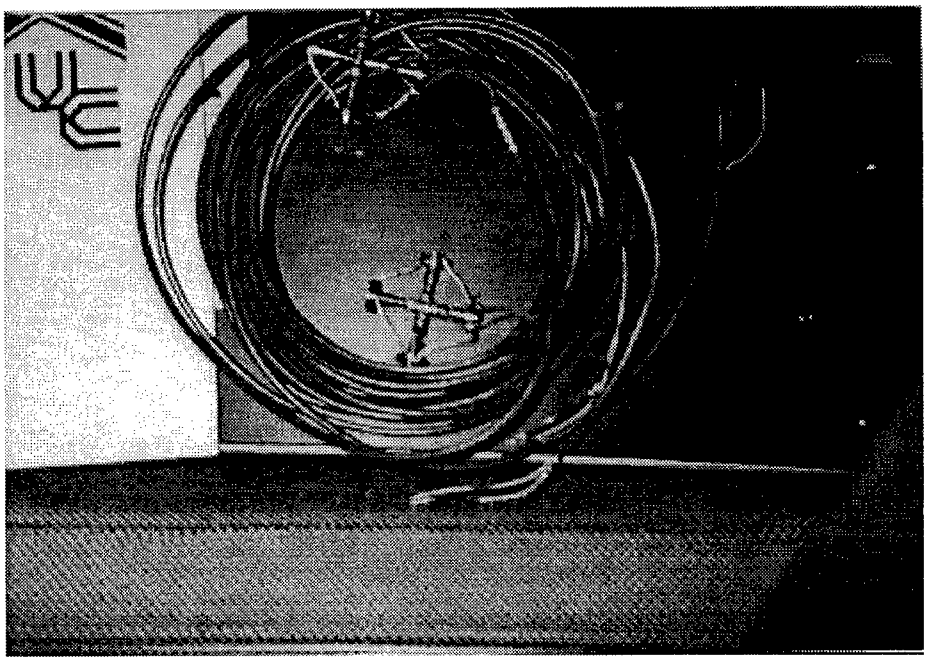

Figure 3.6 Photograph of the keyway vibrating wire gage assembly.

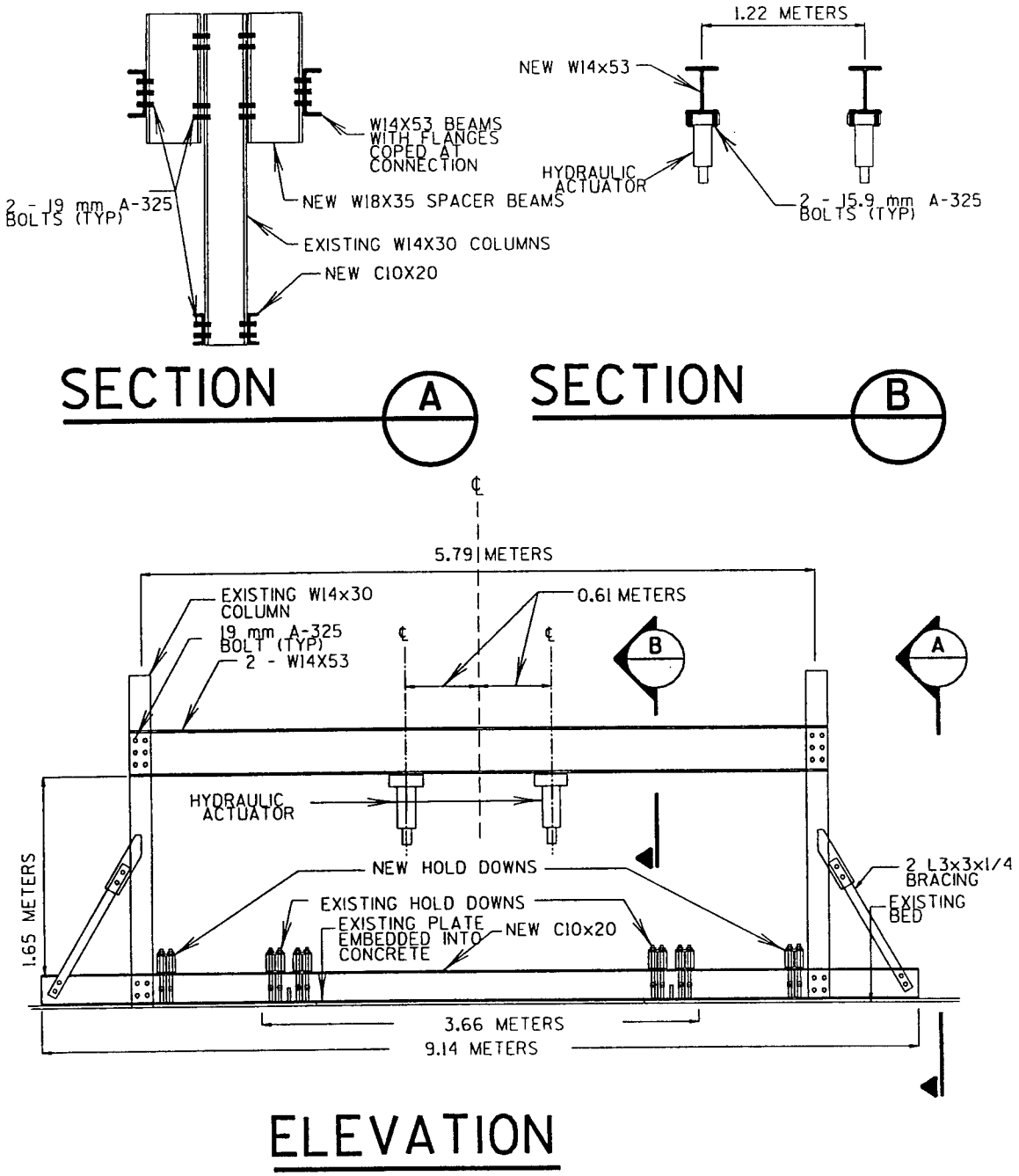

Figure 3.7 Elevation and sections of steel reaction frame.

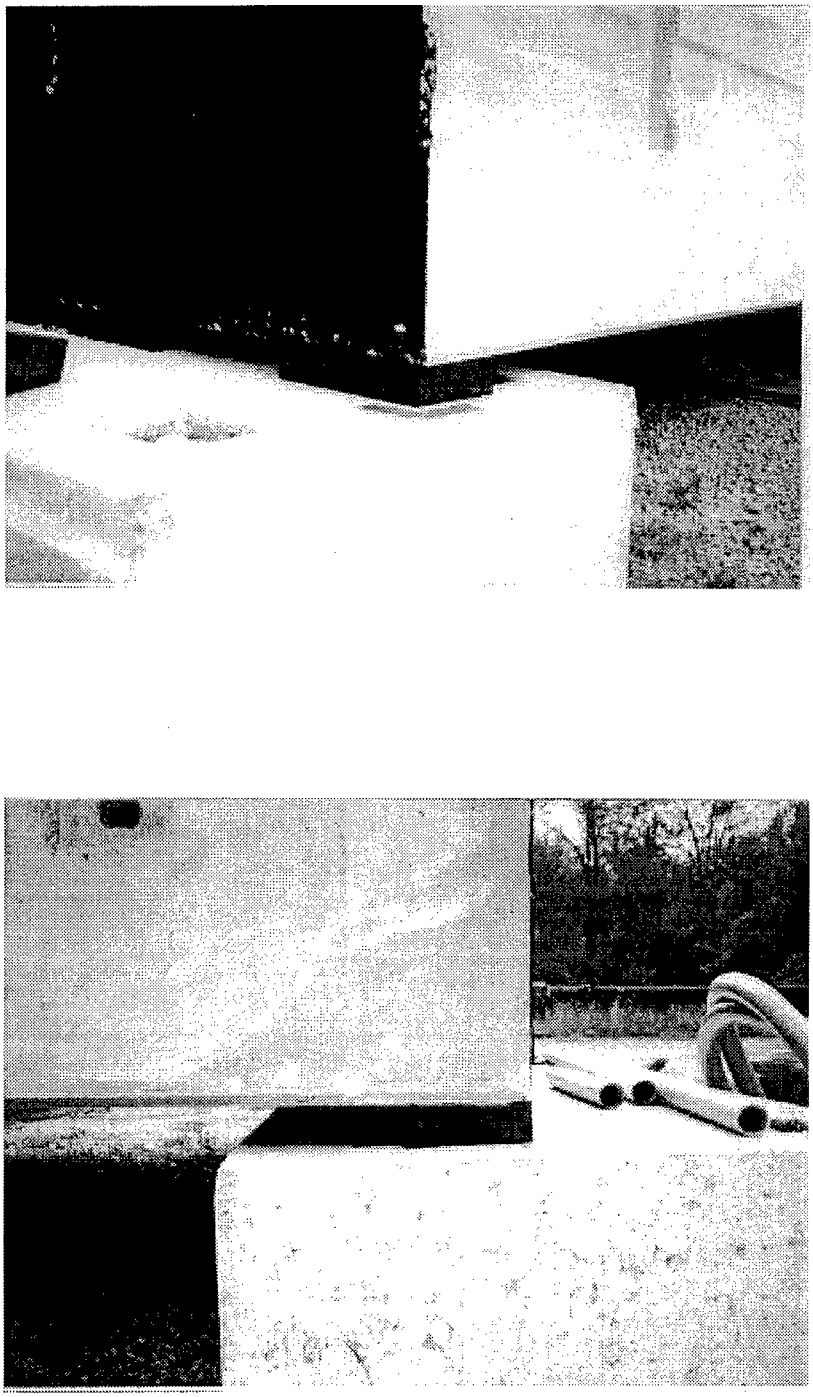

Figure 3.8 Photographs of the bridge abutment.

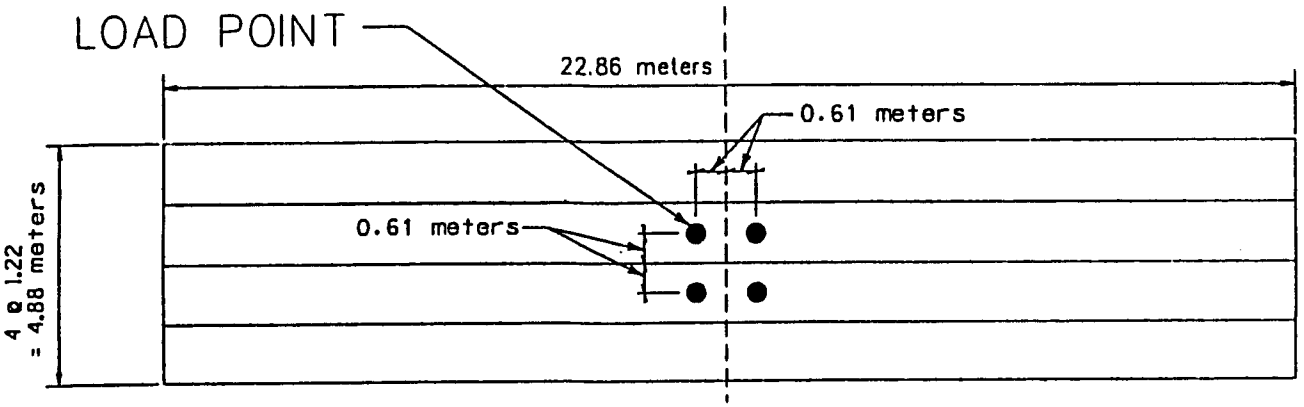

HYDRAULIC ACTUATOR CONFIGURATION

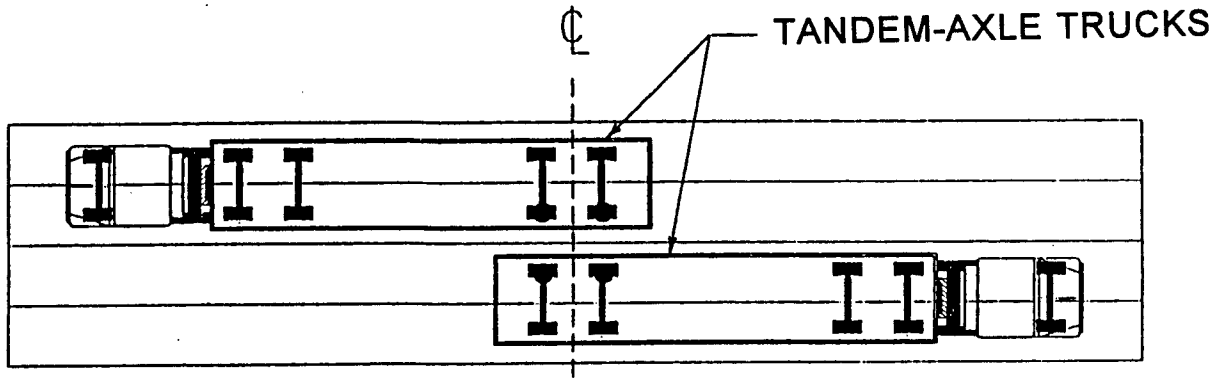

HS20–44 TRUCK SIMULATED LOAD

Figure 3.9 Simulated Truck Loading

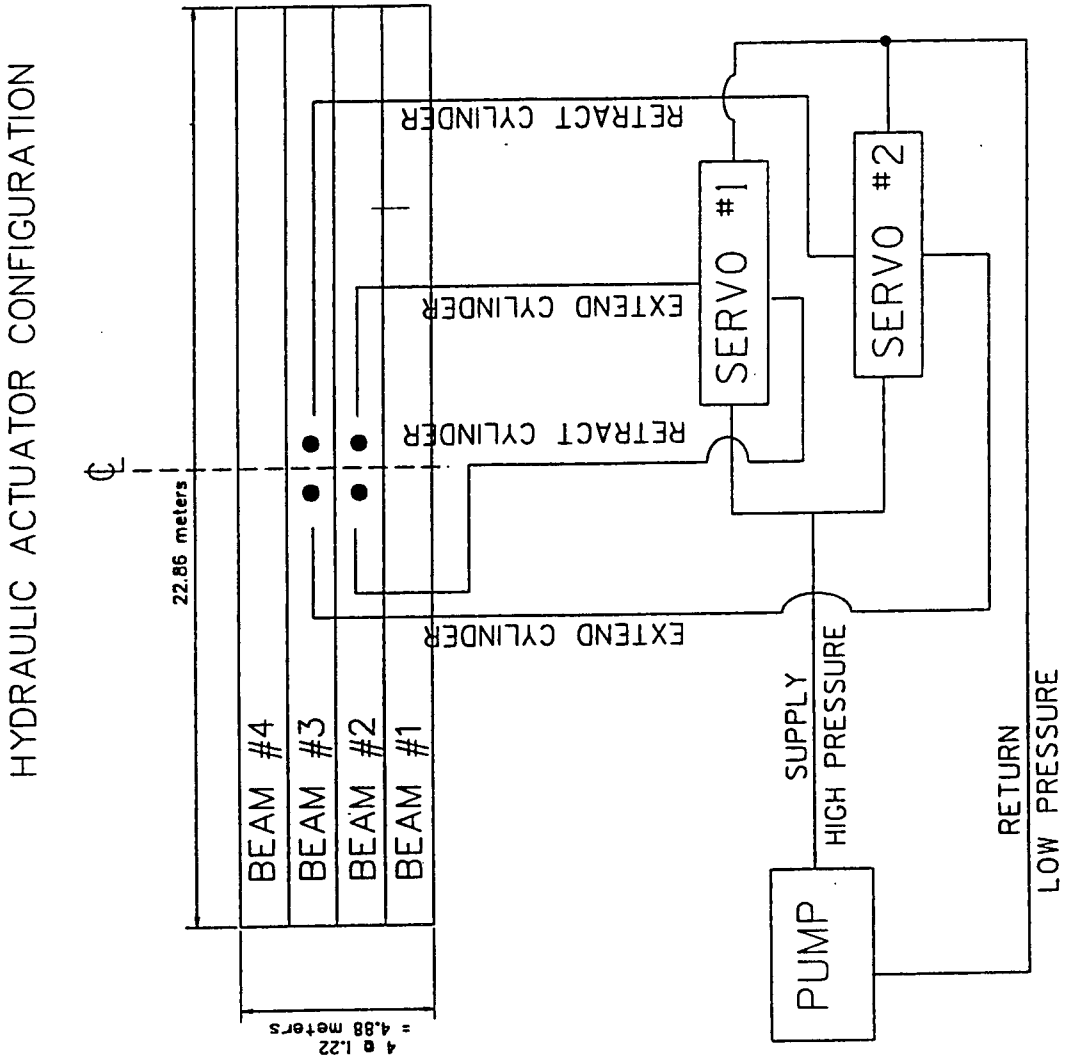

Figure 3.10 Hydraulic power system configuration.

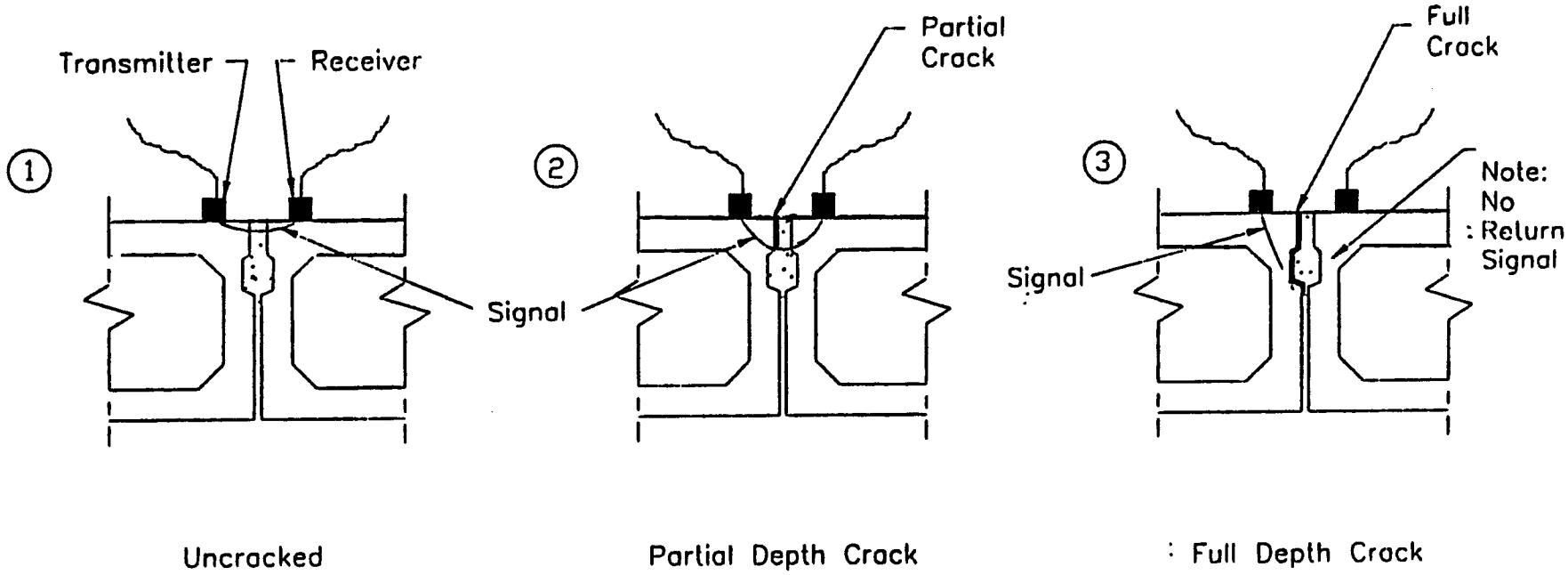

Figure 3.11 Pulse velocity crack detection system.

CHAPTER 4

CONSTRUCTION OF THE BOX GIRDERS

4.1 Construction Strains of Box Girders

During the fabrication of the prestressed concrete beams, instrumentation was installed so that the initial condition of the beam could be determined and any changes in the beams which occurred during testing would be detected (instrumentation described in Chapter 3).

The tendons were prestressed with a hydraulic jack with a stroke capacity of approximately 2 meters (6 feet). Since the strands are stress relieved, they were pulled to 70% of their ultimate strength (0.7 f_{pu}), or 129 kN (28.9 kips) per tendon. Total load in the tendon was determined by the use of a pressure cell on the jack, however, due to friction in the system the reading may not be totally accurate, so the actual elongation of the tendon was checked against the calculated approximate elongation of the tendon under the pretensioning load. During fabrication, all elongations were within tolerance.

Foil strain gages were also placed on the strands to determine the amount of prestress. These gages were placed on one of the wires of the seven-wire tendons and were therefore skewed about 25 degrees from the longitudinal direction. The amount of strain would have been expected to be around 6630 microstrain if the gages had been parallel to the stands. Lower strain values were expected due to the skew of the gages. Multiplying 6630 by the cosine of 25 degrees yields the expected strain of 6010 microstrain (Appendix A). In each girder two tendons were gaged. Table 4.1 shows the measured strains during the prestressing procedure. Strain values measured in the tendons ranged from 5700 to 6004 microstrain and are considered reasonable.

In an attempt to measure loss of prestressing force, readings from the vibrating wire gages in the girders for the second pour (girders interior #2 and exterior #2) were monitored at several intervals. Readings were taken before the concrete was poured, after the concrete was poured, before prestressing strands were cut, after the prestressing strands were cut (See Table 4.2), after the beams were moved into the curing yard, and about three times per week thereafter. Foil gages were also monitored before and after the prestressing tendons were cut (Table 4.3). The foil gages in only one girder (Exterior 1) functioned properly (these gages are easily destroyed during the process of pouring concrete). Tables 4.2 and 4.3 show good agreement in measured strains.

A Geokon GK-403 readout box was used to perform the initial readings on the vibrating wire gages. After about one month, the girders were moved into position on the abutments and the vibrating wire gages were measured using the CR10 datalogger.

Table 4.1- Prestressing Strains Measured by Foil Gages Bonded to Tendons

BEAM	CHANGE IN STRAIN (MICROSTRAIN)
INTERIOR 1 (BEAM #3)	5920
EXTERIOR 1 (BEAM #1)	6004
EXTERIOR 1 (BEAM #1)	5957
INTERIOR 2 (BEAM #2)	5700
INTERIOR 2 (BEAM #2)	5909
EXTERIOR 2 (BEAM #4)	N/A
EXTERIOR 2 (BEAM #4)	5880

Table 4.2 - Change in Strain Before and After Cutting Tendons Measured by Vibrating Wire Gages at the Level of the Tendons

GAGE	CHANGE IN STRAIN (MICROSTRAIN)
INTERIOR 2A TOP	-261.4
INTERIOR 2A BOTTOM	-251.1
INTERIOR 2B TOP	-254.2
INTERIOR 2B BOTTOM	-211.5
EXTERIOR 2 BOTTOM	-236.8

Table 4.3 - Change in Strain Before and After Cutting Tendons Measured by Foil Gages Bonded to the Tendons

GAGE	CHANGE IN STRAIN (MICROSTRAIN)
EXTERIOR 1 TENDON 2	-240
EXTERIOR 1 TENDON 3	-255

4.2 Long Term Strains

Figures 4.1 and 4.2 show the vibrating wire gage data over a period of about 16 months. Figure 4.1 is typical for a gage located 63.5 mm (2.5 inches) from the top of the girder while figure 4.2 is typical for a gage 44.5 mm (1.5 inches) from the bottom face of the girder. Positive values indicate expansive strains while negative strain indicate compression. Zero microstrain is arbitrarily defined to be the strain in the wet concrete immediately after pouring. The initial jump of about -500 microstrain is the change in strain due to the cutting of the prestressing tendons (Tables 4.2, 4.3) and subsequent strains which occur during the first few days (mostly creep and shrinkage). These strains appear together as a jump due to the x axis scale.

Prestressed concrete is known to experience changes in strain due to creep, shrinkage and relaxation of the tendons; therefore, it was expected that the concrete strains would change slowly with time. These changes could be used to measure loss of prestressing force. However, Figures 4.1 and 4.2, show a much different trend There are large variations in daily strains and an overall seasonal change in the strain patterns. These changes are inversely proportional to the temperature of the concrete. Some strain change due to thermal expansion and contraction is expected, but these girders experience a thermal gradient. During the day, the top of the beam is heated directly by the sun while only the increasing air temperature heats the bottom. As a result, the top of the beam gets much hotter than the bottom (Figures 4.1 and 4.2) and expands more. This creates a differential strain field as the top of the beam attempts to "pull" on the bottom and the bottom of the beam restrains the top. The strain field is further complicated by the supports which provide some measure of frictional restraint against expansion and contraction. The net effect is an increase in compressive strain when the beam heats up and a decrease in the compressive strain when the beam cools. These temperature strains are so large (perhaps as much as 250 microstrain over a year) that they mask out any strain attributable to loss of prestress (which would be on the order 40-50 microstrain). Figures 4.1 and 4.2 also show that loss of prestressing force is probably transient. Since the temperature gradient will affect both the concrete and steel stresses, loss of prestressing force would seem to vary with time and temperature.

The differential heating also causes the girder to change camber. Daily changes in camber of 13 mm (0.5") were not unusual. Thus, the behavior of the beam is highly dependant on temperature response.

4.3 Static Testing of Individual Girders

Before grouting the first set of keyways, the individual girders were load tested. The goal of this test was: 1) To find the load vs. deflection characteristics of each girder. 2) To determine the load vs. strain characteristics of the embedded gages. Load was applied to each beam by using two single-acting Enerpac hydraulic jacks. A hand-pump was used to provided fluid pressure to the jacks. The jacks were seated on bearing pads on the girders and pushed up on the reaction frame. Load was applied in 6.40 kN (1.44 kip) increments up to 32.1 kN (7.22 kips) per jack. Every increment, the load was held long enough to read the vibrating wire gages.

Under each girder, three wire potentiometers were mounted, one at each of the quarter points and one at midspan. The internal vibrating wire gages and any working foil strain gages were monitored. A 400 kip load cell was placed on a bearing pad that was seated on the top of the girder to measure load.

The strains in the vibrating wire gages closely matched those strains observed in the foil gages. The wire potentiometers provided similar load vs. deflection curves for the four girders. Figure 4.3 shows a typical load vs. deflection profile from this test. Since the beam remained in the linear range, stiffness is the slope of the graph. An average stiffness value of 7.3 kN/mm (41.7 kips/inch) was determined from the slope of the load vs. deflection graphs. Using the load/deflection data, a value of the modulus of elasticity of the girders was calculated ($E = PL/48\delta I$). The calculation for E is shown in Appendix B. The calculated values of E are higher than those measured from the cylinders. However, some variation is not unexpected. This is because:

1) The beams are made of many different batches of concrete, the cylinders come from a single batch. Batch to batch variations of $\pm$ 10% are not uncommon and variations of $\pm$ 20% are not unreasonable.
2) The concrete at the time of static testing was older than the cylinders (which were tested at 28 days), so some increase in E is expected;
3) The calculation of E from load/deflection data required the use of the moment of inertia, I, which was taken from the ODOT standard drawings and is based on nominal dimensions. The actual value of I will vary slightly from the published value.

However, the values of E calculated from stiffness are still in reasonable agreement with the cylinder values and can be used for subsequent calculations.

Table 4.4 Midspan Stiffness of Individual Girders

GIRDER	STIFFNESS (FROM GRAPHS)	E (CALCULATED FROM STIFFNESS)
	kN/mm (k/in)	MPa (ksi)
EXTERIOR 1 (BEAM #1)	7.21 (41.2)	37,100 (5,380)
INTERIOR 1 (BEAM #3)	6.86 (39.2)	35,300 (5,120)
INTERIOR 2 (BEAM #2)	7.60 (43.4)	39,100 (5,670)
EXTERIOR 2 (BEAM #4)	7.53 (43.0)	38,700 (5,610)

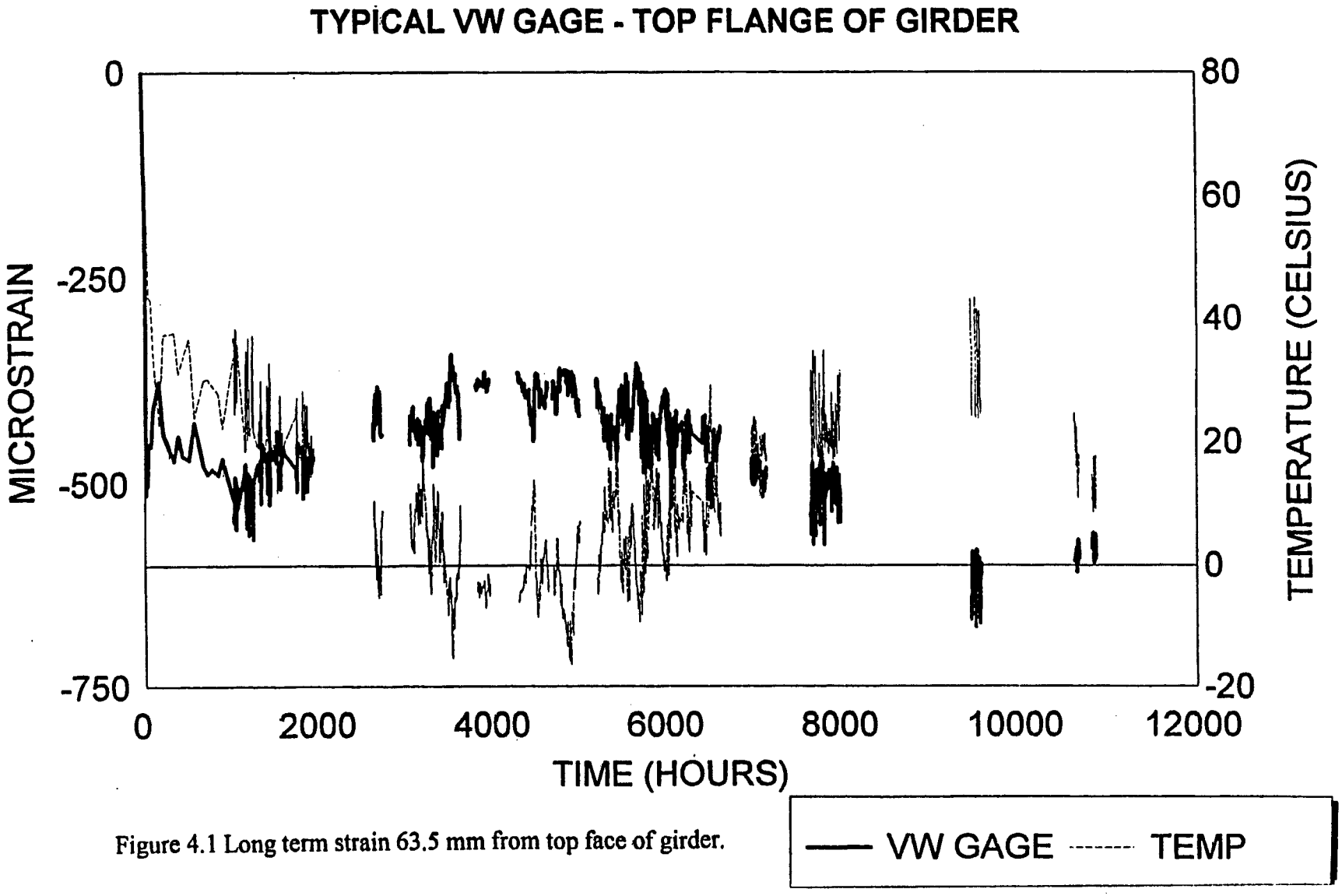

Figure 4.1 Long term strain 63.5 mm from top face of girder.

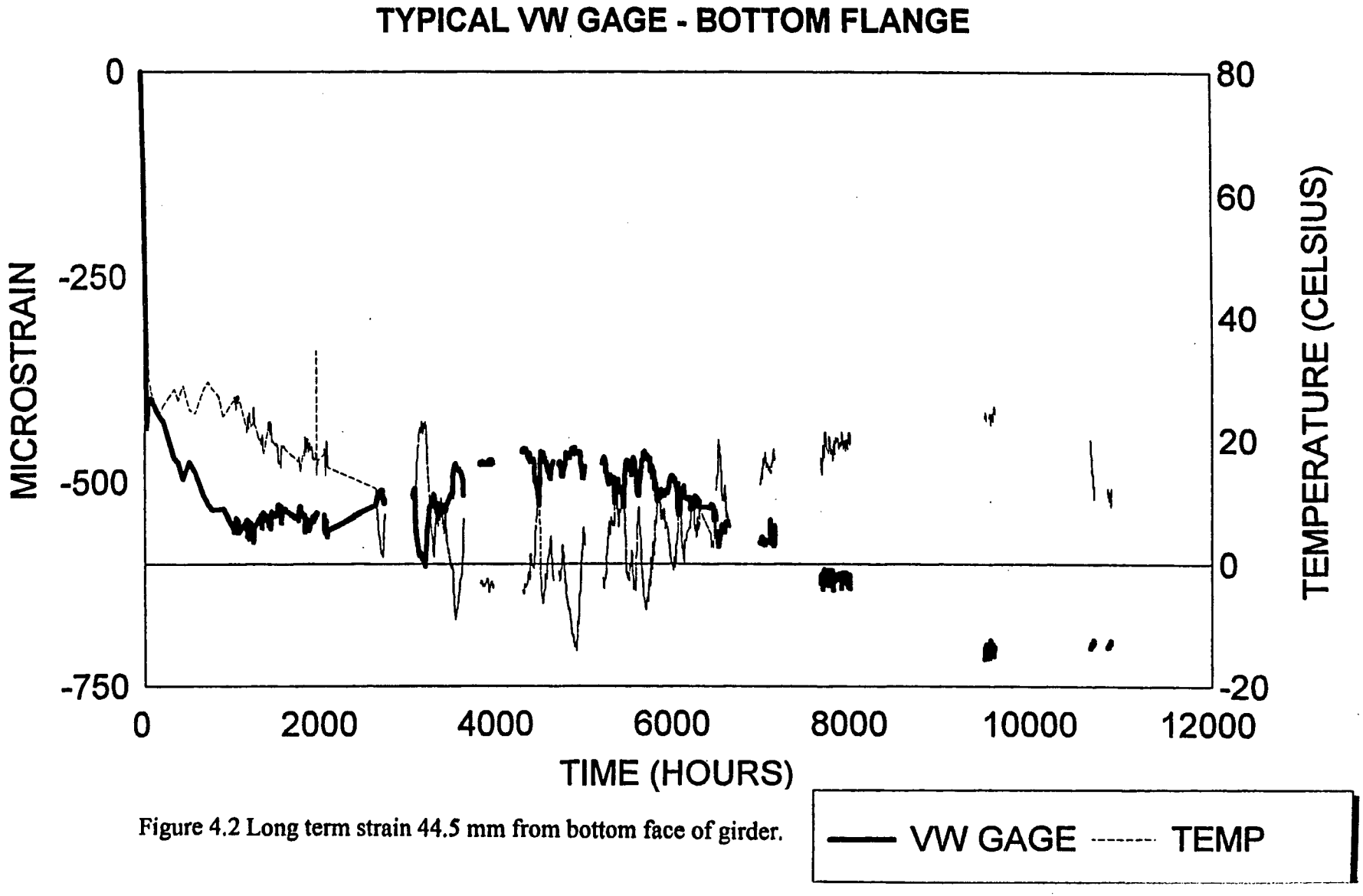

Figure 4.2 Long term strain 44.5 mm from bottom face of girder.

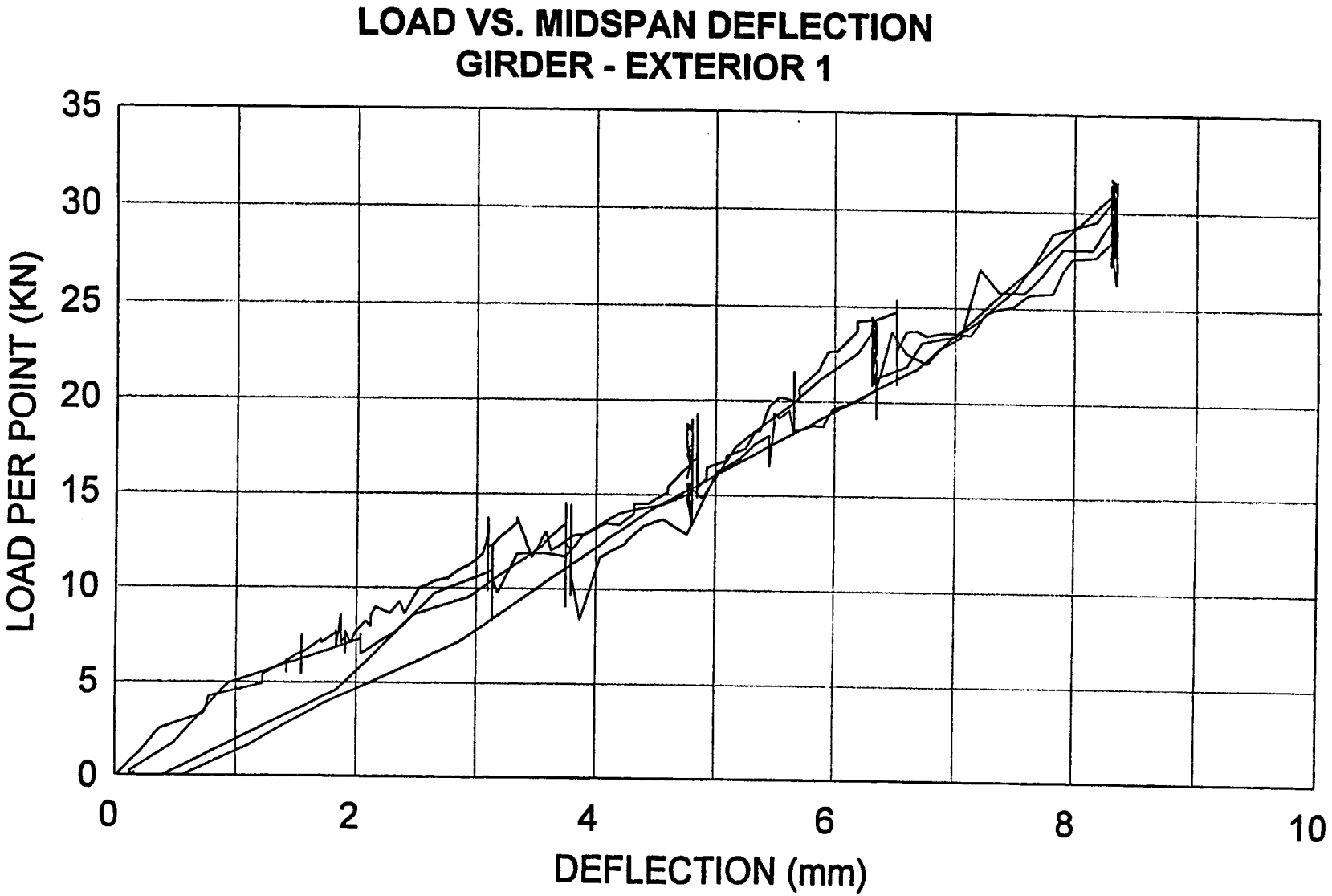

Figure 4.3 **Load Vs. midspan deflection for typical static test of individual girder.**

CHAPTER 5
DYNAMIC LOAD TESTING OF THE BRIDGE

5.1 Objective

The objective of load testing was to monitor the response of the shear keys to simulated truck loading. Hydraulic actuators mounted on a steel reaction frame were used to simulate the wheel load of an truck on both of the interior girders passing at the rate of one every 0.9 seconds (a complete cycle of loading each beam once took 1.8 seconds). At various intervals the loading was stopped and the condition of the shear keys was checked. Static (slow) tests were also performed periodically so that the vibrating wire gages could be monitored. Dynamic monitoring of the vibrating wire gages was not possible because the data acquisition system used for the vibrating wire gages was only capable of monitoring a gage about three times per minute. Another purpose of the static tests was to be able to obtain data from the other instruments free of the noise cause by the harmonic oscillations of the bridge. Static tests were performed after completing approximately the following number of cycles: zero, 100, 1,000, 5,000, 10,000, 25,000, 50,000, 100,000 and every increment of 100,000 up to 1,000,000. Dynamic data was also taken periodically so that if any change occurred, it could be pinpointed to the nearest 50,000 cycles.

5.2 Method of Loading

The four actuators were arranged in a square pattern over the two interior box girders. The hydraulic system was configured so that the two north actuators would move in tandem and the two south actuators would move in tandem. The desired effect was to simulate the wheel load of a single tandem axle passing with one wheel centered on one interior beam followed by the same truck passing with one wheel load centered on the other interior beam (Figure 3.9). As stated earlier, a wheel load of 89 kN (20 kips) was used, so each actuator applied a maximum load of 44.5 kN (10 kips).

The beams were loaded such that a complete load reversal occurred on the center keyway. This was done by making each set of actuators apply a load once every 1.8 seconds and setting the two sets of actuators 180° out of phase. Thus, a complete cycle of applying and completely removing the load on the north interior beam (Beam #2, Figure 5.1) and then applying and completely removing the load from the south interior beam (Beam #3, Figure 5.1) every 1.8 seconds. The speed of 1.8 seconds was as fast a the system could apply load and still achieve a complete load reversal on the center keyway.

5.3 Instrumentation for Dynamic Tests

The bridge and shear keys were instrumented to measure vertical displacements, relative deflections and strains. The external instrumentation scheme for the bottom of the bridge is shown in Figure 5.1. Six DCDT's were placed under the east load points

(610 mm (2 feet) east of midspan)-- one DCDT on either side of the three joints. This configuration was selected to measure global displacement of the bridge as well as any relative displacement across the joints. Relative displacement across the bottom of the joints was also monitored using specially designed relative displacement transducers (deflectometers) which were attached to the soffit of the bridge, two across each keyway. Each relative displacement transducer was a piece of steel with four foil strain gages -- two glued on each side. The design was conceived by El-Esnawi and Huckelbridge (1996). Those made by U.C. differed in two ways. 1) steel was used whereas CWRU used aluminum. 2) U.C. bolted their transducer to the bridge with 6.4 mm (0.25 inch) diameter concrete anchors. CWRU used an epoxy. These gages were calibrated in a mill that had a digital readout accurate to 0.013 mm (0.0005 inches). One end was clamped in a vice and the other was clamped in a chuck. (This simulated the fixed-fixed end conditions that were anticipated on the actual bridge.) The table was moved in 0.013 mm (.0005 in.) increments to calibrate the gages. El-Esnawi and Huckelbridge (1996) reported these transducers to be accurate to 0.00254 mm (0.0001 inches).

Figure 5.2 shows the external instrumentation on top of the bridge. Surface concrete strains near the load points, the spread of the bottom keyway joints and the strains across top keyway joins (transverse joint movements) were measured with omega clip gages. These gages had a slot through which small bolts were fastened into targets. The targets can be attached to any surface with various brands of super glue. The gages were calibrated in an MTS calibrator, which was accurate to 0.254 μm (0.00001 inches). Special care was taken during calibrating and placing of the clip gages on any surface to ensure the targets were as close to the 100 mm gage length as possible. Misplacing targets would have led to incorrect calibration factors. Also, it was observed that the calibration factors varied as much as 16 percent among these gages. Hence, the location of each gage was noted to ensure the correct calibration factor was used. The calibration of these gages appeared to change as the gage heated up, so the gages were allowed to warm up for at least 5 minutes to stabilize them before they were calibrated.

The vibrating wire strain gages embedded in the girders and keyways continued to function (see chapter 3.1.2), but as previously noted, these gages were only monitored during the static (slow) tests. As a result, the vibrating wire gage data is not available during the dynamic tests.

5.4 Data Acquisitions for Dynamic Test

The vibrating wire gages were monitored using a CR10 datalogger and a 16 channel multiplexer. The rest of the gages were monitored using two Strawberry Tree Cards. Each card was plugged into and IBM compatible computer.

5.5.1 Bridge Test #1 – Background

The upper keyway was grouted with non-shrink grout on November 21, 1995. The contractor was allowed to grout the keyways as he normally would. An ODOT approved non-shrink grout was used. No attempt was made to control the water/cement ratio. The contractor made an especially thin grout mixture for the north keyway due to the narrow gap in the throat of this keyway. Approximately 16 – 76 x 152 mm (3 x 6 inch)

cylinders were made for compression testing. Table 5.1 shows the strengths of these cylinders. All cylinders met the required 28-day strength.

After grouting, the bridge was covered with a plastic tarp. Next, a 58,000 kJ (55, 000 BTU) kerosene torpedo heater was run under the bridge for five days to prevent the grout from freezing.

Table 5.1 Shear Key Grout Specimen Strength --Test #1

Keyway ⇒ Age / Curing Method ⇓	North MPa (ksi)	Center MPa (ksi)	South MPa (ksi)
1 Day - air	13 (1.9)	16 (2.3)	20 (3.0)
6 Days - air	28 (4.0)	38 (5.5)	N.A.
28-days- air	45 (6.5)	43 (6.3)	N.A.
28-days - moist	41 (6.0)	35 (5.1)	48 (7.0)

When the compression cylinders were examined three days later, it was noted that they had experienced extreme amounts of shrinkage. The grout cylinders slipped out of the molds when turned up-side-down. The grout cylinder for the north keyway showed the greatest amount of shrinkage.

About two weeks after grouting and after the first severe freeze, the strain gages embedded in the keyways showed large jumps in strain. At about the same time, what appeared to be shrinkage cracks appeared in the center and south keyways. Before any load was ever applied to the bridge, pulse velocity measurements indicated that the center keyway was severely cracked at midspan. At that time it was assumed that improper grout preparation was responsible for the cracks. It was decided that the grout would be removed and the upper keyway regrouted under more favorable weather conditions and with monitoring the water/cement ratio.

However, since the keyways were available for testing, the hydraulic system was run to 41,000 cycles to allow the researchers to practice using the hydraulic and data acquisition systems. During this time, existing superficial cracks in the center and south keyways became severe cracks (Figure 5.3). The north keyway never cracked anywhere along the length of the bridge. At the conclusion of the 41,000 cycle test, the two north actuators applied at total load of 133 kN (30 kips) or 67 kN (15 kips) each in a last attempt to crack the north shear key. This test failed to produce any cracks in the north keyway. Also of interest is the fact that although the south keyway experienced some severe cracking at the ends, it remained intact (i.e. not even a superficial crack) at midspan where the load was applied. Thus, the load did not appear to cause new cracking, but simply propagated the existing cracks. After disassembling the bridge, dye penetration confirmed the severe cracks did penetrate the entire center keyway before any load had been applied.

5.5.2 Results of Test #1

The bridge was tested to 41,000 cycles for test #1. Throughout this test data was periodically taken to determine if any of the strain or displacement gages showed any changes in readings. For this test, severe cracking occurred in the center keyway at midspan where all of the gages were placed. The north and south shear keys did not show any cracks at midspan. Due to the large amount of data, the only results presented here are for cycles 0, 10,000, and 41,000.

Table 5.2 shows the load distribution among the girders when only the two north actuators are applying a total load of 89 kN (20 kips) or 44.5 kN (10 kips) per actuator. Table 5.3 is the load distribution when only the south actuators are applying load. These values are based upon the readings of the internal vibrating wire strain gages embedded in the bottom flange at the level of the prestressing tendons. The total strain in all the gages is summed. Then, the bottom strain in an individual girder is divided by the total strain to arrive at the percentage of strain that girder is withstanding. This percentage of strain is equal to the percentage of load the girder is sustaining. A sample calculation is shown in Appendix C.

The data in tables 5.2 and 5.3 indicated that little change in load distribution occurred throughout Test #1. This is contrary to the assumption that shear key cracking will eliminate the load sharing function of the shear key. It appears the load is sustained mainly by the loaded girder and the adjacent exterior girder, however, the load percentages are the within AASHTO distribution factor of 30%. Also of interest is the fact that even thought the center keyway was severely cracked at midspan, it still transmitted more than 40% of the load. For example, when the north actuators are pushing on the bridge, the south and south-central beams sustain approximately 42% of the load. When the south actuators are pushing on the bridge, the north and north-central actuators sustain approximately 44% of the load. The load was transferred by mechanical interlock, friction between the cracked surfaces of the center keyway at midspan, through the regions where the center shear keys were intact east and west of midspan, or by a combination of these effects.

Probably of most interest from test #1 is the fact that neither the north, nor south keyways cracked at midspan during the test. El-Esnawi and Huckelbridge (1996) had predicted that shear keys under such a loading condition would crack on the first cycle.

Table 5.2 Load Distribution --*North* Actuators Loading Beam #2-- Test #1

GIRDER ⇒ CYCLE ⇓	SOUTH BEAM #4	SOUTH - CENTRAL BEAM #3	NORTH - CENTRAL BEAM #2	NORTH BEAM #1
0	21.1%	22.0%	29.0%	27.8%
10,000	21.0%	21.1%	28.7%	29.1%
41,000	20.9%	21.1%	29.1%	29.0%

Table 5.3 Load Distribution -- *South* Actuators Loading Beam #3--Test #1

GIRDER ⇒ CYCLE ⇓	SOUTH BEAM #4	SOUTH - CENTRAL BEAM #3	NORTH - CENTRAL BEAM #2	NORTH BEAM #1
0	26.2%	28.9%	20.7%	24.1%
10,000	26.5%	29.3%	20.7%	23.4%
41,000	26.6%	28.2%	21.1%	24.1%

5.5.3 Transverse Strains and Movements of Joints --Test #1

Omega clip gages were placed across the joints on top and bottom of the bridge at midspan (see figures 5.1 and 5.2). Tables 5.4 and 5.5 show these measurements at cycles 0, 10,000 and 41,000. Generally, the measurements obtained when the north actuators are pushing on the bridge mirror those with the south actuators pushing. The values presented are the response to both north actuators or both south pushing with a force of 44.5 kN (10 kips) each (89 kN (20 kips) total load to the girder). Values are listed in microstrain ($\mu\varepsilon$) when the transverse gage spanned over intact shear keys and micrometers (μm) when the clip gages spanned over cracks. All of the bottom gages are listed in micrometers since the beams are not grouted at the bottom.

Two transverse keyway clip gages were placed across each of the top joints. Generally, these gages produced output in agreement with each other. The continuity of the top face of the bridge provided by intact keyways results in tensile strains of less than 40 microstrain (usually less than 15 microstrain) across the shear keys. This level of strain is not believed sufficient to initiate a crack in the shear key as cracking strains are usually on the order of 100 - 200 microstrain. At the east load point the intact shear key sustains compressive strains. This may be due to the fact that the girders never sit absolutely square on the abutment, so there is often some tilt to the vertical axis. Since the beam deflects along the vertical axis, there may be some slight lateral movement of the beams. The tilt varies from girder to girder, so adjacent beams will have different lateral movements. This explains the opening and/or closing of the bottom of the joints and also explains why some top joints go into compression.

Generally, Tables 5.4 and 5.5 show no appreciable deterioration over the course of the 41,000 cycles. This conclusion agrees with Tables 5.2 and 5.3, which show that the load distribution did not significantly change either.

Table 5.4 Transverse Keyway Strains and Movements --*North* Actuators Loading Beam #2 -- Test #1

	CYCLE	SOUTH JOINT	CENTER JOINT	NORTH JOINT NE / NW GAGE
TOP	0	-15 με	-15 μM	-40 με / +25 με
TOP	10,000	12 με	-20 μM	-22 με / +30 με
TOP	41,000	6 με	-14 μM	-18 me / +30 με
BOTTOM	0	-3.5 μM	150 μM	N.A.
BOTTOM	10,000	-5.5 μM	80 μM	N.A.
BOTTOM	41,000	-5.0 μM	77 μM	N.A.

+ = compression or closing - = tension or opening

Table 5.5 Transverse Keyway Strains And Movements --*South* Actuators Loading Beam #3 -- Test #1

	CYCLE	SOUTH JOINT	CENTER JOINT	NORTH JOINT
TOP	0	25 με	-16 μM	10 με
TOP	10,000	12 με	-25 μM	10 με
TOP	41,000	12 με	-14 με	4 με
BOTTOM	0	35 μM	68 μM	N.A.
BOTTOM	10,000	27 μM	55 μM	N.A.
BOTTOM	41,000	27 μM	52 μM	N.A.

5.5.4 Relative Vertical Keyway Displacements in Test #1

Two relative displacement transducers and DCDT's were employed to measure the relative vertical keyway displacements across the joints at the bottom of the bridge. It can be noted from Tables 5.6 through 5.9 that the relative displacement transducers rarely agree with each other, nor do they agree with the values from the DCDT's.

There was some indication during testing that the relative displacement transducers were not making accurate measurements. The accuracy depends on creating a fixed end condition in the gage. Due to camber differences between adjacent beams, the ends of the relative displacement transducers had to be shimmed. This appears to have allowed rotation at the end of the relative displacement transducers.

The relative deflections measured by the DCDT's are also inconsistent. This may have been caused by:

1) "Stick/Slip" conditions where the relative movement of the beams changes as frictional contacts are made and lost.

2) Differential thermal movements which occurred during the test.

Table 5.6 Relative Vertical Keyway Displacements -- *North* Actuators Loading Beam #2 - Test #1, Measured using Relative Displacement Transducers

Keyway ⇒	North	North	Center	Center	South	South
Gage ⇒ Cycle ⇓	East	West	Center	West	East	West
0	-30 μM	25 μM	-80 μM	-100 μM	20 μM	-70 μM
10,000	-200 μM	30 μM	70 μM	80 μM	-9 μM	7 μM
41,000	-170 μM	60 μM	60 μM	100 μM	-6 μM	-100 μM

Table 5.7 Relative Vertical Keyway Displacements -- *North* Actuators Loading Beam #2- Test #1 Measured using DCDT's

Keyway ⇒ Cycle ⇓	North	Center	South
0	-60 μM	N.A.	-10 μM
10,000	10 μM	-260 μM	100 μM
41,000	-30 μM	-350 μM	200 μM

Table 5.8 Relative Vertical Keyway Displacements --*South* Actuators Loading Beam #3 Test #1 Measured using Relative Displacement Transducers

Keyway ⇒	North	North	Center	Center	South	South
Gage ⇒ Cycle ⇓	East	West	Center	West	East	West
0	12 μM	-12 μM	-110 μM	-80 μM	30 μM	-80 μM
10,000	-40 μM	-12 μM	-140 μM	-110 μM	20 μM	-65μM
41,000	-40 μM	-11 μM	-140 μM	-110 μM	25 μM	-65 μM

Table 6.9 Relative Vertical Keyway Displacements -- *South* Actuators Loading Beam #3 Test #1 Measured using DCDT's

Keyway ⇒ Cycle ⇓	North	Center	South
0	-20 μM	1100 μM	800 μM
10,000	20 μM	-40 μM	200μM
41,000	-50 μM	-160 μM	100 μM

5.5.5 Crack Investigation -- Test #1

Figure 5.3 shows the crack propagation of Test #1 as measured by the Pulse - Velocity method and confirmed with dye penetration. The center keyway was severely cracked before applying any load to the bridge. This crack propagated only eastward to the abutment. The south keyway had moderate cracks at both abutments which worsened and propagated toward midspan under load. The north keyway did not crack throughout this test. It should be noted that at midspan where the load was applied, neither the north nor the south keyways cracked. At the conclusion of test #1, the south and south-central beams were picked up and separated by cranes without any difficulty, but the north and north-central girders could not be separated. It was necessary to saw-cut the north keyway. This led the hypothesis that the hydraulic system, which was applying the equivalent of an HS20-44 truck plus impact every 0.9 seconds, was not sufficient to initiate shear key cracks. It is not clear if the load was enough to propagate existing cracks or if the propagation was due to thermal movements during the test.

5.6.1 Bridge Test #2 – Background

After test #1, the beams were separated and the keyway was cleaned of all grout. The upper keyway was grouted a second time with non-shrink grout on May 31, 1996. Once again, an ODOT-approved non-shrink grout was used, but this time the water/cement ratio was carefully monitored to assure compliance with manufacturers specifications. Three days after pouring, the keyways had cracked. Severe cracks appeared in the center keyway near the west abutment and in the north keyway near the east abutment. Only moderate cracking was observed in any keyway near midspan. Table 5.10 shows that the grout did achieve the required 35 MPa (5.0 ksi) strength at seven days.

Table 5.10 Shear Key Grout Specimen Strength --Test #2

Keyway ⇒ Age / Curing Method ⇓	North MPa (ksi)	Center MPa (ksi)	South MPa (ksi)
3 Day - air	21 (3.1)	30 (4.3)	26 (3.7)
7 Days - air	36 (5.2)	28 (4.1)	35 (5.0)
14 Days- air	38 (5.5)	37 (5.3)	41 (5.9)
34 Days- air	38 (5.5)	43 (6.2)	37 (5.3)
34 Days - moist	42 (6.1)	36 (5.3)	32 (4.7)

At this time, an investigation (see Chapter 6) of the thermal effects upon the bridge yielded the following results: 1) The longitudinal thermal strains in the top flanges of the girders more than double the strains that would be caused by placing an HS20-44 truck on the bridge. 2) The thermal gradient causes the bridge to camber up as much as 14 mm (0.5 in.) as it heats up. 3) The cracks in the keyways open as much as 1 mm as the bridge cools.

After determining that the cracking was caused by thermal stresses, the beams were tested to 1,000,000 cycles. All of the existing cracks propagated, and this time some new cracks formed. The new cracks formed near the abutments, not near the load, leading the research team to believe these new cracks were caused by thermal stresses, not load (Figure 5.3).

5.6.2 Results Test #2

The bridge was tested to 1,000,000 cycles. Throughout this test data was periodically taken to determine if any of the gages showed any significant changes in reading. Due to the large amount of data, the only results presented here are for cycles 0, 500,000, and 1,000,000.

Tables 5.11 and 5.12 show the load distribution among the girders when the two north or two south actuators are applying a total load of 89 kN (44.5 kN each). The calculation of load distribution is the same as in Tables 5.2 and 5.3.

The data in tables 5.11 and 5.12 indicated that little change in load distribution occurred throughout Test #2. It appears that the loaded girder and the adjacent exterior girder sustain the majority of the load. Slight deterioration can be seen in the center keyway by noting the 0.5% increase in the load sustained by the loaded girder (i.e. in table 6.12 the load sustained by the south-central beam increases from 25.5% to 26.0%.) As in test #1, the broken shear keys continue to function in sharing the load between the girders.

Table 5.11 Load Distribution -- *North* Actuators Loading Beam #2-- Test #2

GIRDER ⇒ CYCLE ⇓	SOUTH BEAM #4	SOUTH - CENTRAL BEAM #3	NORTH - CENTRAL BEAM #2	NORTH BEAM #1
0	24.2%	23.3%	26.4%	26.1%
500,000	23.6%	23.5%	26.2%	26.7%
1,000,000	23.2%	23.4%	26.8%	26.7%

Table 5.12 Load Distribution -- *South* Actuators Loading Beam #3-- Test #2

GIRDER → CYCLE ↓	SOUTH BEAM #4	SOUTH - CENTRAL BEAM #3	NORTH - CENTRAL BEAM #2	NORTH BEAM #1
0	27.5%	25.5%	24.1%	22.9%
500,000	27.0%	25.9%	23.9%	23.2%
1,000,000	27.1%	26.0%	24.0%	22.9%

5.6.3 Transverse Strains and Movements of Joints Test #2

Omega clip gages were placed across the joints on top and bottom of the bridge at midspan. The values presented are the response to both actuators pushing with a force of 44.5 kN each (10 k) on one beam. Deterioration in the center keyway can be noted. At the initial test, only superficial cracks were noted. Tensile strains are developed across center keyway initially, but these strains were not high enough to cause cracking. Clearly, cracking was caused by temperature movements. After it the cracks became more severe, the application of load caused compressive strains, perhaps due to changes in beam alignment due to thermal strains. No change in the movements of the exterior keyways was evident.

Table 5.13 Transverse Keyway Strains and Movements – *North* Actuators Loading Beam #2 -- Test #2

JOINT	CYCLE	SOUTH	CENTER	NORTH
TOP	0	9 με	10 με	20 με
TOP	500,000	9 με	-4 μM	20 με
TOP	1,000,000	9 με	-8 μM	20 με
BOTTOM	0	2 μM	30 μM	40 μM
BOTTOM	500,000	2 μM	50 μM	40 μM
BOTTOM	1,000,000	2 μM	50 μM	40 μM

Table 5.14 Transverse Keyway Strains and Movements -- *South* Actuators Loading Beam #3 -- Test #2

JOINT	CYCLE	SOUTH	CENTER	NORTH
TOP	0	35 με	47 με	10 με
TOP	500,000	35 με	-4 μM	10 με
TOP	1,000,000	35 με	-8 μM	10 με
BOTTOM	0	-40 μM	38 μM	1.8 μM
BOTTOM	500,000	-40 μM	62 μM	1.8 μM
BOTTOM	1,000,000	-40 μM	71 μM	N.A.

5.6.4 Relative Vertical Keyway Displacements in Test #2

Tables 5.15 through 5.18 show the relative vertical keyway displacements. As with Test #1, little correlation is apparent between adjacent gages or between the deflectometers and the DCDT's at the same location. Comparing Tables 5.15-18 with Tables 5.11 and 5.12 show that relative displacements also do not correlate with load distribution (i.e. large relative displacement do not mean a beam is taking a higher percentage of load)

Table 5.15 Relative Vertical Keyway Displacements -- *North* Actuators Loading Beam #2-- Test #2 Measured using Relative Displacement Transducers

Keyway ⇒	North	North	Center	Center	South	South
Gage ⇒ Cycle ⇓	East	West	East	West	East	West
0	12 μM	80μM	50 μM	30 μM	0 μM	-6μM
500,000	20 μM	90μM	95 μM	45 μM	0 μM	-5μM
1,000,000	20 μM	90μM	80 μM	50 μM	N.A.	-5μM

Table 5.16 Relative Vertical Keyway Displacements -- North Actuators Loading Beam #2 -- Test #2 Measured using DCDT's

Keyway ⇒ Cycle ⇓	North	Center	South
0	N.A.	-60μM	350μM
500,000	N.A.	-50μM	0 μM
1,000,000	N.A	-40μM	30 μM

Table 5.17 Relative Vertical Keyway Displacements -- *South* Actuators Loading Beam #3 -- Test #2 Measured using Relative Displacement Transducers

Keyway ⇒	North	North	Center	Center	South	South
Gage ⇒ Cycle ⇓	East	West	East	West	East	West
0	-1 μM	12 μM	40 μM	20 μM	-17 μM	-100 μM
500,000	-1 μM	N.A.	90 μM	35 μM	-14 μM	-100 μM
1,000,000	0 μM	5 μM	80 μM	50 μM	N.A.	-110 μM

Table 5.18 Relative Vertical Keyway Displacements— *South* Actuators Loading Beam #3 — Test #2 Measured using DCDT's

Keyway ⇒ Cycle ⇓	North	Center	South
0	N.A.	0 μM	350 μM
500,000	N.A.	20 μM	0 μM
1,000,000	N.A.	20 μM	20 μM

5.6.5 Crack Investigation of Test #2

Figure 5.4 shows the crack propagation of Test #2 as measured by the Pulse - Velocity method. The center keyway was severely cracked at the west abutment and moderately cracked at the east abutment before applying any load to the bridge. These cracks which propagated toward midspan. The south keyway had moderate cracks at the west abutments propagated past midspan. The north keyway developed cracks at the abutments after cyclic load was applied, but since the cracks appeared away from the load, they may be thermal cracks. At the conclusion of test #2, cranes picked up the south and south-central beams without any difficulty. The north and north-central girders could not be separated easily. It was necessary to place the south beam on top of the north-central beam. This provided more resistance to the lifting load of the cranes, which proved to be enough to break the north keyway. As with test #1, the north shear key did not crack at midspan where the load was applied. Over the course of 1,000,000 shear reversals, the center keyway did not become as severely cracked. It appears that the applied loading has little effect on cracking and crack propagation.

5.7.1 Bridge Test #3 – Background

The lower keyway was grouted with an ODOT-approved non-shrink grout on August 16, 1996. The water/cement ratio was carefully monitored as in test #2. The grout depth was also monitored to avoid grouting both keyways. Cracking was observed only near the abutments three days after pouring. One crack was detected by a clip gage over the keyway near the southeast abutment. The data showed that the crack had occurred the night after the keyways was poured. Table 5.19 shows that the keyway grout achieved the required 35 MPa (5.0 ksi) strength.

Table 5.19 Shear Key Grout Specimen Strength -- Test #3

Keyway ⇒ Age / Curing Method ⇓	North MPa (ksi)	Center MPa (ksi)	South MPa (ksi)
6 Day - air	23 (3.3)	41 (6.0)	35 (5.1)
42 Days - air	52 (7.5)	51 (7.4)	51 (7.4)
42 Days - moist	44 (6.4)	55 (8.0)	58 (8.4)

The hydraulic system was run to 1,000,000 cycles. Only one crack propagated a total of 1 meter.

5.7.2 Results of Test #3

The bridge was tested to 1,000,000 cycles during test #3. Throughout this test, data was periodically taken to determine if any of the gages showed significant changes in readings. Due to the large amount of data, the only results presented here are for cycles 0, 500,000, and 1,000,000.

Tables 5.20 and 5.21 again show load distribution between the beams. The data indicated that no change in load distribution occurred throughout test #3. This would be expected in the case where none of the shear keys show any sign of deterioration at midspan.

Table 5.20 Load Distribution -- *North* Actuators Loading Beam #2 -- Test #3

GIRDER ⇒ CYCLE ⇓	SOUTH BEAM #4	SOUTH - CENTRAL BEAM #3	NORTH - CENTRAL BEAM #2	NORTH BEAM #1
0	22.9%	24.3%	25.0%	27.8%
500,000	23.1%	24.2%	24.8%	27.9%
1,000,000	23.2%	23.9%	25.0%	27.7%

Table 5.21 Load Distribution -- *South* Actuators Loading Beam #3-- Test #3

GIRDER ⇒ CYCLE ⇓	SOUTH BEAM #4	SOUTH - CENTRAL BEAM #3	NORTH - CENTRAL BEAM #2	NORTH BEAM #1
0	26.1%	25.0%	24.6%	24.2%
500,000	26.3%	25.4%	24.2%	24.2%
1,000,000	26.4%	25.1%	24.4%	24.1%

5.7.3 Transverse Keyway Strains and Movements of Test #3

Omega clip gages were placed across the joints on top and bottom of the bridge at midspan. Tables 5.22 and 5.23 shows these measurements at 0, 500,000 and 1,000,000 cycles. No deterioration of the keyways was noted in test #3.

Table 5.22 Transverse Keyway Movements -- *North* Actuators Loading Beam #2-- Test #3

JOINT	CYCLE	SOUTH	CENTER	NORTH
TOP	All	0.0 μM	-2 μM	2 μM
BOTTOM	All	-3 μM	-20 μM	25 μM

Table 5.23 Transverse Keyway Movements -- *South* Actuators Loading Beam #3 -- Test #3

JOINT	CYCLE	SOUTH	CENTER	NORTH
TOP	All	-1 μM	-2 μM	1 μM
BOTTOM	All	25 μM	-20 μM	-3 μM

5.7.4 Relative Vertical Keyway Displacements in Test #3

Tables 5.24 - 27 show relative displacement data. As before, this data does not correlate well with any measured or observed data.

Table 5.24 Relative Vertical Keyway Displacements -- *North* Actuators Loading Beam #2 -- Test #3 Measured using Relative Displacement Transducers

Keyway ⇒	North	North	Center	Center	South	South
Gage ⇒ Cycle ⇓	East	West	East	West	East	West
0	8 μM	-3 μM	3 μM	-30 μM	N.A.	N.A.
500,000	-270 μM	-8 μM	3 μM	-30 μM	N.A.	N.A.
1,000,000	N.A.	N.A.	3 μM	-30 μM	N.A.	N.A.

Table 5.25 Relative Vertical Keyway Displacements -- *North* Actuators Loading Beam #2 -- Test #3 Measured using DCDT's

Keyway ⇒ Cycle ⇓	North	Center	South
0	-20 μM	85 μM	-100 μM
500,000	-20 μM	60 μM	160 μM
1,000,000	-20 μM	80 μM	0 μM

Table 5.26 Relative Vertical Keyway Displacements -- *South* Actuators Loading Beam #3 -- Test #3 Measured using Relative Displacement Transducers

Keyway ⇒	North	North	Center	Center	South	South
Gage ⇒ Cycle ⇓	East	West	East	West	East	West
0	N.A.	0 μM	3 μM	-32 μM	N.A.	N.A.
500,000	N.A.	1 μM	4 μM	-32 μM	N.A.	N.A.
1,000,000	N.A.	N.A.	4 μM	-32 μM	N.A.	N.A.

Table 5.27 Relative Vertical Keyway Displacements -- *South* Actuators Loading Beam #3 -- Test #3 Measured using DCDT's

Keyway ⇒ Cycle ⇓	North	Center	South
0	-30 μM	70 μM	-120 μM
500,000	-20 μM	70 μM	250 μM
1,000,000	-30 μM	80 μM	10 μM

5.7.5 Crack Investigation of Test #3

Figure 5.5 shows the crack propagation of test #3 as measured by the Pulse - Velocity method. Cracking occurred in all the keyways at both abutments. Only the south keyway had severe cracking at the east abutment. This was the only crack that propagated. Over the one million cycles it propagated 1 meter. At the conclusion of test #3, none of the girders could be removed without saw-cutting the keyways. The results show the neutral axis keyway was much more resistant to cracking.

5.8.1 Bridge Test # 4 - Background

The upper keyway was grouted with an ODOT-approved epoxy grout. Sandblasting along the entire length of each of the keyways was performed two days prior to grouting as is required by ODOT. University of Cincinnati graduate students performed the grouting, while under the direct supervision of the product manufacturer's representative. Construction precautions such as wearing chemical resistant gloves and full length clothing was adhered to due to the chemical nature of the product being used. The product used was Master Builders Ceilcote 648 CP Plus epoxy grout mixture. This mixture consisted of three parts: Ceilcote 648 CP Plus grout liquid (Part A), Ceilcote 648 CP Plus Hardener (Part B), and Ceilcote 648 CP Plus grout aggregate. The hardener and the liquid first had to be mixed thoroughly for three minutes with a jiffler (a.k.a. jiffy) mixer attached to a high-speed industrial drill. The proportions for this mixing were as follows. By weight 3.46 kg (7.63 lbs.) of hardener (part B) was added to 9.17 kg (20.2 lbs.) of grout liquid (Part A) and vigorously mixed for three minutes. This combination was then added to an electric paddle mixer. Immediately following three bags of grout aggregate, each weighing 21.3 kg (47 lbs.), were added to the liquid chemicals in the mixer. This was then completely mixed for two minutes according to the recommendations of the manufacturer. From the mixer the grout was poured into a wheelbarrow, and then into a 19 liter (5 gallon) bucket. This bucket was carried to the device constructed for pouring the grout into the narrow keyways (see Figure 5.6). This device roughly resembled a long flat funnel or a trough. The upper opening was .254 m (10 in.) and the bottom opening was 12.7 mm (0.5 in.). The overall length of the device was .86 m (34 in.). The consistency of the grout was such that it poured smoothly through the trough into the keyways. The gaps at the upper throat of the keyways were approximately 19.0 mm (.75 in.), 25.4 mm (1 in.), and 38.1 mm (1.5 in.) for the south, north, and center keyways respectively.

Clean up of the epoxy grout required the use of the methyl ethyl ketone. One possible problem with epoxy grouts for field use is disposal of this solvent. Method for safe and effective disposal do exist and contractors using the epoxy grout should contact local environmental officials for disposal instructions.

Four – 101 x 203 mm (4 x 8 inch) cylinders were made for compression testing. Two – 152 x 304 mm (6 x 12 inch) cylinders were made for determining the modulus of elasticity of the epoxy grout. Table 5.28 shows that the epoxy grout did achieve the required 35 MPa (5 ksi.) seven day strength. The modulus of elasticity was determined from the 28-day specimens and resulted in an average value of 247 MPa (1705 ksi), as can be seen in Table 5.29.

Table 5.28 Shear Key Grout Specimen Strength --Test #4

Keyway ⇒ Age / Curing Method ⇓	Test 1 MPa (ksi)	Test 2 MPa (ksi)	Average MPa (ksi)
7 Day - air	59 (8.6)	57 (8.2)	58 (8.4)
28 Days - air	59 (8.5)	61 (8.8)	60 (8.7)

Table 5.29 Shear Key Grout Modulus of Elasticity – Test #4

Keyway ⇒ Age / Curing Method ⇓	Test 1 MPa (ksi)	Test 2 MPa (ksi)	Average MPa (ksi)
28 Days - air	252 (1740)	242 (1670)	247 (1705)

While the grout was setting, the keyways were observed to produce bubbles on the surface. Investigation showed that grout was expending the trapped air from the grouting process. Examination of the test cylinders showed the same phenomenon. However, no air pockets were found inside the cylinders, and the grout had a good consistency. When the keyways were examined the day after grouting, it was observed that the grout had notable shrinkage at the top of all of the keyways. When the compression cylinders were examined one day later, it was noted that they had experienced some amount of shrinkage, similar to that seen in the keyways. However, no cracking of the keyway was observed after grouting, as was confirmed by the pulse velocity testing performed at zero cycles. Also of interest, was that the grout could be seen to have absorbed into the side of the keyway. It was visually apparent that the grout liquid and hardener had completely bonded itself to the sides of the keyways.

5.8.2 Results of Test # 4

The bridge was tested to 1,000,000 cycles as in the previous tests. Throughout this test data was periodically taken to determine if any of the strain or displacement gages showed any changes in readings. For this test, no cracking was observed at any point during the testing. Due to the large amount of data, the only results presented here are for cycles 0, 500,000, and 1,000,000.

Tables 5.30 and 5.31 show the load distribution after 1,000,000 cycles. The results are similar to the previous 3 tests.

Table 5.30 Load Distribution --*North* Actuators Loading Beam #2 -- Test #4

GIRDER ⇒ CYCLE ⇓	SOUTH BEAM #4	SOUTH - CENTRAL BEAM #3	NORTH - CENTRAL BEAM #2	NORTH BEAM #1
1,000,000	22.6%	24.2%	26.3%	26.9%

Table 5.31 Load Distribution -- *South* Actuators Loading Beam #3--Test #4

GIRDER ⇒ CYCLE ⇓	SOUTH BEAM #4	SOUTH - CENTRAL BEAM #3	NORTH - CENTRAL BEAM #2	NORTH BEAM #1
1,000,000	25.9%	26.5%	23.8%	23.8%

5.8.3 Transverse Strains and Movements of Joints --Test # 4

Omega clip gages were placed across the joints on top and bottom of the bridge at midspan (see figures 5.1 and 5.2). Tables 5.32 and 5.33 show these measurements at cycles 0, 500,000 and 1,000,000. Values are listed in microstrain ($\mu\epsilon$) because the transverse clip gages always spanned over intact shear keys. All of the bottom gages are listed in micrometers since no grout was present at the bottom of the bridge

The two transverse keyway clip gages placed across each of the top joints, generally produced output in agreement with each other. Again the continuity of the top face of the bridge, provided by intact keyways, resulted in tensile strains of less than 15 microstrain across the shear keys. This level of strain was not sufficient to initiate a crack in the shear key.

Tables 5.32 and 5.33 show no appreciable deterioration over the course of the 1,000,000 cycles. This conclusion agrees with Tables 5.30 and 5.31, which show that the load distribution did not significantly change either.

Table 5.32 Transverse Keyway Strains and Movements --*North* Actuators -- Test #4

JOINT	CYCLE	SOUTH	CENTER	NORTH
TOP	0	-6 με	11 με	15 με
TOP	500,000	-5.5 με	10.5 με	14 με
TOP	1,000,000	-5 με	11 μM	14.5 με
BOTTOM	0	-201 μM	-18 μM	N.A.
BOTTOM	500,000	-159 μM	-20 μM	N.A.
BOTTOM	1,000,000	-198 μM	-18 μM	N.A.

Table 5.33 Transverse Keyway Strains and Movements --*South* Actuators -- Test # 4

JOINT	CYCLE	SOUTH	CENTER	NORTH
TOP	0	-13 με	11 με	15 με
TOP	500,000	-12.5 με	10.5 με	15 με
TOP	1,000,000	-13 με	11 με	14.5 με
BOTTOM	0	-1110 μM	-28 μM	N.A.
BOTTOM	500,000	-1110 μM	-28 μM	N.A.
BOTTOM	1,000,000	-1068 μM	-27 μM	N.A.

5.8.4 Relative Vertical Keyway Displacements in Test # 4

As in previous tests, relative displacements were measured. As before, individual measurements do not correlate well with each other or with any measured quantity. However, it is of interest to note that relative displacements for the epoxy grout are an order of magnitude larger than those for nonshrink grout. This is because the epoxy grout is a much more flexible system.

Table 5.34 Relative Vertical Keyway Displacements -- *North* Actuators Loading Beam #2 -- Test # 4 Measured using Relative Displacement Transducers

Keyway ⇒	North	North	Center	Center	South	South
Gage ⇒ Cycle ⇓	East	West	Center	West	East	West
0	N.A.	1.5 μM	-40 μM	-11.5 μM	7 μM	-1 μM
500,000	-100 μM	5.5 μM	-44 μM	-13 μM	4 μM	-6 μM
1,000,000	-92 μM	11 μM	-35 μM	-8 μM	20 μM	-1.5 μM

Table 5.35 Relative Vertical Keyway Displacements -- *North* Actuators Loading Beam #2-- Test # 4 Measured using DCDT's

Keyway ⇒ Cycle ⇓	North	Center	South
0	- 600 μM	320 μM	-500 μM
500,000	-1038 μM	805 μM	805 μM
1,000,000	-125 μM	-70 μM	195 μM

Table 5.36 Relative Vertical Keyway Displacements --*South* Actuators Loading Beam #3 -- Test # 4 Measured using Relative Displacement Transducers

Keyway ⇒	North	North	Center	Center	South	South
Gage ⇒ Cycle ⇓	East	West	Center	West	East	West
0	N.A.	1.5 μM	-32 μM	-28.5 μM	32 μM	-3 μM
500,000	-100 μM	5.5μM	-35 μM	-28 μM	26 μM	-14 μM
1,000,000	-92 μM	11 μM	-24 μM	-1.7 μM	-18 μM	-1.5 μM

Table 5.37 Relative Vertical Keyway Displacements -- *South* Actuators Loading Beam #3 -- Test # 4 Measured using DCDT's

Keyway ⇒ Cycle ⇓	North	Center	South
0	-560 μM	380 μM	-520 μM
500,000	-980 μM	885 μM	930 μM
1,000,000	-50 μM	-115 μM	145 μM

5.8.5 Crack Investigation -- Test #4

The Pulse - Velocity method was again employed in test #4 to determine if there were any cracks. At various intervals during the 1,000,000 cycles the bridge was tested using this method. Figure 5.7 shows that there were only minor deviations of transmission time, well within acceptable error, in any of the keyways during the entire course of this test. At no time were any cracks detected visually nor did the Pulse – Velocity data indicate any cracking. At the conclusion of the test none of the girders could be removed without saw-cutting the keyways along the entire length.

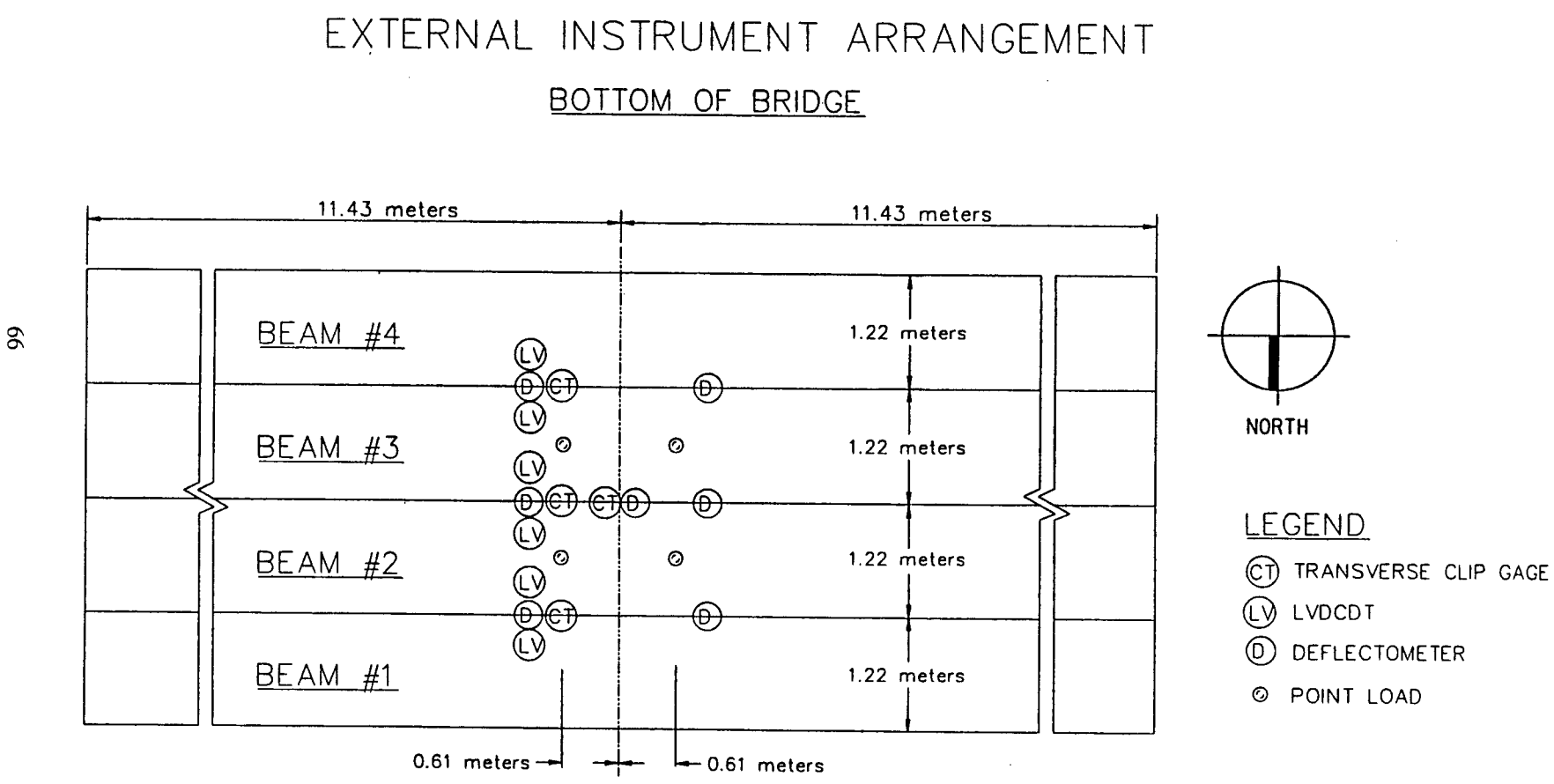

Figure 5.1 **External instrument arrangement — bottom of bridge.**

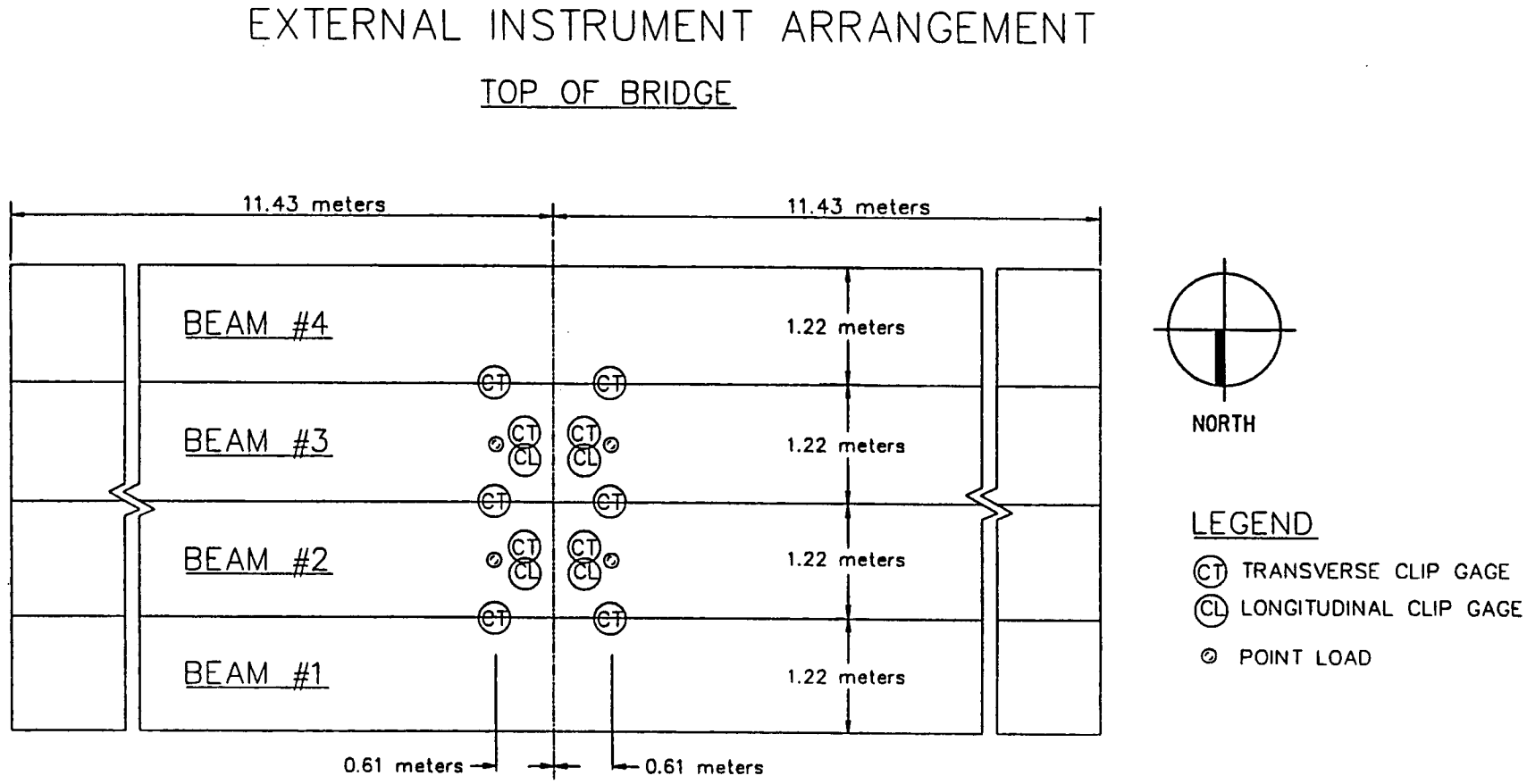

Figure 5.2 **External instrument arrangement — top of bridge.**

CRACK PROPAGATION FOR TEST 1

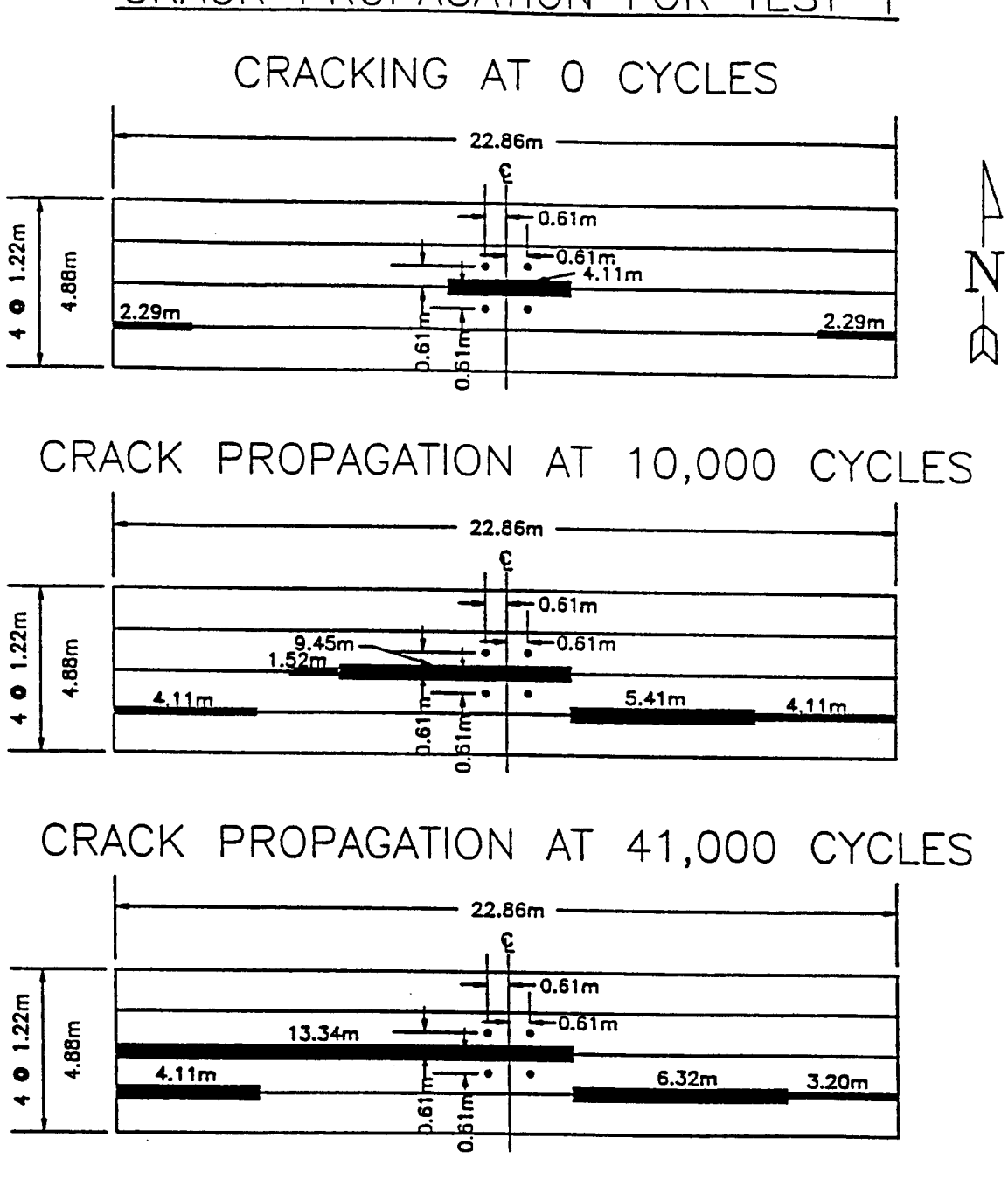

SEVERE CRACKING – CRACKED COMPLETELY THROUGH AS INDICATED BY PULSE VELOCITY

MODERATE CRACKING – PARTIALLY CRACKED AS INDICATED BY PULSE VELOCITY

NO CRACK OR SUPERFICIAL CRACKING

LOAD POINT

Figure 5.3 Crack propagation for Test #1.

CRACK PROPAGATION FOR TEST 2

CRACKING AT 0 CYCLES

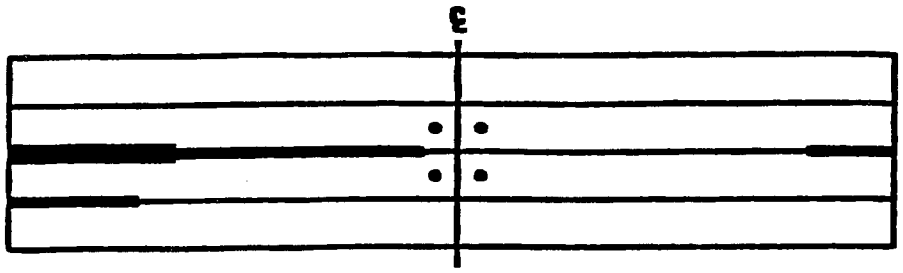

CRACK PROPAGATION AT 100,000 CYCLES

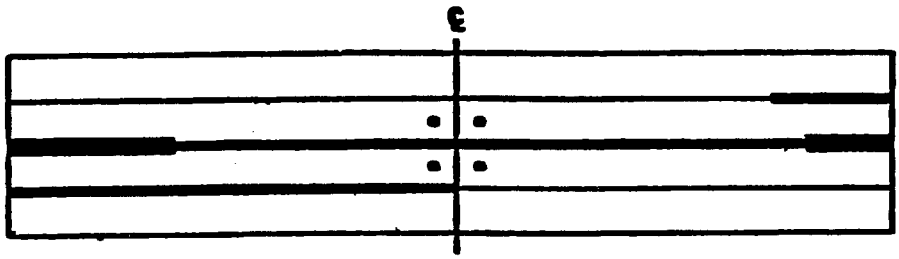

CRACK PROPAGATION AT 500,000 CYCLES

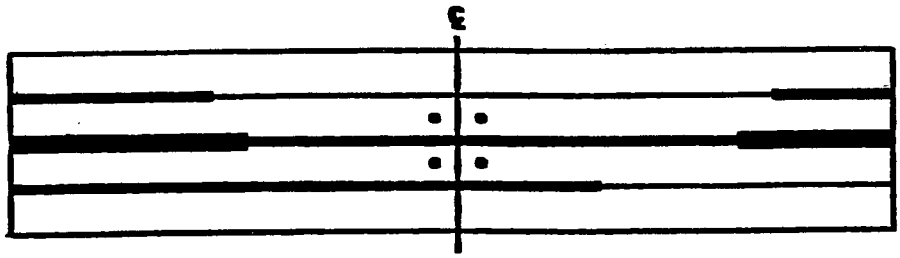

CRACK PROPAGATION AT 1,000,000 CYCLES

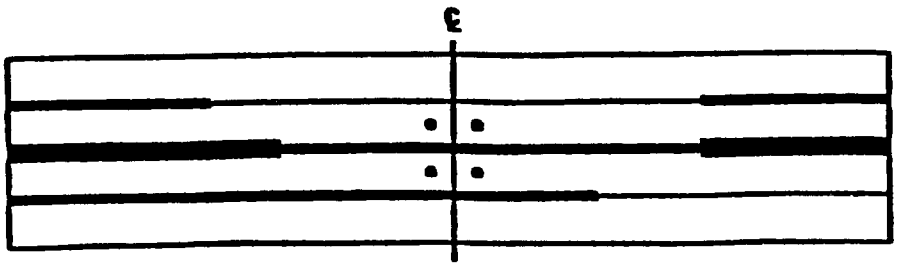

Figure 5.4 Crack propagation for test #2.

Figure 5.5 Crack propagation for test #3.

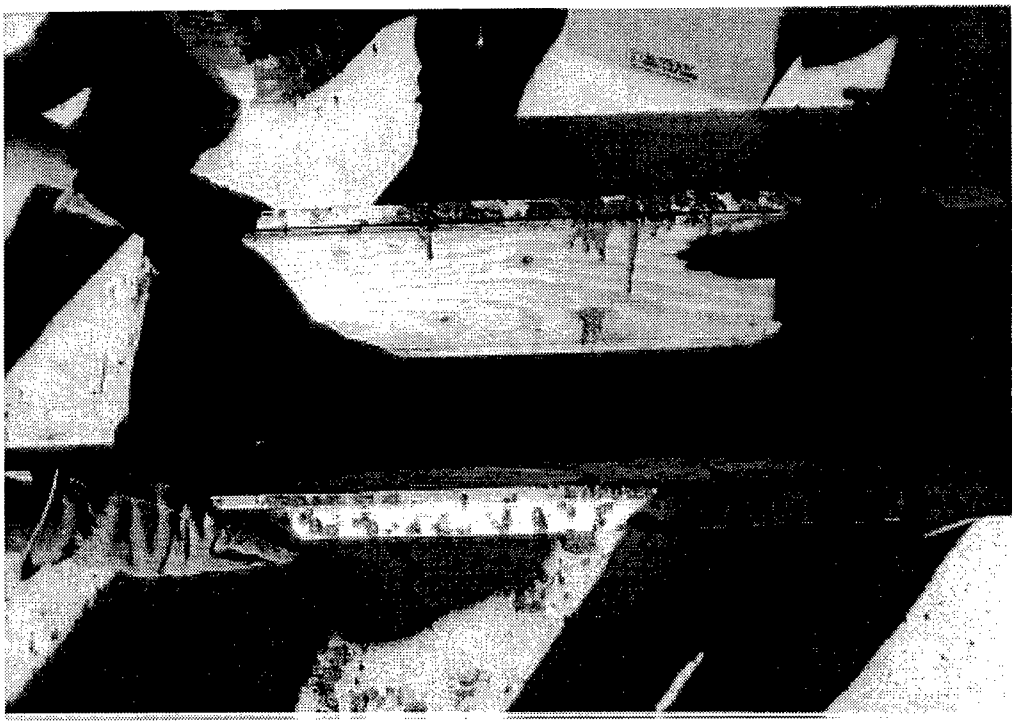

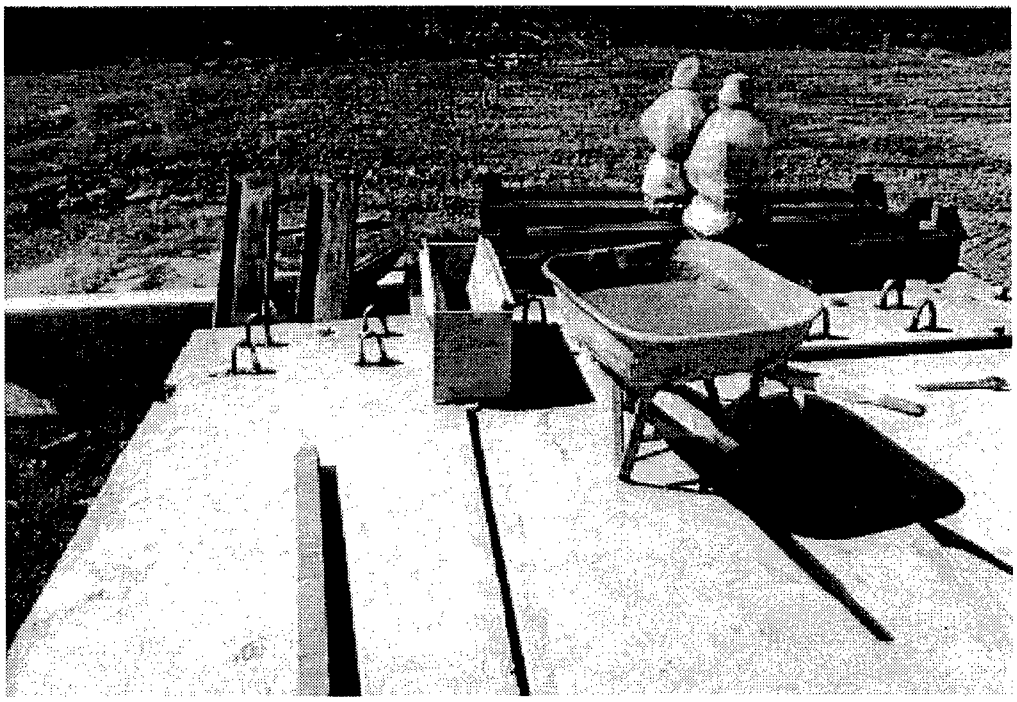

Figure 5.6 Photographs of the trough device used to grout the keyways.

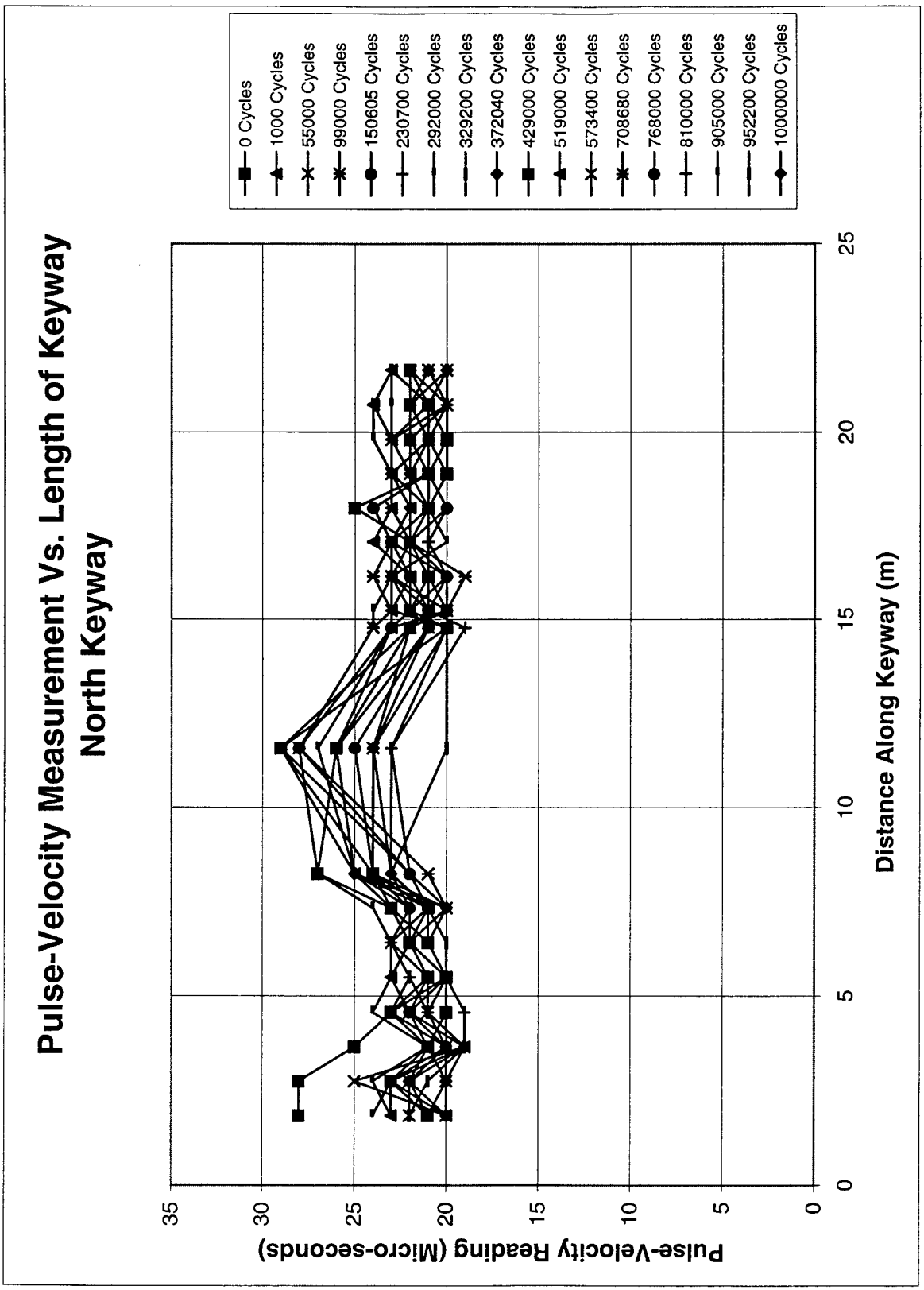

Figure 5.7 Pulse-Velocity readings for test #4

CHAPTER 6

THERMAL MOVEMENTS OF THE BRIDGE

6.1 Introduction

In the literature on keyways, thermal effects are not considered as a cause of cracking. In most cases, cracking is blamed on improper grouting and/or truck loading. However, these tests show that thermal effect is very important.

As noted in Chapter 5, the first test consisted of casting the upper keyway with nonshrink grout. The grouting was done in November. To guard against possible freezing of the grout, the bridge was heated while the grout cured. In retrospect, this heating may have done more harm than good. The heater was placed under the bridge and the bottom was heated more than the top creating a thermal gradient and causing deformations in the bridge. When the heat was removed, the girder deformations changed because the thermal gradient was reversed (the sun heats the top of the beam). These thermal movements probably contributed to cracking the keyway. Later, the beams experienced a hard freeze which definitely cracked the keyways. This cracking is shown by a large jump in the keyway strain which occurred during the freeze.

Since it was initially assumed the freeze was alone responsible for the keyway cracks in test #1, the upper keyway was removed and grouted for the second time in May. For this second test, the grout, the water/cement ratio, and the grouting process itself were carefully controlled. Three days later, the researchers returned to the bridge and noticed severe cracks in the keyways. These cracks could not be caused by freezing as no freeze occurred. The grout compression specimens did not show any sign of the severe shrinkage that had been observed in the specimens from test #1, so shrinkage did not appear to explain the cracks. The water/cement ratio had carefully monitored to assure compliance with manufacturers specifications and the grouting operation was carefully monitored so improper grout preparation could not have been the cause of the cracks.

The next hypothesis was that the cracking was caused by thermal effects. Up to this time (beginning of test #2) large thermal strains had been observed in the vibrating wire gages (see chapter 4), but these strains seemed to be longitudinal and did not appear to cause stress in the keyways. However, the vertical movement and any transverse strains had not been measured. By using DCDT's and clip gages, additional thermal deflections and strains were measured. Crack openings were also measured.

6.2 Thermal Testing

For this test, thermal load was provided by the sun. As noted in Chapter 4, the sun heats the top of the bridge while the bottom remains cooler. The thermal gradient causes strains in the beams.

Gages on the bridge were monitored as the bridge gained and lost thermal energy during the course of several days. The instrumentation scheme and data acquisition system used were the same as for the dynamic testing (Chapter 5.3). To avoid collecting excessively large amounts of data, the systems were set to take data at intervals ranging

from once every 10 minutes to once every 60 minutes. Due to the long time intervals between readings, the vibrating wire gages could also be monitored.

6.3 Test Results

Data was taken over the course of several sunny days during early June. The thermal vertical deflection of the bridge is shown in Figure 6.1. This graph shows 8.3 mm (0.33 inches) of thermal camber, which was typical. Deflections as high as 13 mm (0.51 inches) were recorded. By comparison, Figure 6.2 shows the load vs. vertical deflections for the bridge during a static test. With about 178 kN (40 kips) of load applied the bridge deflects about 5.6 mm (0.22 inches). The maximum thermal deflection is more than twice that caused by the simulated truck load while the typical deflection is approximately equal to the deflection caused by the truck load.

Figures 6.3 compares the strains caused by applying the 178 kN (40 kip) midspan load with the thermally induced strains. Again, it can be seen that the strain gradient from the load testing (approx. 90 με) is very close to the strain gradient from the thermal effects (approx. 60 με). Figure 6.4 shows that the change in top flange strain is much greater that experienced in the bottom flange, again explaining the large thermal movement .

Of particular interest are the transverse thermal strains observed. Several extra clip gages were placed spanning the keyways as well as on the girders in the transverse direction. Figure 6.5 shows a clip gage place over a keyway crack located about 2.7 meters (9 feet) west of midspan. This crack occurred before the bridge had experienced any applied mechanical load. Figure 6.6 shows the strains occurring at an uncracked location spanning the keyway. These figures show large transverse deformations of the bridge. These movements appear to be too large to simply be transverse expansion of contraction of the beams due to temperature.

A better explanation is found from examining all the transverse data. During the day, the heat from the sun caused the beams to camber upward. During this time, it was found the some joints experienced an opening at the top of the joint and closing at the bottom of the joint. Other joints experience closing at the top and opening at the bottom when the beams camber up. At night, when the beams cool and camber down, opposite transverse movements are found. The probable explanation is that the beams do not sit square on the abutment and the vertical axes of the cross sections are not parallel (this is certainly true of the center joint, which is crowned). As the beams camber up or down, they follow their own vertical axis and, since the axes are not parallel, the beams do not move parallel to each other (Figure 6.7) causing the observed opening and closing of the joints. As shown in Figure 6.6, the transverse strains can be on the order of 300 με or more. This magnitude of strain is sufficient to cause keyway cracking.

The transverse thermal movements caused one problem for the researchers. When the pulse velocity was used to detect cracks, some cracks seemed to disappear and then later reappear. It was found that the thermal movements were causing temporary crack closures. Thus, it was necessary to check for cracks at various times during the day since at any point in time the thermal movements might close a given crack.

6.4 Summary

The data clearly shows that the beam experiences large deformations due to thermal gradients. These thermal gradients cause large longitudinal strains and cambering of the bridge. However, the thermal movements also cause transverse strains in the bridge. Transverse keyway strains, of sufficient magnitude to cause cracking, were measured. Therefore, it appears that the thermal strains crack the keyways.

These observations lead to several interesting conclusions:

1) If the shear keys crack due to thermal movements, the cracking occurs very early on. This explains why Huckelbridge, El-Esnawi and Moses (1995) found cracking so soon after the shear keys were regrouted. It is very possible that shear keys crack before the construction phase is ended.

2) The applied loads also cause transverse strains in the keyways, but the measured strains are an order of magnitude too small to cause cracking. It appears that crack initiation is due to thermal movements.

   During the loading phase, the cracks propagated. However, since the beams could not be insulated from the weather during the loading phase it is not clear if the load propagated the cracks or if the propagation was due to additional thermal strains.

3) This may also explain why the neutral axis keyway showed less initial cracking. The neutral axis would be subject to lower levels of strains from thermal gradients and the transverse strains generated at the neutral axis would not be large enough to crack the keyways.

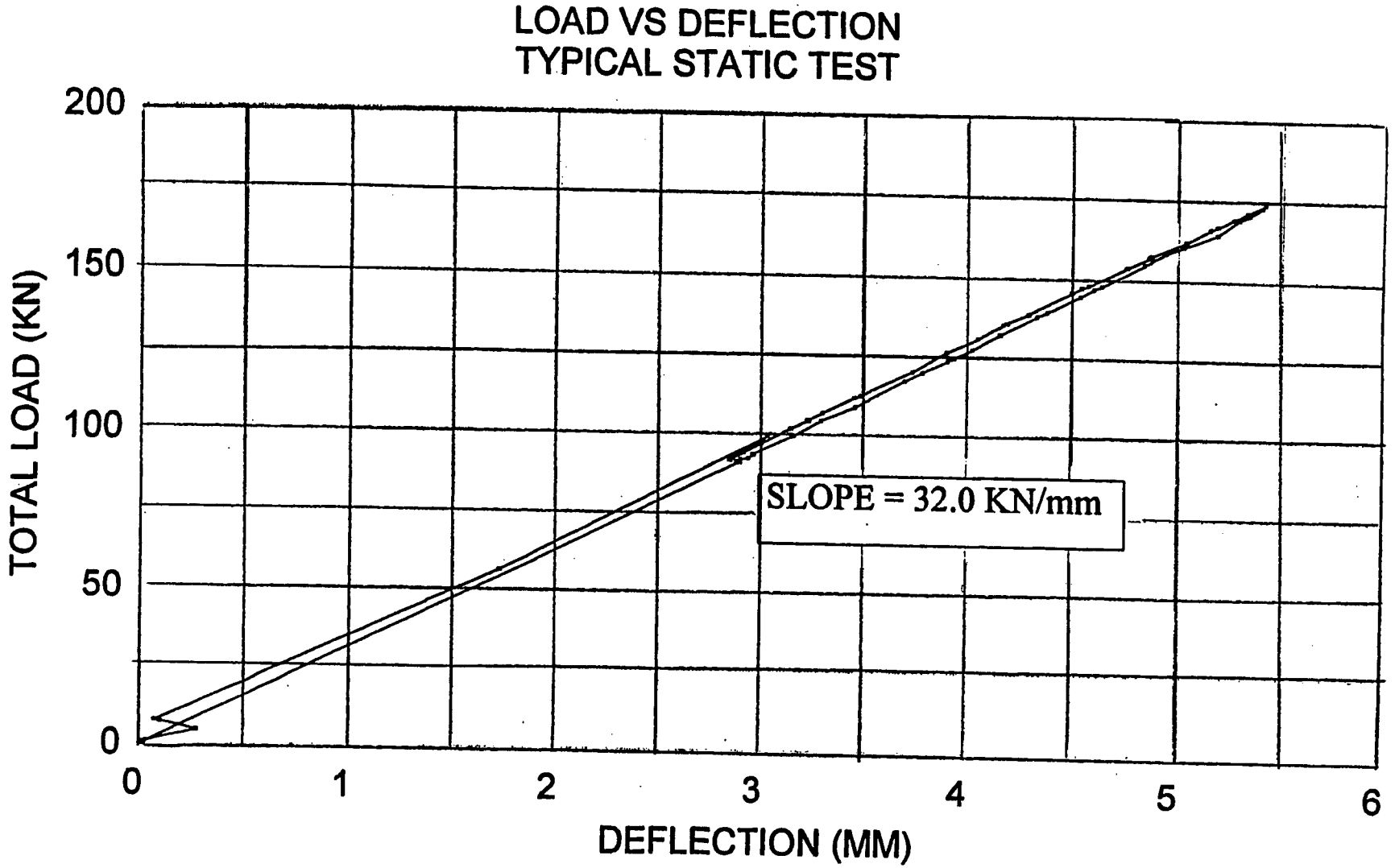

Figure 6.1 **Load Vs. midspan deflection for typical static test of bridge.**

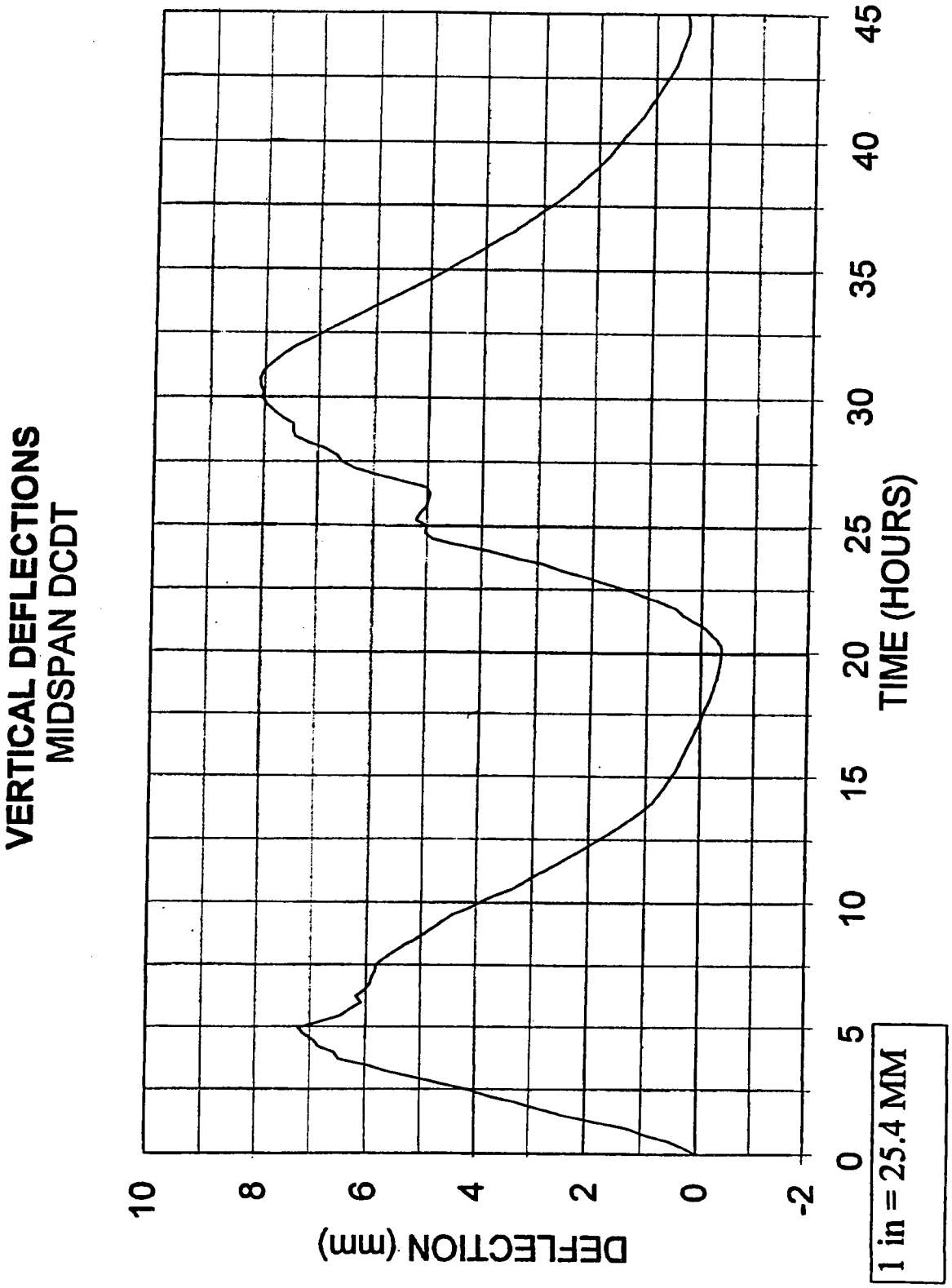

Figure 6.2 **Vertical midspan deflection caused by thermal loads.**

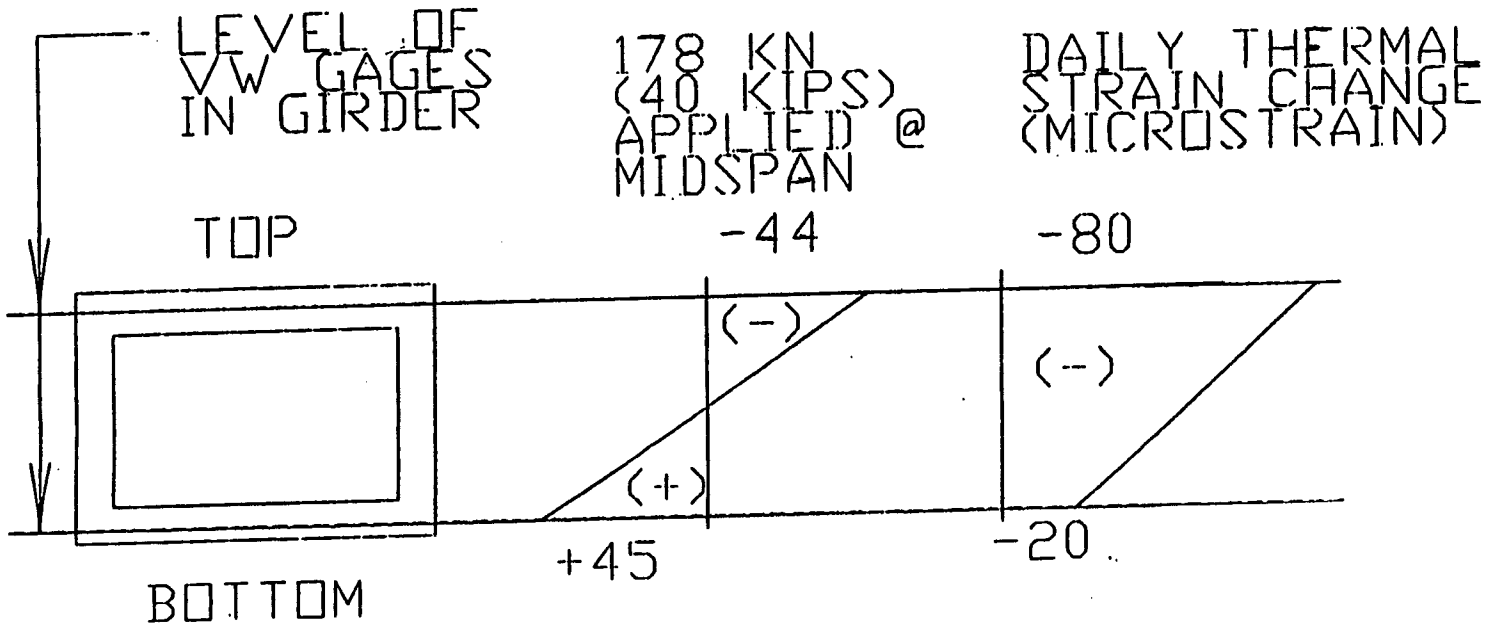

Figure 6.3 **Top and bottom flange strains Vs. 178 kN (40 kip) midspan load.**

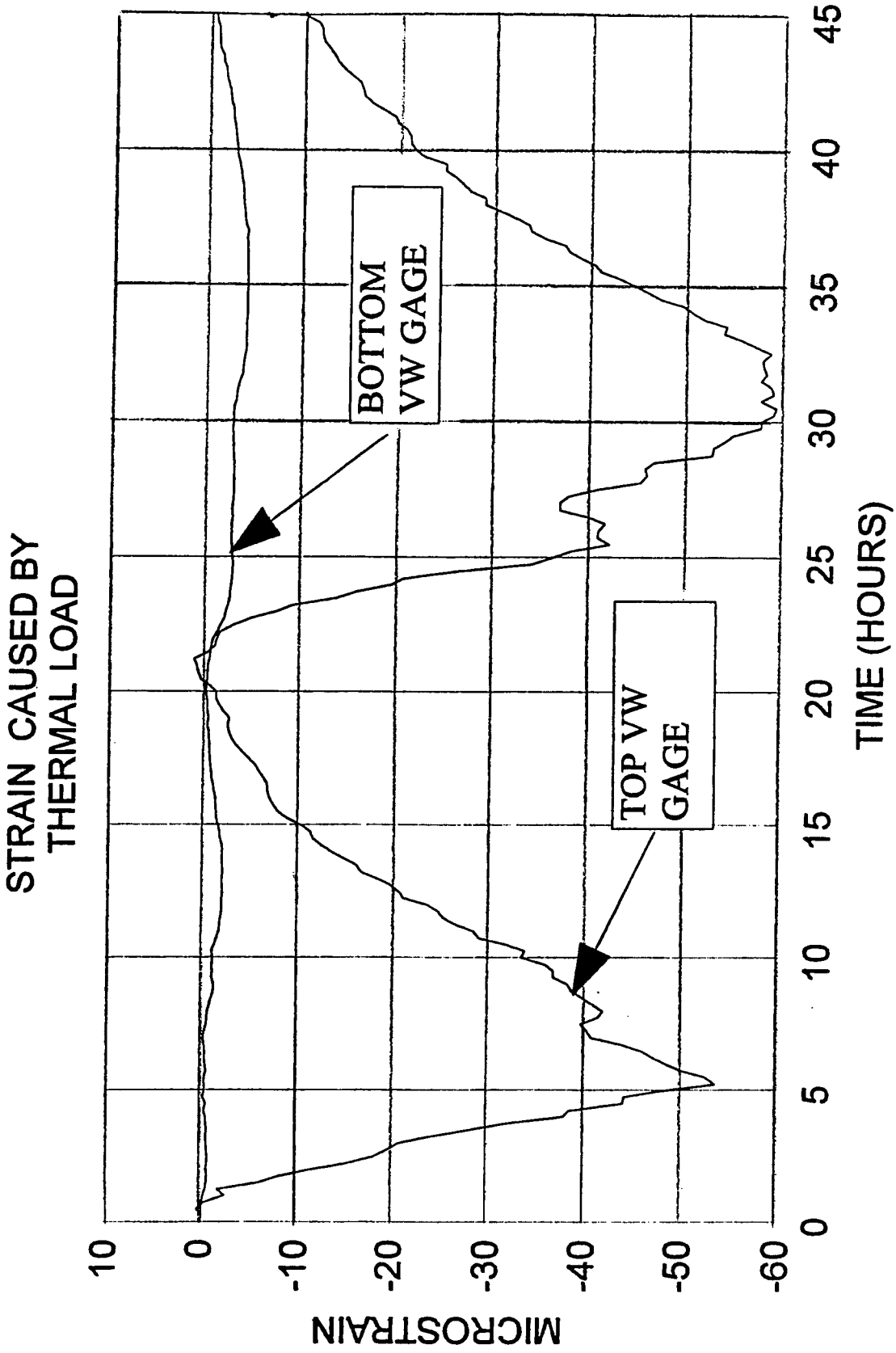

Figure 6.4 **Top and bottom flange thermal strains vs. time.**

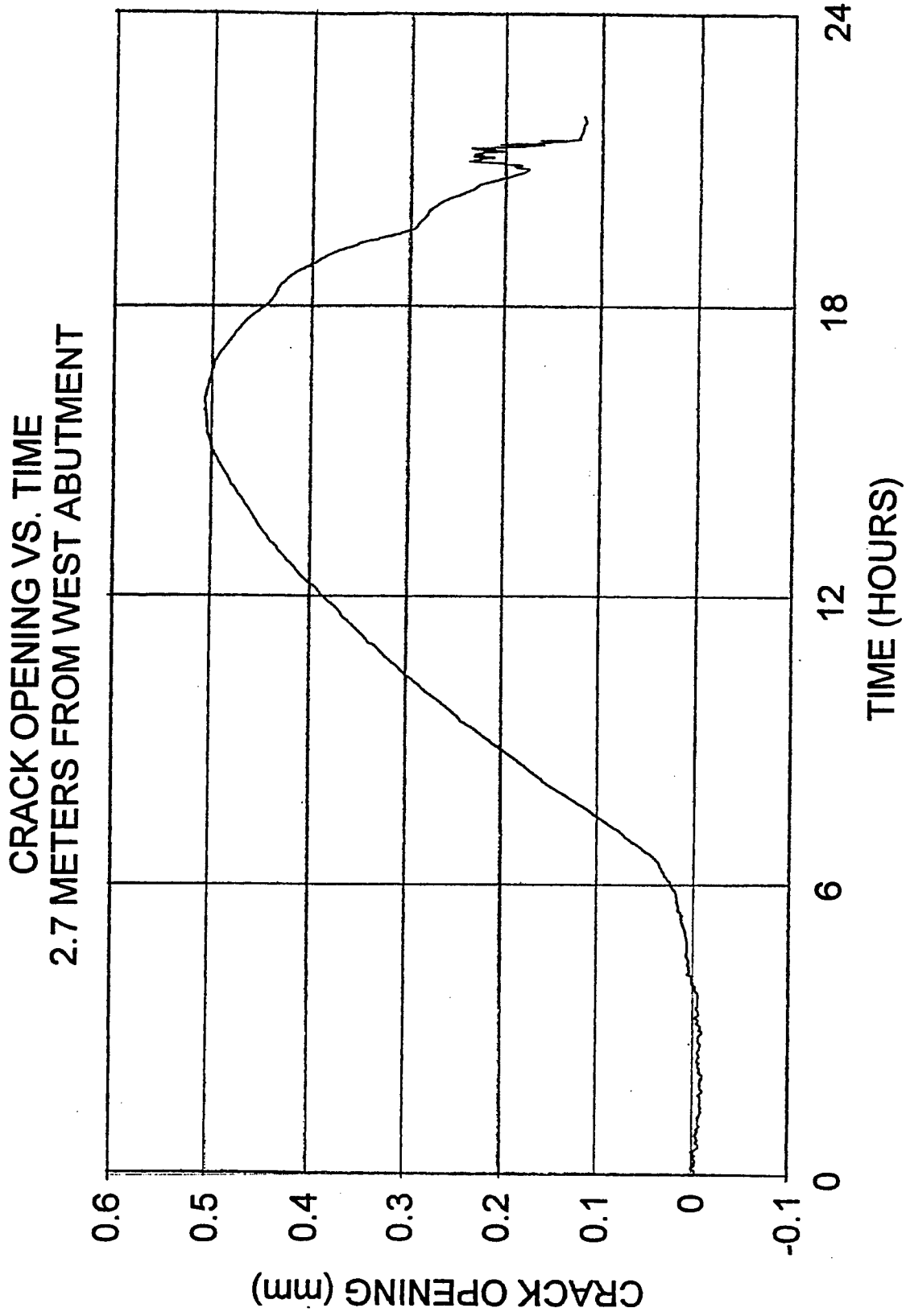

Figure 6.5 **Thermally induced transverse keyway movements at a cracked location.**

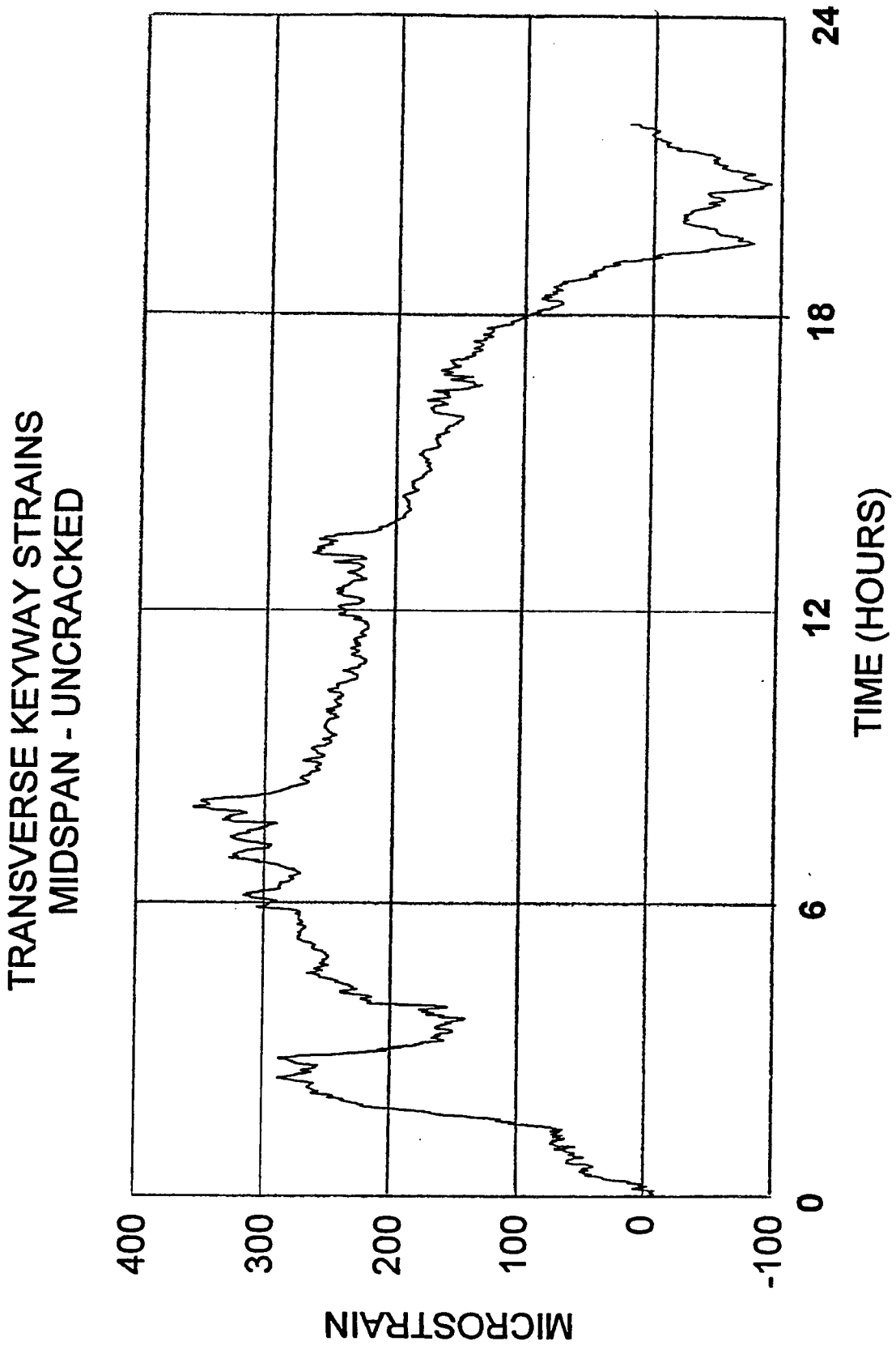

Figure 6.6 **Thermally induced transverse keyway strain at an uncracked location.**

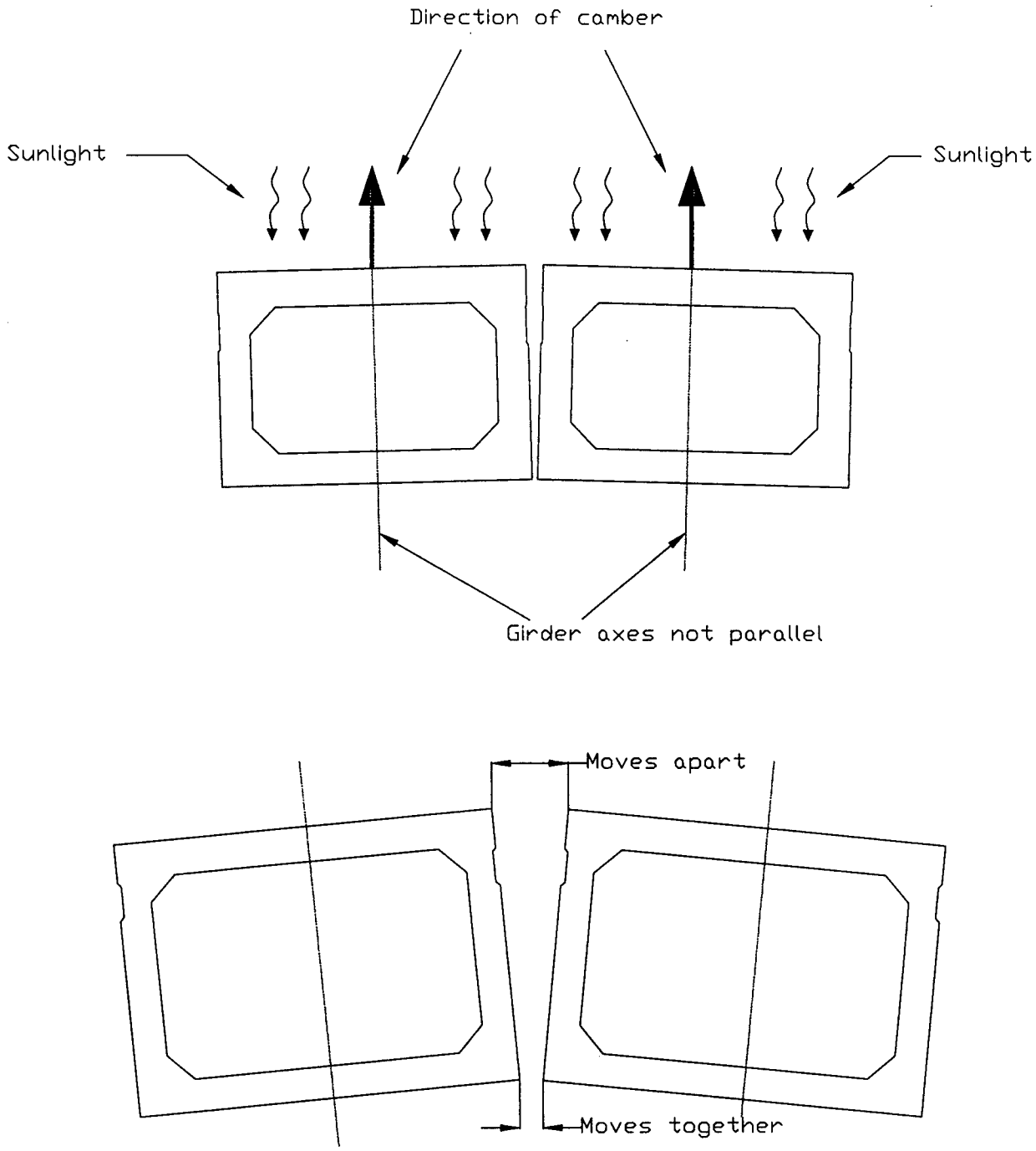

Figure 6.7 Joint Movement

CHAPTER 7

SUMMARY, CONCLUSIONS AND RECOMMENDATIONS

7.1 Summary of the Project

A full size portion of an adjacent box girder bridge was constructed to evaluate different shear key details. The bridge consisted of four (4) ODOT B33-48 girders, each 22.9 m (75 feet) long. Three separate keyway details were tested:

a) The current ODOT standard keyway using nonshrink grout.
b) A keyway of the same dimensions as the current standard, but moved down to the neutral axis of the beams. For this detail, only the actual keyway area was grouted with nonshrink grout, the throat area from the top of the keyway to the top of the beam was not grouted.
c) The current ODOT standard keyway grouted with epoxy grout.

The bridge was loaded in the center of flange of the two middle beams at midspan. Each beam was loaded by a pair of actuators which applied a total load of 89 kN (20 kips). This load corresponds to the wheel load of an HS-20-44 truck with impact. The beams were loaded alternately so that a complete shear reversal was achieved in the keyways. Loading continued for 1,000,000 cycles. Bridge response was monitored by numerous instruments and a computerized data acquisition system.

7.2 Test Summaries

7.2.1 Summary of Test #1 (Top Keyway Grouted)

Test #1 was a test of the current ODOT standard keyway with nonshrink grout. The keyways were grouted in November. The contractor was allowed to grout the keyways as he normally would with no attempt was made to control the water/cement ratio. After grouting, the bridge was covered with a plastic tarp, and a 58, 000 kJ (55,000 BTU) torpedo heater was run under the bridge for five days to prevent the grout from freezing. About two weeks after grouting and after the first severe freeze, the strain gages embedded in the keyways showed large jumps in strain. At the same time, what appeared to be shrinkage cracks appeared in the center and south keyways. Before any load was ever applied to the bridge, pulse velocity measurements indicated that the center keyway was severely cracked at midspan. Since it appeared that weather had cracked the keyways, the decision was made to grout the upper keyway in more typical weather conditions.

However, it was decided that the cracked keyways should still be subjected to a shortened tested. A total of 41,000 cycles were run. During this time, existing cracks in

the center keyway at midspan and the south keyway near the abutments became severe cracks which completely penetrated the keyway. The south keyway did not crack at midspan. The north keyway did not crack anywhere along its length. After disassembling the bridge, dye penetration confirmed the severe cracks did penetrate the center keyway at midspan before any load had been applied. Of particular interest in test #1 is the fact that neither the north nor the south keyway cracked at midspan where the load was applied and the keyways were expected to crack.

7.2.2 Summary Test # 2 (Top Keyway Grouted)

This was a repeat of test #1. The grouting was done in May and the water/cement ratio was carefully monitored to assure compliance with manufacturers specifications. Three days after pouring, the keyways had cracked. Severe cracks appeared in the center keyway near the west abutment and in the north keyway near the east abutment. Only superficial cracking was observed in any keyway near midspan.

At this time, an extensive investigation of the thermal effects upon the bridge yielded the following results: 1) The maximum longitudinal thermal strains in the top flanges of the girders are more than double the strains that would be caused by parking a HS20-44 truck on the bridge. 2) The thermal gradient causes the bridge to camber up as much as 14 mm (0.55 inches) as it heats up. 3) Transverse strains in the keyways, due to thermal loading, are of sufficient magnitude to crack the keyways.

The load was applied for 1,000,000 cycles. All of the existing cracks propagated, but no new cracks were formed. Measurement of transverse keyway strains during loading show that the strain from loading are an order of magnitude below that required for cracking. It does not appear that the loading initiated any cracking. It is not clear whether crack propagation was due to loading or additional thermal movements.

7.2.3 Summary of Test #3 (Neutral Axis Keyway Grouted)

In test #3, the ODOT standard keyway was moved down to the neutral axis. The water/cement ratio was monitored as in test #2. The grout depth was also monitored to avoid grouting the throat above the keyway. El-Esnawi and Huckelbridge (1995) suggested that flexure of webs under loading applied a transverse tension to the top of keyways. Elimination of the grout at the top of the keyway eliminates this tension.

Cracking was observed only directly over the abutments three days after pouring. The most severe crack was detected over the keyway near the southeast abutment. The data show that the crack had occurred the night after the keyways were poured. However, the cracks were < 1 m (3.25 feet) in length. The beams were loaded for 1,000,000 cycles. Only one crack propagated a total of 1 m (3.25 feet). The neutral axis keyways seemed to be more resistant to cracking. This is probably because the thermal movements are the neutral axis are smaller.

7.2.4 Summary of Test # 4 (Top Keyway Grouted With Epoxy Grout)

This test consisted of grouting the current ODOT standard keyway with epoxy grout. Construction and placement of the epoxy grout was closely monitored, and the grouting was done under reasonable weather conditions in April. Unlike the previous

tests, no cracking was observed at any point during the course of the test. As before, the beams were loaded for 1,000,000 cycles and was not enough to induce cracking in the keyways. Temperature induced strains were also not enough to produce cracking in the keyways.

7.3 Conclusions

Based on the test results, it appears that the epoxy grouted keyways are most resistant to cracking. The neutral axis keyway experiences some slight cracking, but is more resistant to cracking than the current ODOT standard keyway. The current ODOT standard keyway is least resistant to cracking. All cracking seems to be thermally induced.

More specific conclusions are:

1) Initial cracking of the current ODOT standard shear key design for a box girder bridge appears to occur while the grout is relatively young and seems to be the result of temperature strains. As the top of the beams heat up and cool down, the beams change camber. Because the beams do not sit perfectly square on the abutment, the vertical axes of the girders are slightly tilted. When the beams heat up and camber or cool down and decamber, the beams move along their vertical axis. Since this axis is slightly tilted, the beams also move slightly from side to side causing either transverse opening or closing of the joints. When the keyway is grouted to the top, these transverse openings cause tensile or compression strains in the keyways. Transverse temperature induced tensile strains of sufficient magnitude to crack the keyways were measured and can occur in either warm or cold weather. The cracks due to temperature strains are localized in given areas of the beam and may go partially or entirely through the shear keys.

2) For the current ODOT standard shear key design, transverse strains in the keyways measured during loading are an order of magnitude less than required for cracking. Therefore, loading does not appear to cause the initial cracking in the keyways.

3) The neutral axis keyway proposed by CWRU appears to resist cracking much better that the current keyway design., but some cracking is still found. The improved behavior is probably due to the fact that the temperature induced movements at the neutral axis are smaller. However, since this keyway is not grouted to the top of the beams, an empty space exists above the keyway where water and debris can collect. In a real field situation, this area needs to be sealed.

4) For both the current ODOT standard keyway and the proposed neutral axis keyway, cracks which formed from thermal movements propagated during the loading period. Crack propagation is a difficult phenomenon to understand. Due to high stress concentrations at crack tips, it is possible that a load which is insufficient to start cracking may cause a crack to propagate. Therefore, it is possible that, even though the applied load did not cause cracking, it may have propagated the existing cracks. Another possibility is that continued thermal movements of the bridge propagated the cracks. A third possibility is that

propagation is due to combination of thermal and load effects. Since the size of the beams required outdoor testing, it is not possible to insulate the beams from thermal movement and, therefore, not possible to separate load and temperature induced effects. However, since most of the cracking and most of the crack propagation occurred near the abutments, temperature is probably more responsible for crack propagation than loading.

5) The epoxy grouted shear keys did not crack. However, the result of this test are not sufficient to say that epoxy is the best choice for the keyways. It is important to note that there are several possible problems with the use of epoxy grout:

   a) Epoxy grouts have a coefficient of thermal expansion which is three (3) times that of concrete. During extreme changes in temperature, this incompatibility of thermal coefficients may cause high stresses in the keyways. During the tests reported here, the maximum ambient temperature change was about $\pm$ 12 ° C ($\pm$ 20° F). This did not crack the keyways. However, it is possible to have temperature swings of 60 ° C (110 ° F) during the course of a year. If the keyways are grouted on a very hot day, there may be problems in the winter when the temperatures may reach -20°C (0° F). More study is needed on the thermal incompatibility.

   b) After grouting, all tools must be cleaned with methyl ethyl ketone (MEK), a powerful organic solvent. This solvent presents some slight hazard to the humans and a large environmental hazard. If epoxy grouts are used, ODOT will need to specify an environmentally sound method of disposal of the epoxy and the MEK.

6) Uncracked shear keys exhibited full load distribution and the current AASHTO distribution factor for these girders (30%) was a reasonable upper bound for maximum load distribution. During the short term duration of these tests, cracked shear keys exhibited almost a negligible reduction in load sharing capabilities so data from this research does not indicate that the simple presence of a cracked shear key will result in loss of load transfer and overloading an individual girder. The most severe shear key cracks resulted in less than a 10% reduction in load distribution between the box girders. However, it is possible that over a long period of time a given keyway could deteriorate to the point where load distribution is compromised. The data also shows that relative deflections of the girders are inconsistent and cannot be used to determine the presence of cracks or loss of load distribution.

8.3 Recommendations

1) Use of non-shrink grout in the current keyway design will result in keyway failures due to thermal movements. This design should be discontinued or modified to include transverse post-tensioning.

2) Moving the keyway to the neutral axis is one possible alternative to the current design. This new design performed much better than the current design. It should be noted that the neutral axis keyway did experience some minor cracking at the abutments. This study evaluated relatively short term performance and it is possible that, over long periods of time, the observed cracking may become severe. A more complete, long term study of the neutral axis keyway is needed.

3) Both the CWRU study and this study showed epoxy keyways to be very resistant to cracking. However, it is recommended that the effects of the incompatibility of the coefficient of thermal expansion between concrete and epoxy be studied over a wide range of temperature variations before epoxy is considered for adoption.

4) Many states require varying amounts of transverse post-tensioning after the keyway grout has reached a specified strength. The new AASHTO LRFD code penalizes an adjacent box girder bridge with a high distribution factor unless 1.75 MPa (250 psi) of transverse post tensioning is supplied along the entire keyway. While this provision seems unreasonable, it still points out that transverse post-tensioning, perhaps combined with the neutral axis keyway, might be a more crack resistant design.

5) An attempt should be made to gain a better understanding of the thermal movements of the girders and bridge since it is clear that the shear key cracking is thermally induced.

6) It appears that the keyway problem is really two separate problems. In one case, it is desirable to prevent cracking as cracking may lead to loss of load transfer. In the second case, the more common problem is that cracking allows leakage of salt laden water which damages the beams through corrosion. It may be wise to separate these problems.

   This study shows that, in the short term, the presence of a crack does not affect load distribution. A longer term study should be conducted to see how severe the cracking needs to be to prevent load transfer and if such cracking is likely to occur. It is possible that a design which allows cracking may be acceptable if load transfer still occurs.

   For the problem of leakage, the shear keys should be sealed. One possibility is to use the neutral axis keyway, which is more resistant to cracking, and fill the open throat (recall that this keyway is not grouted to the top of the beams) with a high quality sealant which will prevent leakage even if the keyways crack.

REFERENCES

AASHTO (1992), *Standard Specifications for Highway Bridges*, 15th Edition, American Association of State Highway and Transportation Officials, Washington, D. C., 1992.

Collins, M. P. and Mitchell, D. (1990). *Prestressed Concrete Structures*, Prentice Hall, Englewood Cliffs, N. J., 1990.

Dunker, K. F., and Rabbat, B. G. (1992), "Performance of Highway Bridge in the United States - The First 40 Years," *PCI Journal*, Vol. 37, No. 3, May/June 1992, p. 61.

El-Esnawi, H. H. (and A. A. Huckelbridge, Advisor) (1996), *Evaluation of Improved Shear Key Design for Multi-Beam Prestressed Concrete Box Girder Bridges*, a Thesis Submitted to the Faculty of the Department of Civil Engineering in Partial Fulfillment of the Requirements for the Degree of Doctor of Philosophy, Department of Civil Engineering, Case Western Reserve University, Cleveland, Ohio, January, 1996.

El-Remaily, A., Tadros, M. K., Yamane, T., and Krause, G. (1996), "Transverse Design of Adjacent Prestressed Concrete Box Girder Bridges," *PCI Journal*, Vol 41, No. 4, July/August, 1996, pp. 96-107.

Gulyas, R. J., Wirthlin, G. J., and Champa, J. T. (1995), "Evaluation of Keyway Grout Test Methods for Precast Concrete Bridges," *PCI Journal*, Vol. 40, No. 1, January/February, 1995, pp. 44-57.

Halsey, J.T. (and R. A. Miller, Advisor) (1996), *Destructive Testing of Forty-Year-Old Prestressed Concrete Bridge Beams*, A Thesis Submitted to the Faculty of the Division of Research and Advanced Studies of the University of Cincinnati in Partial Fulfillment of the Requirements for the Degree of Master of Science, Department of Civil and Environmental Engineering, University of Cincinnati, Cincinnati, Ohio, 1996.

Hlavacs, G. M., Long, T., Miller, R. A., and Baseheart, T. M. (1997), "Nondestructive Determination of Response of Shear Keys to Environmental and Structural Cyclic Loading," In *Transportation Research Record 1574*, TRB, National Research Council, Washington, D.C., 1997, pp. 18-24.

Huckelbridge, A. A., El-Esnawi, H. H., and Moses, (1995), "Shear Key Performance in Multibeam Box Girder Bridges," *Journal of Performance of Constructed Facilities*, Vol. 9, No. 4, November, 1995, pp. 271-285.

Lall, J., Alampalli, S. and DiCocco, E. F.(1998), "Performance of Full Depth Shear Keys in Adjacent Prestressed Box Beam Bridges", PCI Journal, Vol. 33, No. 2, Mar/Apr. 1998, pp. 72 - 79.

Leslie, J. R., and Cheeseman, W. J. (1949), "An Ultrasonic Method of Studying Deterioration and Cracking in Concrete Structures", *ACI Journal*, Vol. 21, No. 1, January, 1949, pp. 17-36.

Miller, R. A. and Parekh K. (1994), "Destructive Testing of Deteriorated Prestressed Box Bridge Beam", In *Transportation Research Record 1460*, TRB, National Research Council, Washington, D.C., 1994, pp. 37-44.

PCI Design Handbook, 4th Ed., Prestressed, Precast Concrete Institute, Chicago, Illinois, 1992.

Swartz, S. E. (1991), "Dye Techniques to Reveal the Fracture Surface of Concrete in Mode I," *Experimental Techniques*, Vol. 15, No. 3, May/June, 1991, pp. 29-34.

Yamane, T., Tadros, M. K., and Arumugasaamy, P. (1994), "Short to Medium Span Precast Prestressed Concrete Bridges in Japan," *PCI Journal*, Vol. 39, No. 2, March/April, 1994, pp. 74-100.

APPENDIX A

Expected Prestressing Strain

Properties:

$E := 28500 \text{ ksi}$

$A := 0.153 \text{ in}^2$

$f_{pu} := 270 \text{ ksi}$

$f := 0.7 * f_{pu}$

$:= 0.7 * 270 \text{ ksi}$

$:= 189 \text{ ksi}$

Force Applied to Tendons := P

$P := f * A$

$:= \frac{f}{E} := \frac{189}{28500} := 6630\mu$

$:= 0.153 * 189$

$:= 28.9 \text{ kips}$

Skew of Foil Strain Gages $:= 25^0$

$f_{measured} := 6630 * \cos 25$

$:= 6010\mu$

APPENDIX B

Calculation of Stiffness of Girders

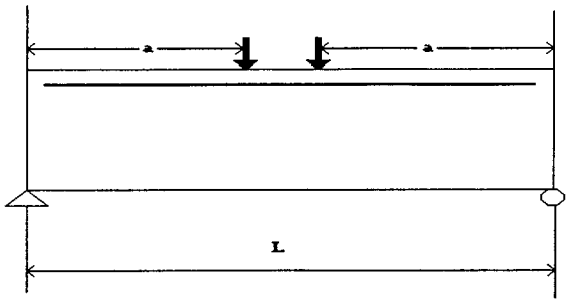

Properties:

a := 34.75 feet

L := 73.5 feet

k := 43.0 kips/inch

I := 110,000 in^4

$$\frac{P}{\Delta_{max}} := \frac{k}{2}$$

Note: k is based upon two load points.

$$\Delta_{max} := \frac{Pa}{24EI}\left(3L^2 - 4a^2\right)$$

$$EI := \frac{ka}{48}\left(3L^2 - 4a^2\right)$$

EI := 611,976 k in^2

E := 5560 ksi

APPENDIX C

Sample Calculation for Determining Percentage of Load Withstood by a Girder

Data used to create one value in Table 6.3
Test #1 -- Zero cycles -- Both south actuators pushing with 44.5 kN each.
Percentage of load sustained by the south-central girder which (INT1).

Raw Vibrating Wire Gage Data

GAGE	ZERO STRAIN	LOADED STRAIN	CHANGE IN STRAIN
INT 1A BOTTOM	2138.2	2164.0	25.8
INT 1B BOTTOM	1908.2	1933.6	25.4
EXT 1	1979.2	2000.5	21.3
INT 2A BOTTOM	2051.3	2069.8	18.5
INT 2B BOTTOM	2162.3	2180.5	18.2
EXT 2	2124.7	2147.9	23.2

GIRDER	AVERAGE CHANGE IN STRAIN
EXT 1 (BEAM #1) (NORTH)	21.3
INT 2 (BEAM #2) (NORTH-CENTRAL)	18.35
INT 1 (BEAM #3) (SOUTH-CENTRAL)	25.6
EXT 2 (BEAM #4) (SOUTH)	23.2

$$\%\text{SOUTH} - \text{CENTRAL} := \frac{25.6}{25.6 + 21.3 + 18.35 + 23.2} := 28.9\%$$

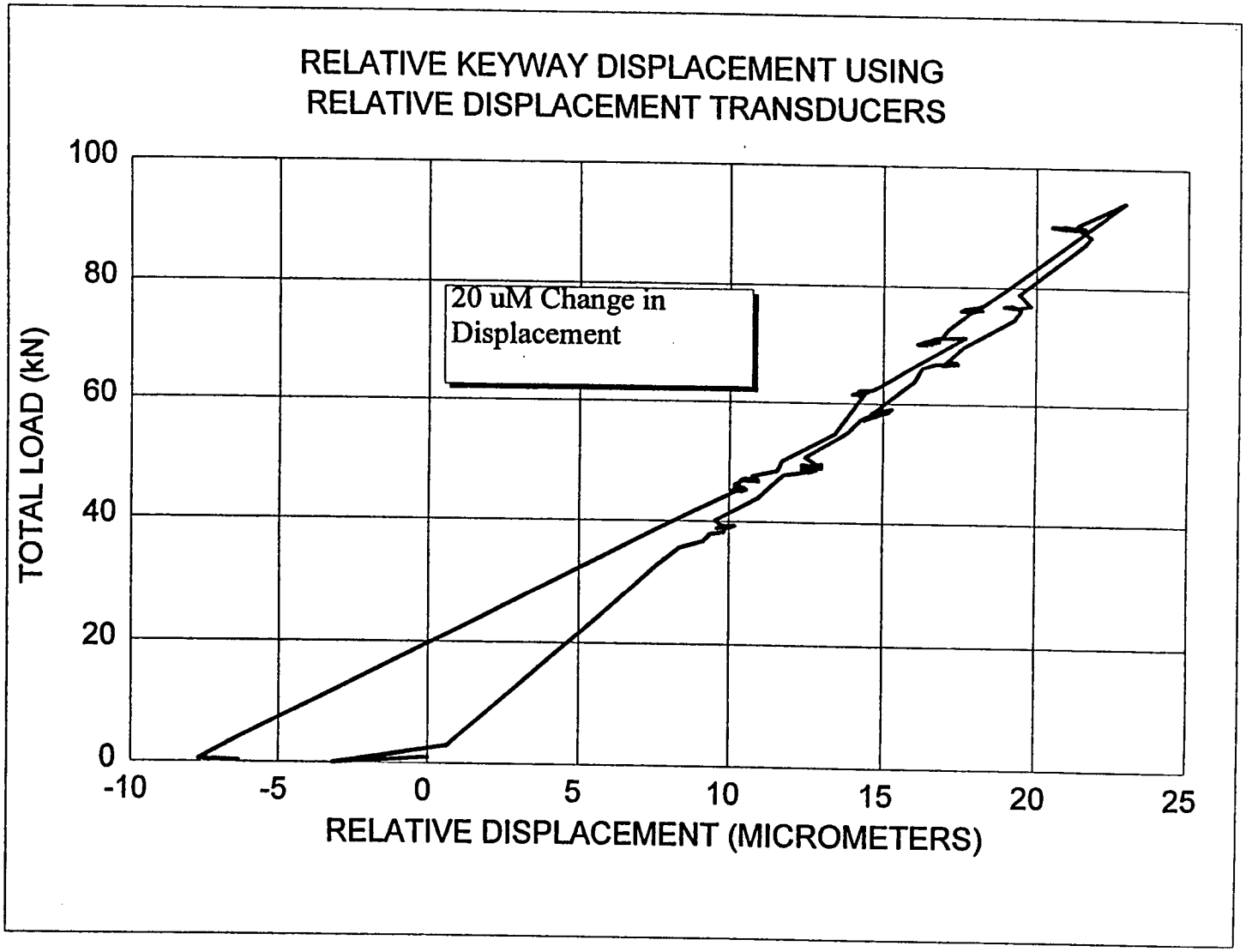

APPENDIX D: Graph Used to Obtain a Value in Table 5.6 -- South East Shear Key -- Zero Cycles

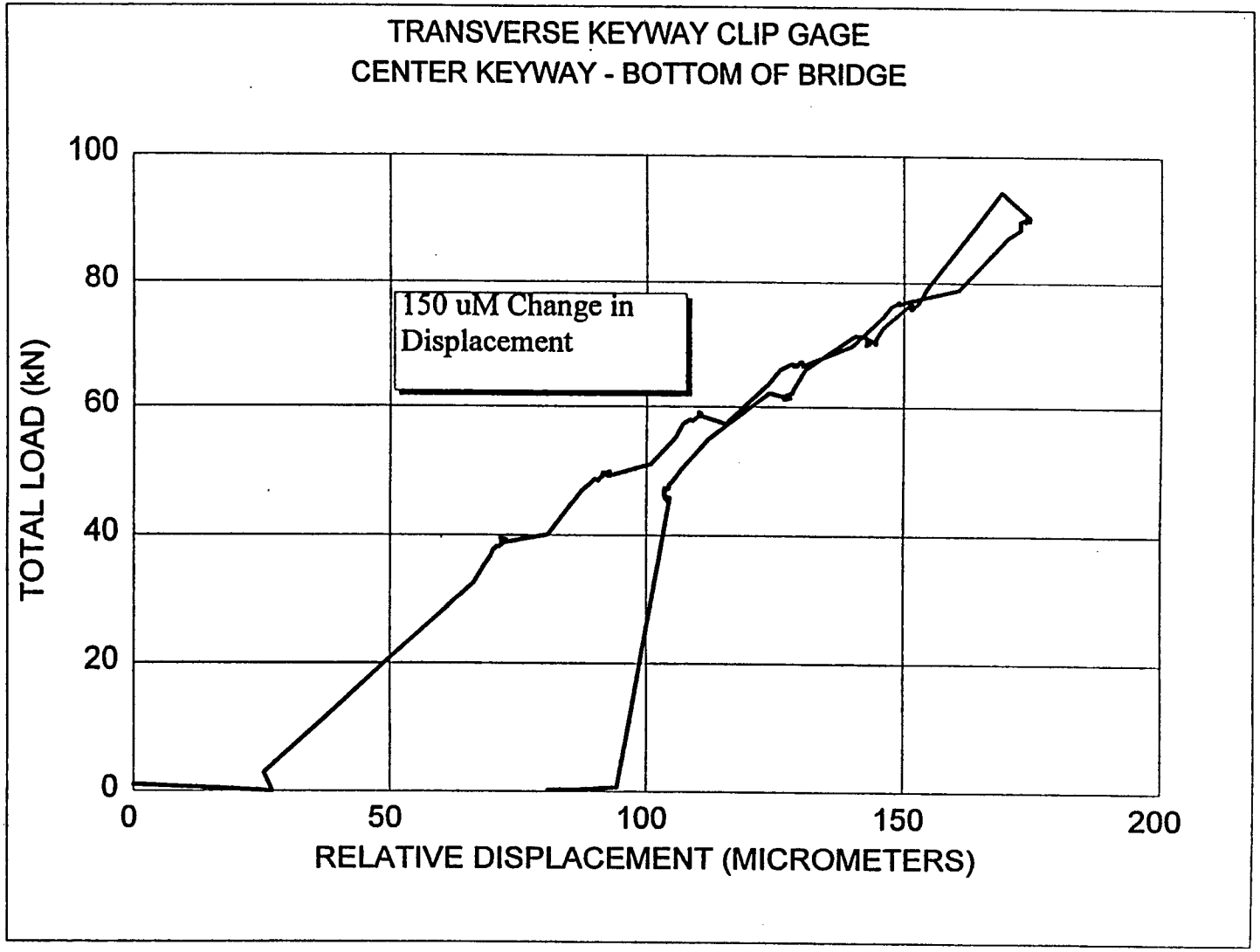

APPENDIX E: Graph Used to Obtain a Value in Table 5.4 -- Center Shear Key -- Bottom Clip Gage --Zero Cycles

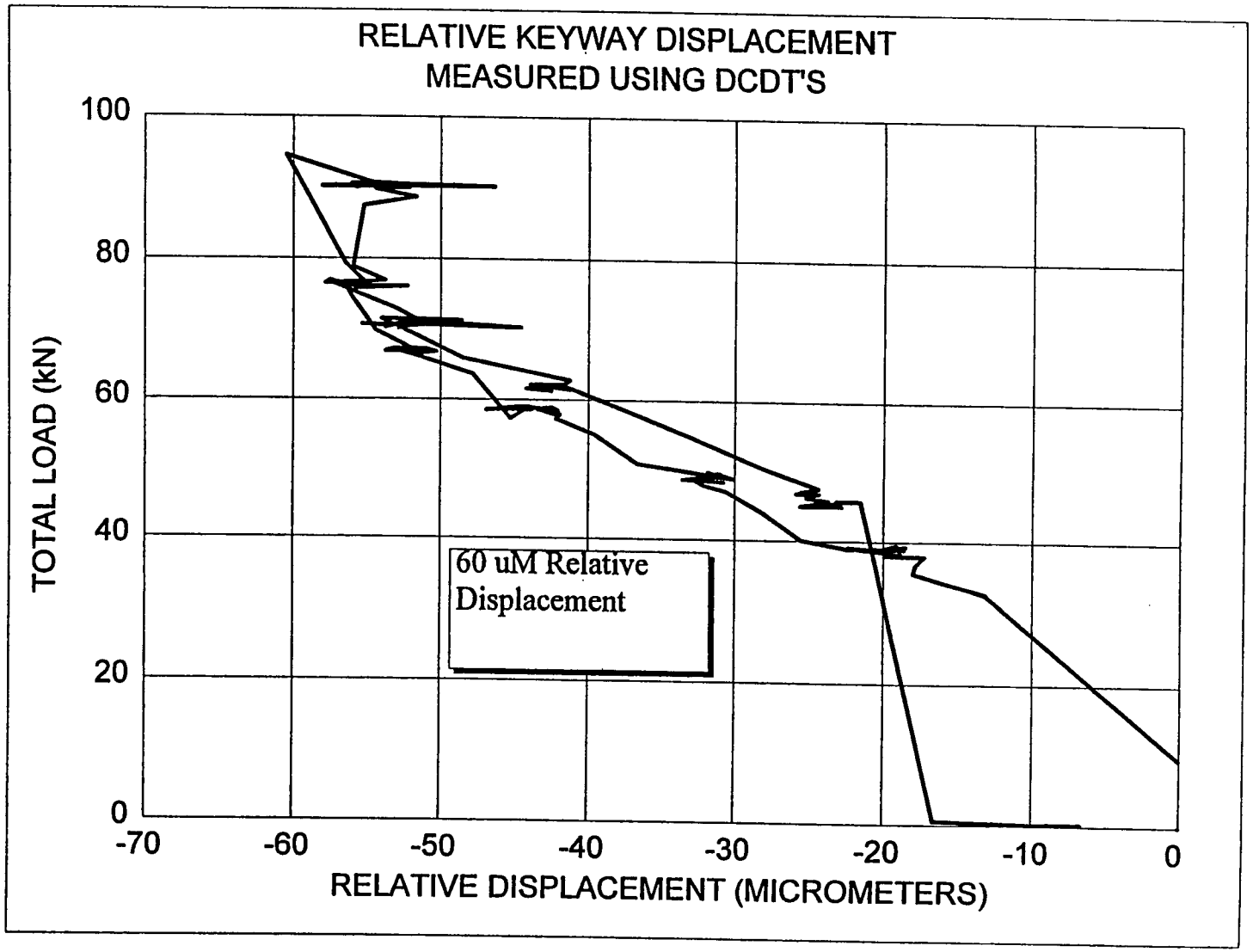

APPENDIX F: Graph Used to Obtain a Value in Table 5.7 -- North Shear Key -- Zero Cycles